**The Thesis Committee for Frank Edward Schalla**
**Certifies that this is the approved version of the following thesis:**

# Effects of flush slab supports on the hydraulic performance of curb inlets and an analysis of design equations

**APPROVED BY**
**SUPERVISING COMMITTEE:**

Ben R. Hodges, Supervisor

Michael E. Barrett

# Effects of flush slab supports on the hydraulic performance of curb inlets and an analysis of design equations

**by**

**Frank Edward Schalla, B.S.C.E.**

**THESIS**

Presented to the Faculty of the Graduate School of

The University of Texas at Austin

in Partial Fulfillment

of the Requirements

for the Degree of

**Master of Science in Engineering**

**The University of Texas at Austin**

**May, 2016**

# Acknowledgements

This thesis is based upon research supported by the Texas Department of Transportation, Research and Technology Implementation Office, Project 0-6842.

I'd like to first thank my advisor, Dr. Ben R. Hodges, for his support, trust, and enthusiasm for fluid dynamics. Additionally, I'd like to thank Dr. Michael Barrett, who through his insight and experience, has kept the project focused and has saved me countless hours. I would like to thank Muhammad Ashraf for his valuable contributions to this project. I would like to thank Alfredo Hijar and the rest of my co-workers at the Center for Research in Water Resources who have graciously helped with model construction. I would like to thank Jim Buttles for his advice and constant willingness to support me. Finally, I'd like to thank my family, friends and the EWRE community.

# Effects of flush slab supports on the hydraulic performance of curb inlets and an analysis of design equations

Frank Edward Schalla, M.S.E.

The University of Texas at Austin, 2016

Supervisor: Ben R. Hodges

The new Texas Department of Transportation curb inlet uses 6 inch flush slab supports for the top slab of a curb inlet. HEC-22, which provides design equations used by TxDOT, states flush slab supports can reduce an on-grade inlet's interception capacity by as much as 50%, yet does not provide any guidance on quantifying these effects. Full-scale physical modeling of the TxDOT curb inlet on-grade was performed to investigate the effects of flush slab supports on hydraulic performance. In addition, the modeled curb inlet is compared with HEC-22 and other curb inlet design equations. No measurable difference in interception capacity or ponded width was found between curb inlets with flush slab supports and without. For the 5 ft modeled curb inlet a combination of Guo and MacKenzie (2012) design equation and HEC-22 align best, yet neither align with every tested slope combination. HEC-22 design equations were found to over-predict the 15 ft modeled curb inlet by an average factor of 2.3:1. No other design equations were found to accurately predict hydraulic performance for the 15 ft modeled curb inlet.

# Table of Contents

# List of Tables

# List of Figures

# CHAPTER 1: INTRODUCTION

## 1.1 INTRODUCTION

This chapter summarizes the current state of knowledge surrounding curb inlets, curb inlet slab supports, their effect on curb inlet performance, common curb inlet design equations, and the objective and scope of this thesis.

Storm drain inlets are used to collect and direct stormwater runoff from roadways into storm drainage systems. They are commonly installed in urban environments within gutters or medians. Storm drain inlets decrease the risk of vehicle hydroplaning, roadway flooding and adjacent property flooding. Over 1,500,000 traffic accidents nationwide are associated with wet pavement (Pisano et al., 2008), which may have contributing factors from or are caused by hydroplaning.

Figure 1 shows common types of storm drain inlets taken from the Federal Highway Administration's third edition of the Urban Drainage Design Manual (Brown et al., 2009—herein HEC-22).

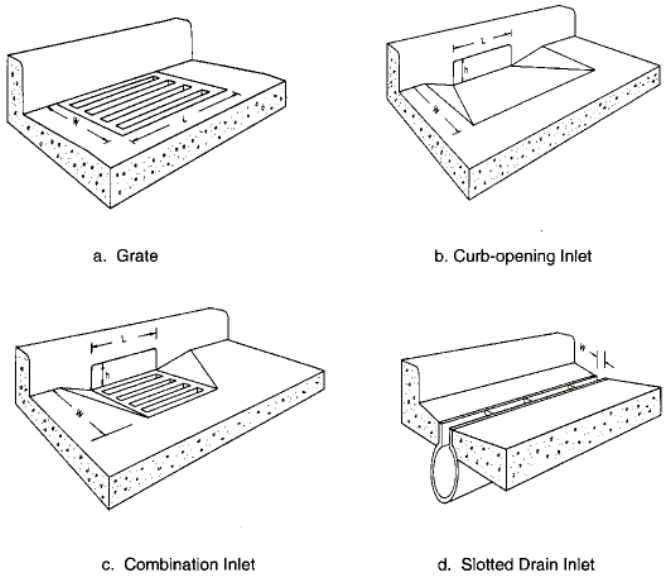


Figure 1. Common types of storm drain inlets (Figure 4-4 in HEC-22).

The common types of storm drain inlets are grate, curb-opening (or curb), combination, and slotted drain. Storm drain inlets are either installed on a constant slope (on-grade), or at the bottom of a sag vertical curve, (sag configuration). This thesis only studies on-grade curb inlets. The curb inlet poses less of a risk to motorist or bicyclists compared to a grate or combination inlet (TxDOT, 2014). The curb inlet is also less prone to clogging compared to a grate or slotted drain inlet (HEC-22).

Storm drain inlet spacing along a roadway is dependent upon the water depth at the curb (over which water flows outside of the roadway) and ponded width (the spread of water on the roadway). Figure 2 shows both water depth at the curb (or depth of flow, y) and ponded width (T).

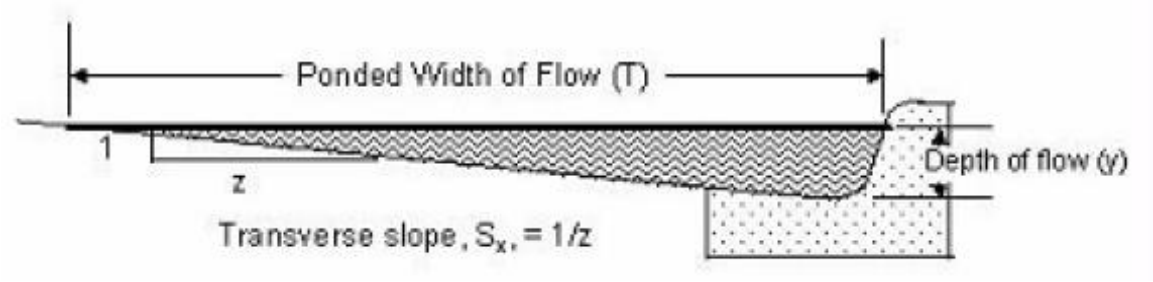


Figure 2. Profile view of a roadway and ponded flow (Figure 10-10 in TxDOT, 2014).

For a particular design storm, a storm drain inlet is installed once either the water depth is above the curb height or a maximum ponded width has been reached ($T_{max}$). The maximum ponded width is often defined by roadway type (e.g. principle arterial, local roads and streets). A plan view of the curb inlet design process is shown in Figure 3. After a storm drain inlet intercepts water off of the roadway the ponded width and depth of water decrease significantly (often reducing to zero) and the process of spacing and installing an inlet repeats.

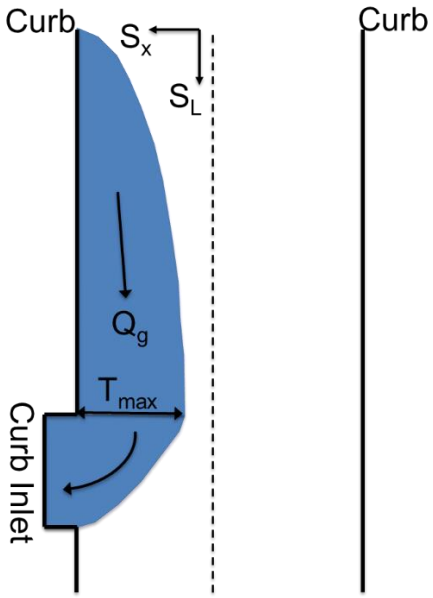


Figure 3. Plan view of a curb inlet design; $S_x$ is the cross slope, $S_L$ is the longitudinal slope, $Q_g$ is the gutter flow rate, and $T_{max}$ is the maximum ponded width.

The length of a curb inlet required to intercept 100% of the flow upstream ($Q_g$) is a function of longitudinal slope ($S_L$), cross slope ($S_X$), the flow rate upstream of the curb inlet ($Q_g$) and roadway roughness. A curb inlet's hydraulic performance, or the intercepted flow off of the roadway, increases with increasing curb inlet length, increasing cross slope and decreasing longitudinal slope (HEC-22).

### 1.2 TxDOT Curb Inlets and Slab Supports

The new Texas Department of Transportation (TxDOT) pre-cast curb inlet outside roadway, Type PCO (Figure 4 and 5), uses 6 inch flush slab supports for the top slab when extensions are used on the right, left, or both sides of the main inlet. The accepted curb inlet design standard is HEC-22, which is implemented within the TxDOT Hydraulic Design Manual (TxDOT, 2014). HEC-22 notes that, "Top slab supports placed flush with the curb line can substantially reduce the interception capacity of curb openings. Tests have

shown that such supports reduce the effectiveness of openings downstream of the support by as much as 50%." HEC-22 recommends that supports should be "recessed several inches from the curb line and rounded." However, HEC-22 does not provide any citation for studies supporting these recommendations. Furthermore, no information is provided on quantifying the effects of flush slab supports. Thus, the effects of such supports on the interception capacity (herein referred to as hydraulic performance) of the new TxDOT pre-cast curb inlet outside roadway (herein TxDOT curb inlet) cannot be determined from prior literature.

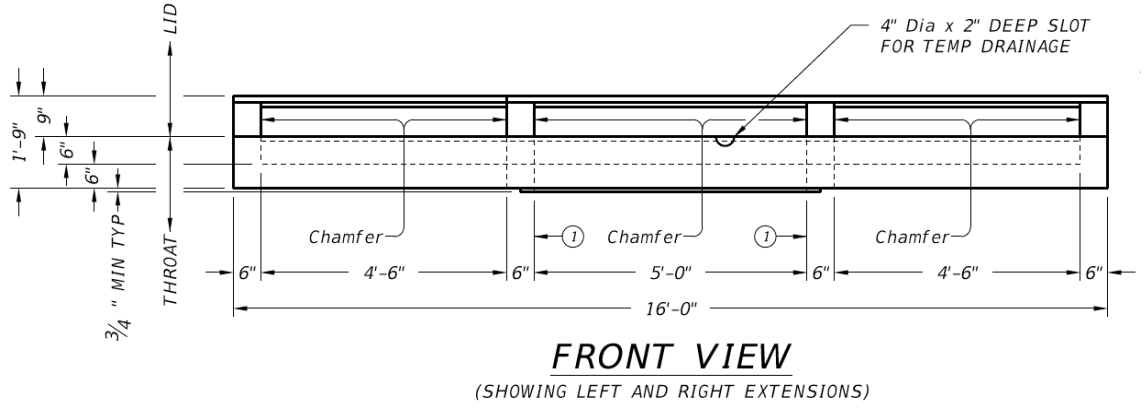


Figure 4. Front view of new TxDOT Precast Curb Inlet Outside Roadway (Type PCO) extracted from TxDOT file presd03.dgn (January 2015 revisions).

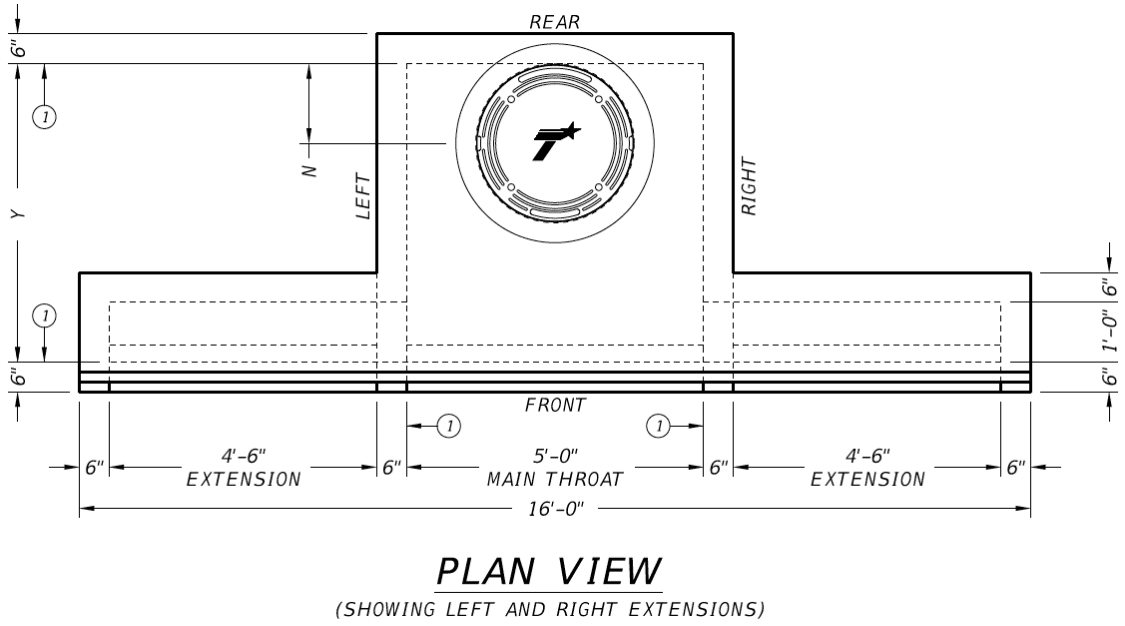


Figure 5. Plan view of new TxDOT Precast Curb Inlet Outside Roadway (Type PCO) extracted from file presd03.dgn (January 2015 revisions).

Previous studies have investigated curb inlet hydraulic performance using physical models (e.g., Hammond and Holley, 1995; Fiuzat et al., 2000) or numerical simulations (Fang et al., 2010). However, no prior studies specifically examined the differences in curb inlet performance when slab supports were present or not.

### 1.3 PREVIOUS STUDIES

Curb inlet hydraulic performance for roadway drainage has been studied for more than 60 years, as summarized in reviews of Holley et al. (1992), Hammonds and Holley (1995), Thompson et al. (2003), and Jiang (2007). None of these reviews mention investigations of the effects of slab supports, although some research clearly used models that included slab supports (e.g., Hammonds and Holley, 1995; Comport and Thornton, 2012). Further review of the literature (Table 1) has not provided any evidence for the

contention of HEC-22 that flush slab supports have a 50% reduction in hydraulic performance.

It is clear that flush slab supports are used in practice despite the HEC-22 admonition, e.g., as shown in Denver's Drainage Criteria Manual (their Photograph ST-1, 2002). Likewise, experiments have included flush slab supports, e.g., as shown in Hammonds and Holley (their Figure 4, 1995). Furthermore, Comport and Thornton (2012) conducted tests of the Colorado Type R inlet with 1-1/4 inch diameter rods for slab support, and sag configurations were considered by Guo (2006) and Guo et al. (2009). However, none of these experiments specifically looked at how the slab supports affected an inlet's hydraulic performance or might alter the standard design equations of HEC-22.

Table 1. Literature reviewed to look for evidence of the HEC-22 statement that flush slab supports cause a 50% reduction in hydraulic performance. No evidence was found.

| | |
|---|---|
| Izzard (1977) | McEnroe et al. (1999) |
| Bowman (1988) | Fiuzat et al. (2000) |
| Hotchkiss and Bohac (1991) | Spaliviero et al. (2000) |
| Soares (1991) | Kranc et al. (1998, 2001) |
| Holley et al. (1992) | Guo (2006) |
| Uyumaz (1992, 1994, 2002) | Jiang (2007) |
| Hotchkiss (1994) | Fang et al. (2010) |
| Hammond and Holley (1995) | Comport and Thorton (2012) |
| MacCallan and Hotchkiss (1996) | Guo and MacKenzie (2012) |
| McEnroe and Wade (1998) | |

Although no prior experiments have directly studied the effects of flush slab supports, Hotchkiss and Bohac (1991) and Soares (1991) studied the effects of altering a curb inlet's entrance and exit transitions with the desire to improve an inlet's hydraulic performance. Their experiments tested a number of sharp and smooth entrance and exit transitions, yet none had any significant effects on an inlet's hydraulic performance or reducing the standing wave which occurred at the end of the inlet opening. As shown in

Figure 6, slab supports can also cause standing waves, which indicates the HEC-22 recommendation to recess and round slab supports is likely credible. The standing waves at slab supports are likely similar to hydraulic effects at entrances and exits and might be similarly difficult to mitigate or alter to increase hydraulic performance.

Curb inlet modifications have been successful in increasing an inlet's hydraulic performance. One example of this is a canted curb inlet, where the upstream opening is recessed beyond the curb line. Another example is a curb and gutter transition, where the curb and gutter transition to a depressed curb inlet (Figure 7). A canted design provided hydraulic performance increases similar to a curb and gutter transition (Hotchkiss and Bohac, 1991). Similarly, a curb and gutter transition effectively extend the physical length of the inlet, increasing hydraulic performance (Hammond and Holley, 1995).

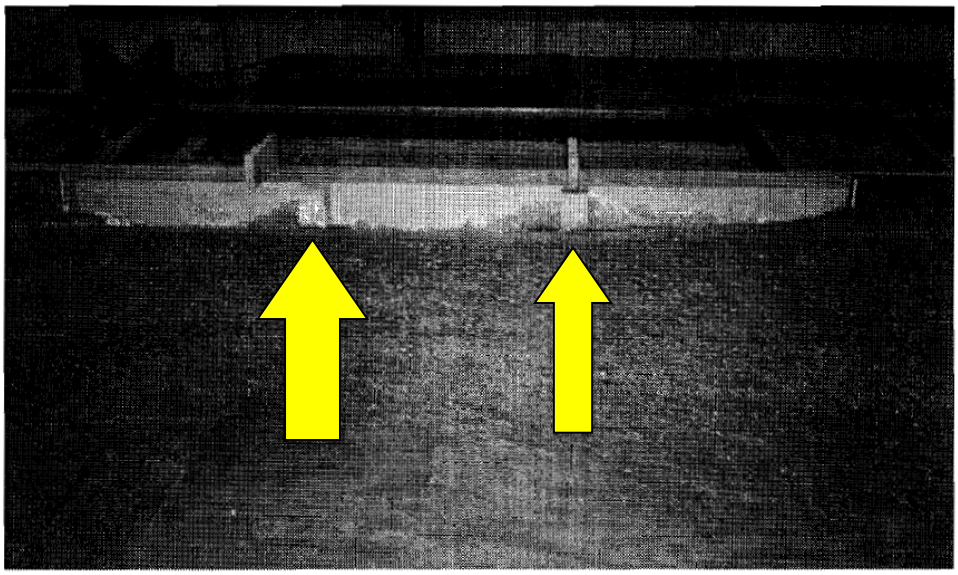

Figure 6. Photograph from Appendix C in Hammonds and Holley (1995), with arrows added. Experiments with modular sections for a 15 ft depressed inlet TxDOT Type C and D. Although the figure was poorly reproduced in the PDF digitization, it is still possible to observe the build up of waves associated with the two supports (arrows).

Figure 7. Depressed on-grade curb inlet with flush slab support (Denver's Drainage Criteria Manual, Photograph ST-3, pg. ST-20).

Arguably, numerical simulations could provide a means of analyzing curb inlet configurations for various types of slab supports (or no supports at all). Fang et al. (2010) used numerical simulations (FLOW-3D) of the TxDOT Type C and D inlets previously studied in the laboratory by Hammonds and Holley (1995). Unfortunately neither Fang et al. (2010) nor the dissertation of Jiang (2007) provide confidence that FLOW-3D is correctly representing the complex flows around slab supports. In particular, the numerical model was calibrated from Subramanya and Awasthy (1972) experimental data, which was generated in a study of side-weir flow without any internal slab supports. Thus, the ability of the FLOW-3D model (or any other model) to predict the effects of supports—either recessed or flush with the curb—is as yet unproven.

## 1.4 STATE OF THE ART FOR CURB INLET DESIGN

The basic approach of HEC-22 is used throughout the USA and is implemented within TxDOT (2014). Alternative approaches (particularly for grate inlets) have been proposed (Gomez and Russo, 2005, 2011; Comport and Thorton, 2012), yet much of the basic research has focused on fitting different coefficients to experimental data for specific curb inlets (Holley et al., 1992; Kranc et al., 2001; McEnroe and Wade, 1998; McEnroe et al., 1999; Uyumaz, 1992, 2002). It is difficult to extrapolate from such focused studies to general applications or for TxDOT curb inlets.

The HEC-22 design procedures for curb inlets on-grade are based on computing an inlet efficiency (E), defined from the intercepted flow rate ($Q_i$) by the inlet and the total gutter flow rate upstream of the inlet ($Q_g$) in a ratio:

$$E = \frac{Q_i}{Q_g} \tag{1}$$

The bypass flow ($Q_b$) that continues in the gutter downstream of the inlet is obtained by mass conservation as

$$Q_b = Q_g - Q_i \tag{2}$$

HEC-22 uses an empirical equation for the required length of a non-depressed curb opening inlets for 100% interception (i.e., E = 1) using the symbol $L_T$, defined as

$$L_T = K_u Q_g^{0.42} S_L^{0.3} \left( \frac{1}{n S_x} \right)^{0.6} \tag{3}$$

where $K_u$ = 0.817 (SI) or 0.6 (English), $S_L$ is the longitudinal slope, $S_x$ is the cross slope, and n is the Manning's roughness coefficient. Where the installed curb inlet length ($L_c$) is less than $L_T$ for the design $Q_g$, HEC-22 recommends an efficiency equation for use with eq. (1) of the form

$$E = 1 - \left(1 - \frac{L_c}{L_T}\right)^{1.8} \quad (4)$$

It follows that the bypass flow is obtained by manipulating eqs. (1)-(4) to obtain

$$Q_b = Q_g \left(1 - \frac{L_c}{L_T}\right)^{1.8} \quad (5)$$

which is Eq. (10-13) in TxDOT (2014).

Note that $L_T$ is the fundamental theoretically-based and empirically-adjusted parameter for curb inlet design in HEC-22 and represents the expected curb inlet length for interception of the design gutter flow using theory developed by Izzard (1950). Izzard's (1950) theoretical model presumes a single continuous opening with a smoothly changing free surface—a description that does not match the observed flow with slab supports as shown in Figure 6.

HEC-22 extends the non-depressed inlet equations (above) for use with depressed curb inlets by defining an equivalent cross slope, $S_e$, to replace $S_x$ in eq.(3):

$$S_e = S_x + S_w' E_o \quad (6)$$

where $S_w'$ is the cross slope of the depressed gutter section measured from the cross slope of the pavement, and $E_o$ is the ratio of flow in the depressed section to the total gutter flow. The depressed gutter section cross slope measured from the pavement cross slope, $S_w'$, is defined as

$$S_w' = \frac{a}{W} \quad (7)$$

where a is the depth of gutter depression and W is the width of gutter depression. Equation (7) is a variation of $S_w$, which is shown in Figure 5 and is defined as

$$S_w = S_x + \frac{a}{W} \quad (8)$$

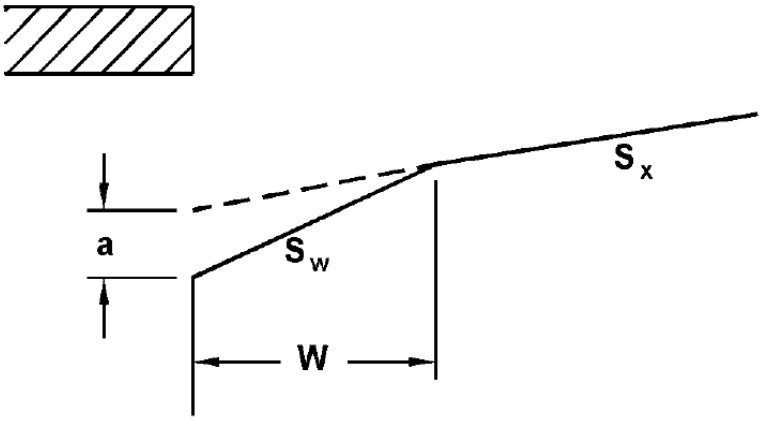


Figure 8. Side view of a depressed curb opening inlet and variables within eq. (6) and (8) (Figure 4-13 in HEC-22).

For a depressed curb inlet eq. (3) becomes

$$L_T = K_u Q_g^{0.42} S_L^{0.3} \left( \frac{1}{n S_e} \right)^{0.6} \tag{9}$$

i.e., the same form and exponents as eq. (3) are retained, but the revised geometry $S_e$ is substituted for $S_x$. The above is identical to Eq. (10-12) in TxDOT (2014).

Although capturing the entire design gutter flow (i.e., $L_c = L_T$, E=1, $Q_b = 0$) might seem preferable, the power relationship in eq. (4) implies that reductions of installed curb length ($L_c < L_T$) are not linearly related to the efficiency. It follows that a relatively small bypass can allow a significantly shorter inlet. Using the HEC-22 approach with eq. (4) above, an inlet length that is 81% of $L_T$ (19% reduction in length) leads to 5% bypass (95% interception), which is conservative compared to studies of Fiuzat (2000) and Izzard (1977), who noted inlet lengths that were 75% of $L_T$ had only 5% bypass. This concept is implemented within TxDOT (2014), where a bypass flow up to 0.5 cfs is allowed where capturing the entire design gutter flow is not necessary.

Because of the importance of the $L_T$ in gutter design, the lack of any way to quantify the effect of slab supports on either $L_T$ or the computation of E is a significant deficiency in the state of the art.

## 1.5 Comparison of Curb Inlet Design Equations & Charts

Table 2 provides a summary of curb inlet studies over the past 25 years that are available in the literature. These studies typically caution that their design equations cannot be used beyond their specific tests, and clearly a relatively small range of inlet lengths have been examined.

Table 2. Curb inlet studies from the recent literature.

| Study | State/Country Specific | Design Method | Equation Components | Based on Theory | Inlet Length, ft | Transition | Depression | Slab Support |
|---|---|---|---|---|---|---|---|---|
| Bowman (1988) | South Carolina | Chart | N/A | No | 4, 8, 12, 16 | 3 ft US/DS | 2 in | Unknown |
| Hotchkiss and Bohac (1991) | Nebraska | Chart | N/A | No | 6 | 5 ft US/DS | 5 in | No |
| Soares (1991) | South Carolina | Equation | $E = f(K, L_c, T, S_x, S_L)$ | No | 4, 8, 12, 16 | 3 ft US/DS | 2 in | Unknown |
| Holley et al. (1992) | Texas | Equation | $q_L = f(Y)$ | Yes | 5, 10, 15 | 10 ft US/DS | Yes | No |
| Uyumaz (1992, 1994, 2002) | Turkey | Equation | $E = f(K, L_c, h, T, F, S_x, S_L)$ | Yes | 1.25, 2.5, 3.75 | Yes | Yes | No |
| Hotchkiss (1994) | Nebraska | Chart | N/A | No | 6 | 5 ft US/DS | 5 in | No |
| Hammond and Holley (1995) | Texas | Equation | $q_L = f(Y)$ | Yes | 5, 15 | 5 ft US/DS | 3 in, 4 in | Yes |
| MacCallan and Hotchkiss (1996) | Nebraska | Equation | $E = f(S_L, S_x, Q_g)$ | No | 6 | 5 ft US/DS | 5 in | No |
| Kranc et al. (1998, 2001) | Florida | Equation & Chart | $Q_i = f(Q_g, S_x, S_L)$ | No | 4 | 4 ft US/DS | 3 in | Yes |
| McEnroe and Wade (1998) | Kansas | Equation & Chart | $Q_i = f(K, L_c, S_x, S_L)$ | No | 4, 6, 8, 10, 12 | 10 ft US, 5 ft DS | Y | No |
| McEnroe et al. (1999) | Kansas | Equation & Chart | $Q_i = f(K, L_c, S_x, S_L)$ | No | 3.94*, 8.86*, 14.10* | 2.5 ft US/DS | 3 in | No |
| Fiuzat et al. (2000) | South Carolina | Equation | $E = f(K, L_c, T, S_x, S_L)$ | No | 4, 8, 12, 16 | 3 ft US/DS | 2 in | Unknown |
| Spaliviero et al. (2000) | United Kingdom | Equation | $E = f(Q_g, Y, L_c)$ | Yes | 1.64*, 4.92* | No | No | No |
| Jiang (2007) | Texas | FLOW-3D | N/A | Yes | 5, 15 | 5 ft US/DS | 4 in | Yes |
| HEC-22 (2009) | USA | Equation | $L_T = f(K, Q_g, S_L, S_e/S_x, n)$ | Yes | Varies | N/A | Varies | N/A |
| Fang et al. (2010) | Texas | FLOW-3D | N/A | Yes | Varies | 5 ft US/DS | 3 in, 4 in | Yes |
| Comport and Thorton (2012) | Colorado | Equation | $L_T = f(K, Q_g, S_L, S_e/S_x, n)$ | Yes | Varies | N/A | Varies | N/A |
| Guo and MacKenzie (2012) | Colorado | Equation | $L_T = f(K, Q_g, S_L, S_e/S_x, n)$ | Yes | Varies | N/A | Varies | N/A |

Abbreviations: US - upstream of inlet, DS - downstream of inlet, E - efficiency, K - study specific coefficient, $L_c$ - inlet length, T – ponded width on road, $S_x$ - cross slope, $S_L$ - longitudinal slope, $q_L$ - intercepted inlet flow per effective unit length, Y - normal water depth at curb upstream of inlet, h - curb inlet opening height, F – Froude number, $Q_i$ - intercepted flow rate, * - length converted from meters, $Q_g$ - gutter flow rate upstream of inlet, $L_T$ - curb inlet length to capture 100% of flow, $S_e$ - equivalent cross slope.

A major difference between these studies is whether the authors started from equations derived from theory (such as HEC-22, e.g., Hammond and Holley, 1995; Uyumaz, 2002) or if they developed a purely empirical fit (e.g., MacCallan and Hotchkiss, 1996; Fiuzat et al., 2000). Studies using purely empirical fitting should only be applied to inlets matching the tested inlet.

For the Colorado Type R depressed curb inlet, Comport and Thorton (2012) and Guo and MacKenzie (2012) developed revised sets of coefficients and exponents for the $L_T$ computation of eq. (9) from HEC-22, which can be written in a general depressed curb inlet form as

$$L_T = N\, Q_g^a\, S_L^b \left( \frac{1}{n\, S_e} \right)^c \tag{10}$$

The different recommendations are shown in Table 3 and graphed in Figure 9. Although these results show a significant departure from HEC-22, the accuracy of Comport and Thornton (2012) has been questioned by Russo and Gomez (2014), whose experiments supported HEC-22, albeit for grate inlets (Gomez and Russo, 2005 & 2011). Furthermore, the presence of a negative exponent for b in the Comport and Thorton (2012) implies a departure from the physics of the theoretical model used to develop $L_T$, indicating that their approach is an empirical fit.

Table 3. Regression coefficients and exponents from the literature for eq. (10).

| | **N [SI (English)]** | **a** | **b** | **c** |
|---|---|---|---|---|
| HEC-22 / TxDOT (2014) | 0.817 (0.6) | 0.42 | 0.3 | 0.6 |
| Comport and Thornton (2012) | 0.493 (0.176) | 0.62 | -0.021 | 0.49 |
| Guo and Mackenzie (2012) | (0.38) | 0.51 | 0.06 | 0.46 |

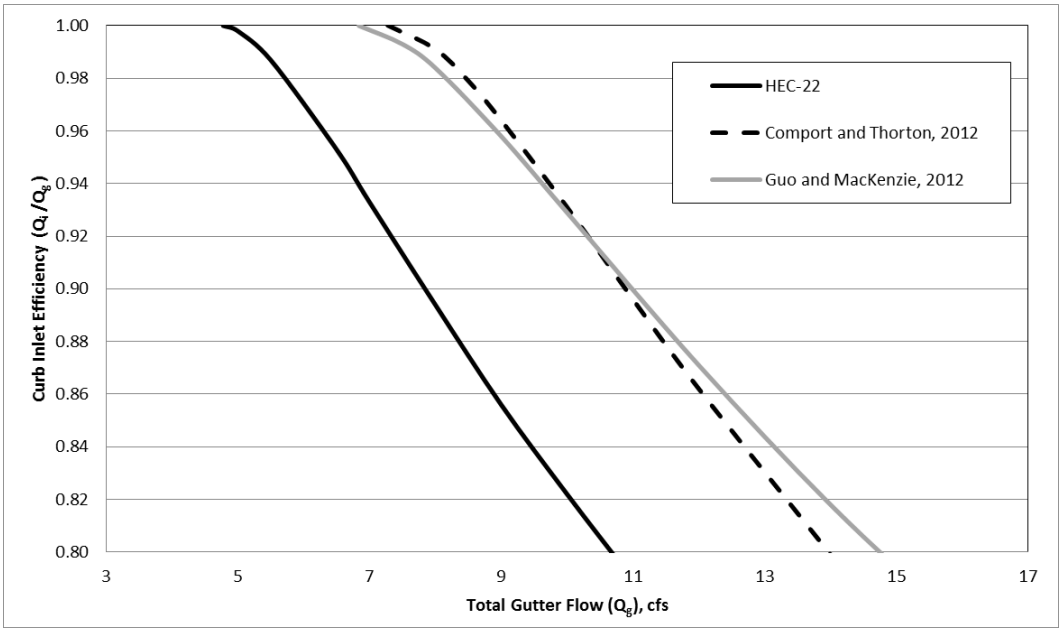


Figure 9. A 15 foot curb inlet efficiency comparison from Table 3. Road Geometry: $S_x$ = 2%, $S_L$ = 2%, n = 0.0166.

### 1.6 INCLUDING SLAB SUPPORTS IN CURB INLET DESIGN EQUATIONS

None of the studies discussed above explicitly include the effects of flush slab supports within a curb inlet. Given the existing data and methods, a designer has three options within the context of HEC-22. As Case 1, the designer could ignore the supports and use sum of the inlet openings as the $L_c$ for a single long inlet. This approach presumes that the slab supports are a simple interruption of the smooth inlet flow. As Case 2, the designer could include the slab supports within the total inlet length, taking the distance from the entrance to exit as $L_c$. This approach presumes that the interruption of the flow by the slab supports is balanced by a local increase of the interception around the supports. Finally, as Case 3 the designer could treat adjacent inlets as a series of individual inlets, where the bypass from the upstream inlet becomes the gutter flow for the next inlet. This approach presumes that the flow at the slab support is a normal flow, i.e., similar to the assumptions used for the upstream gutter conditions for a single inlet, which seems

unlikely. Indeed, none of these cases are rigorously supported by the derivation of $L_T$ or the efficiency relationship shown in eq. (4). Appendix A derives the efficiency equations for Case 1, Case 2, and Case 3 to illustrate the different solutions that could be obtained. Figure 10 is a graph of the efficiency curves for the three derived cases.

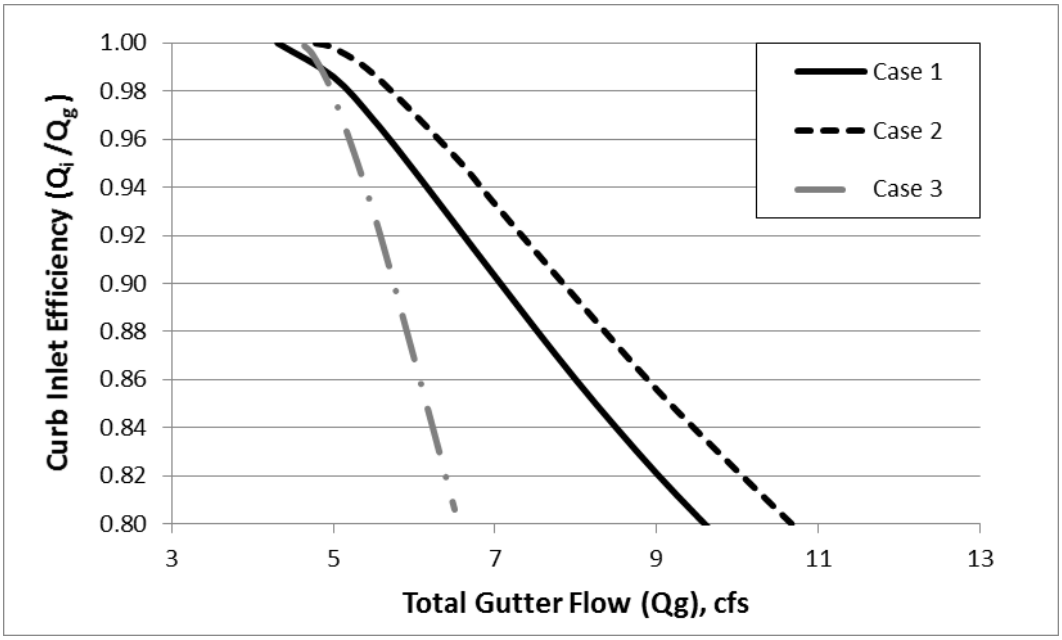


Figure 10. Case 1, Case 2 and Case 3 efficiency curves for a 15 foot curb inlet. Road geometry: $S_x$ = 2%, $S_L$ = 2%, n = 0.0166.

### 1.7 On Experiment Scaling

Laboratory experiments have been conducted at both full scale (1:1) and at geometrically reduced scales. Russo and Gomez (2012) provided a discussion of the Comport and Thornton (2012) inlet experiments with a question as to whether the use of a 1:3 scale model is appropriate for such flows. Similarly, Argue and Pezzaniti (1996) argued that full-scale experiments might be necessary to correctly capture urban drain performance, particularly for considerations of debris flow.

From dimensional analysis, the flow at a curb inlet should be governed by geometric parameters, the Froude number (Fr), and the Reynolds number (Re). Geometric scaling of the experiments is accompanied with Froude number scaling of the flow. This is represented by eq. (11) and derived in Appendix A, where $L_{prototype}$ and $L_{model}$ are the geometric lengths of the prototype and model, respectively.

$$\frac{Q_{prototype}}{Q_{model}} = \left( \frac{L_{prototype}}{L_{model}} \right)^{5/2} \tag{11}$$

Experimental scaling requires the assumption that Reynolds number effects are invariant over a wide range of scales. Matching both the Re and Fr requires a full-scale model if water is used as the experimental fluid.

Although hydraulic experiments for a wide range of structures have traditionally been conducted with Fr scaling, there is a question as to whether the Re effects can be neglected for curb inlet flow, particularly at the apex of the cross-section triangle (where the flow depth is thin compared to the gutter) or in the turbulence caused by a slab support. Arguably, the standing wave produced by a slab support should dominate the Re effects, so Fr scaling might not be detrimental. However, there does not appear to be any studies that conclusively determine whether Fr scaling produces the same curb inlet behavior as a full-scale model.

## 1.8 Thesis Objective and Scope

Curb inlet studies over the past 20 years have largely been focused on providing the hydraulic performance of specific inlets. Evidence of inlet/end wall effects (see §1.3) supports the HEC-22 recommendation to avoid slab supports. However, slab supports are a structural necessity for long inlets and cannot be simply dismissed as an inefficient or unacceptable design practice. Unfortunately, there has been no attempt to develop a

theoretical model (i.e. Izzard, 1950; HEC-22) to account for the presence of slab supports, nor has there been any attempt to quantitatively investigate the effects of slab supports on an inlet's hydraulic performance.

A physical experimental model is used herein to study the effects of slab supports on a curb inlet's hydraulic performance. The model allows for testing a varying curb inlet lengths with and without slab supports over a range of road geometries (i.e. $S_L$, $S_x$). The physical model data are then analyzed to observe what effect slab supports have, if any, on a curb inlet's hydraulic performance.

The physical model data is also compared to HEC-22 design equations. This comparison assesses how accurate HEC-22 and other design equations are (i.e. Comport and Thorton, 2012; Guo and MacKenzie, 2012) at predicting a curb inlet's hydraulic performance for TxDOT on-grade curb inlets (Type PCO).

# CHAPTER 2: PHYSICAL MODEL & METHODOLOGY

## 2.1 PHYSICAL MODEL

The physical model is located in the Center for Research in Water Resources (CRWR) laboratory at the J.J. Pickle Research Campus of The University of Texas at Austin. The physical model was originally constructed for Holley et al. (1992), and built as a 3:4 scale representation of one lane of a roadway with adjustable longitudinal and cross slopes. It has been used for a variety of projects (e.g. Hammond and Holley, 1995; Qian et al., 2013) and modified according to projects' specific needs.

The physical model has a length of 64 ft (19.05 m) and operational surface (framed by two curbs) width of 10.5 ft (3.2 m). The physical model has a steel structure supporting a wood deck, curbs and headbox. The steel structure is supported at 4 locations, each near a corner of the physical model. One corner sits on a ball bearing, acting as a pivot point and allowing the other three corners to be raised and lowered independently by crane hoists (Figure 11 and 12). This provides a full range of longitudinal and cross slope combinations.

A 12 inch diameter pipe, reduced to 4 inch pipe and valve, provides the water supply into a headbox at the upstream end of the physical model. Water is taken from an exterior holding tank by 2 pumps operating in parallel. The pumps were designed to discharge 7 cfs (Holley et al., 1992).

The model's road surface is sealed with layers of fiberglass and resin. The surface is textured with a mean diameter particle size of 1.3 mm (Hammond and Holley, 1995). Recent roughness calculations performed by Qian et al. (2013) show an average Manning's roughness coefficient of 0.0166, which is discussed further in §2.4.

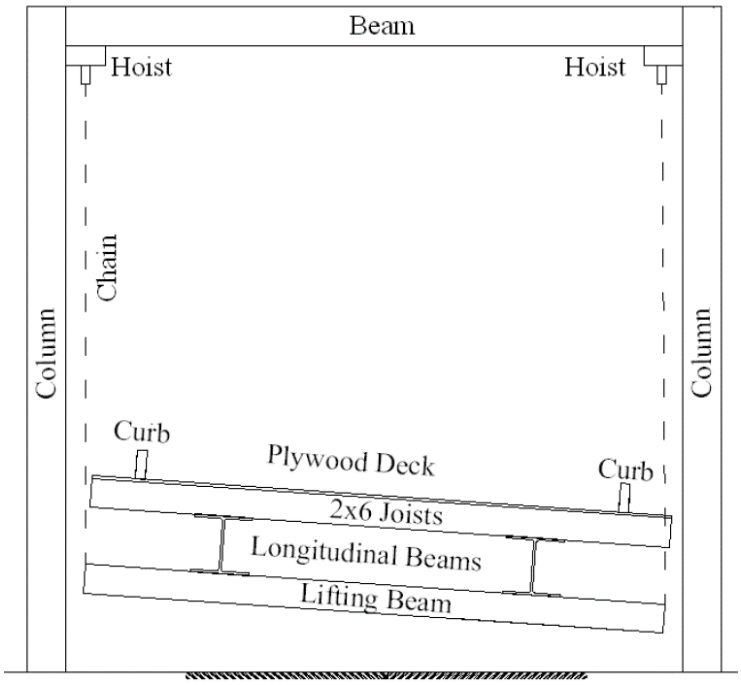


Figure 11. Upstream support cross section (Qian et al., 2013).

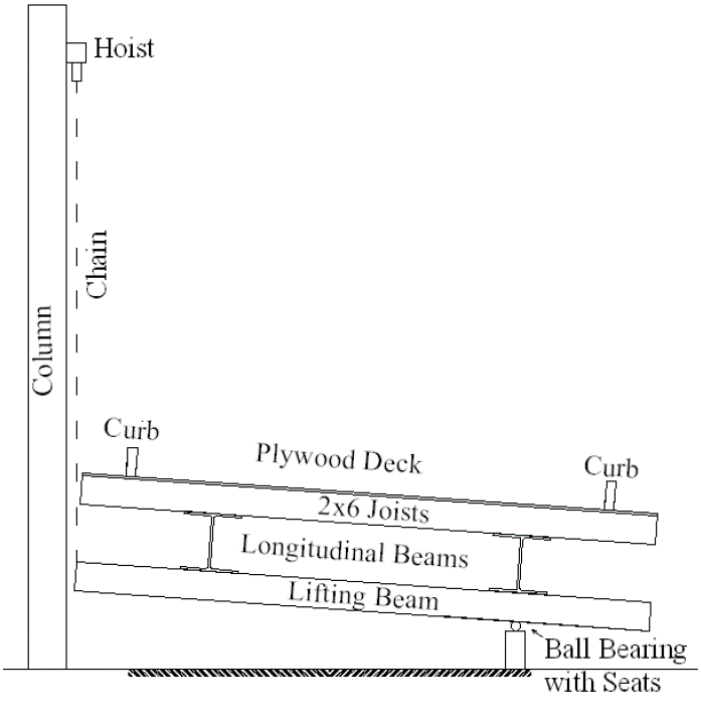


Figure 12. Downstream support cross section (Qian et al., 2013).

## 2.2 PHYSICAL MODEL MODIFICATIONS

A variety of modifications were required for the present study. Figure 13 shows the overall layout of the physical model and modifications. The TxDOT on-grade curb inlet was added to the existing physical model and depressed 3 inches beyond the normal gutter line (Figure 14). Internal slab supports were constructed to be easily installed and removed from the curb inlet opening. Curb and gutter transitions were constructed upstream and downstream of the curb inlet (Figure 15). The curb inlet and curb and gutter transitions were constructed according to TxDOT design plans (Figure 4, 5 and 16 are the curb inlet design plans and Figure 17 is the curb and gutter transition design plans). The roadway surfaces for the curb inlet and curb and gutter transitions were textured and sealed by layering epoxy sealant and graded sand. The one construction exception was the exclusion of 6 inch end walls on either side of the curb inlet opening, which are annotated in Figure 18. The 6 inch end walls do not contribute to the curb inlet opening length. This exclusion is expected to have minimal effect on the overall performance of the curb inlet[1].

Three V-notch weirs and their approach channels were also constructed to measure flow rates from each of the three curb inlet sections (Figure 19). Three flumes directed water from each curb inlet section to their respective V-notch weir approach channels. Finally, the inlet pipe was modified to a manifold with valves, and the headbox was modified to increase control of the water entering the roadway (Figure 20).

Appendix A outlines the construction and modifications in more detail and include additional design plans.

[1] The exclusion of the end walls was unintentional. Future studies are planned to check whether the effects are significant.

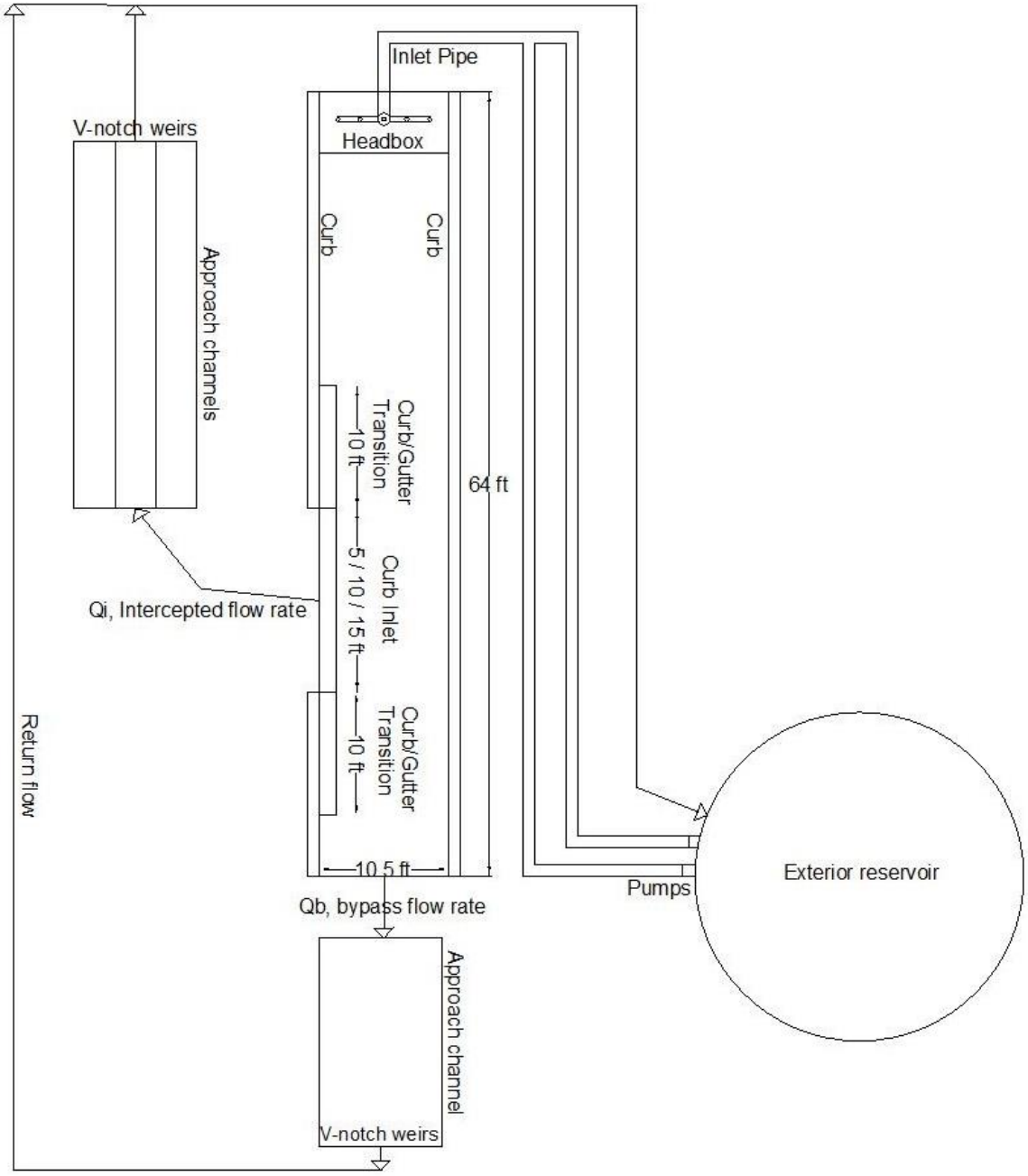


Figure 13. Definition sketch of physical model with modifications.

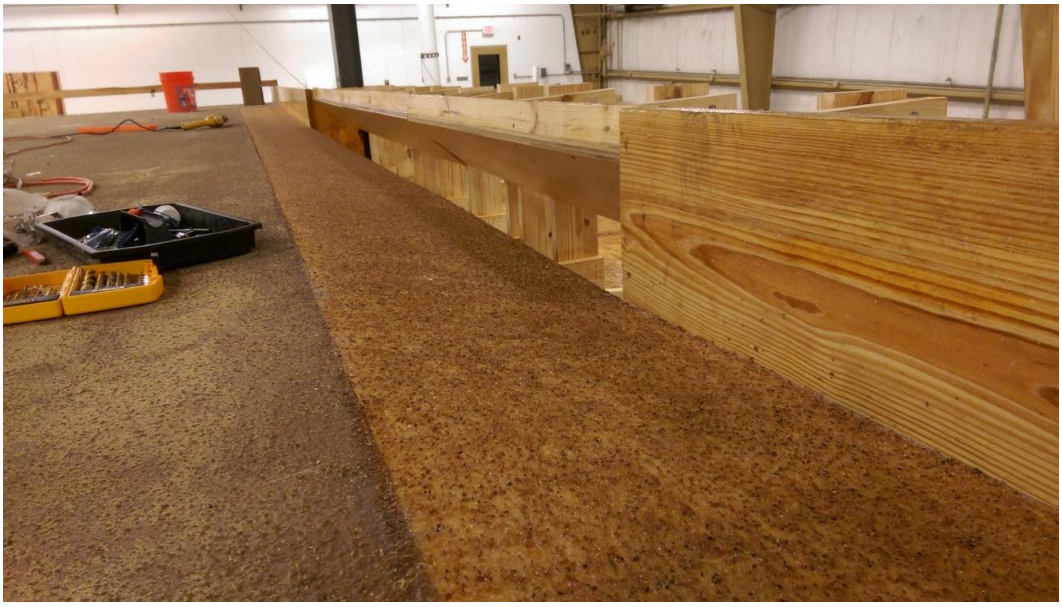

Figure 14. Fifteen foot TxDOT curb inlet without internal slab supports.

Figure 15. Upstream curb and gutter transition and TxDOT curb inlet.

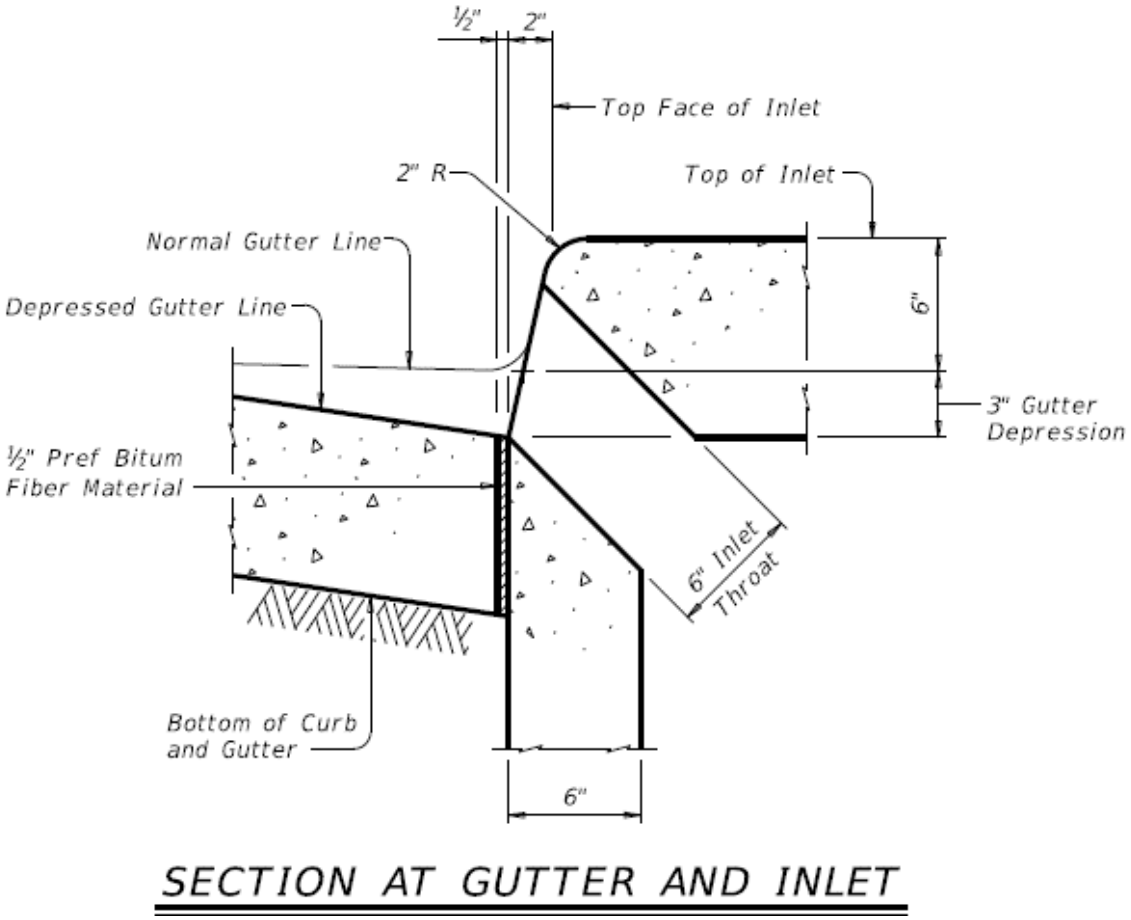


Figure 16. Profile view of TxDOT curb inlet design, extracted from TxDOT file prestd13.dgn (January 2015 revisions).

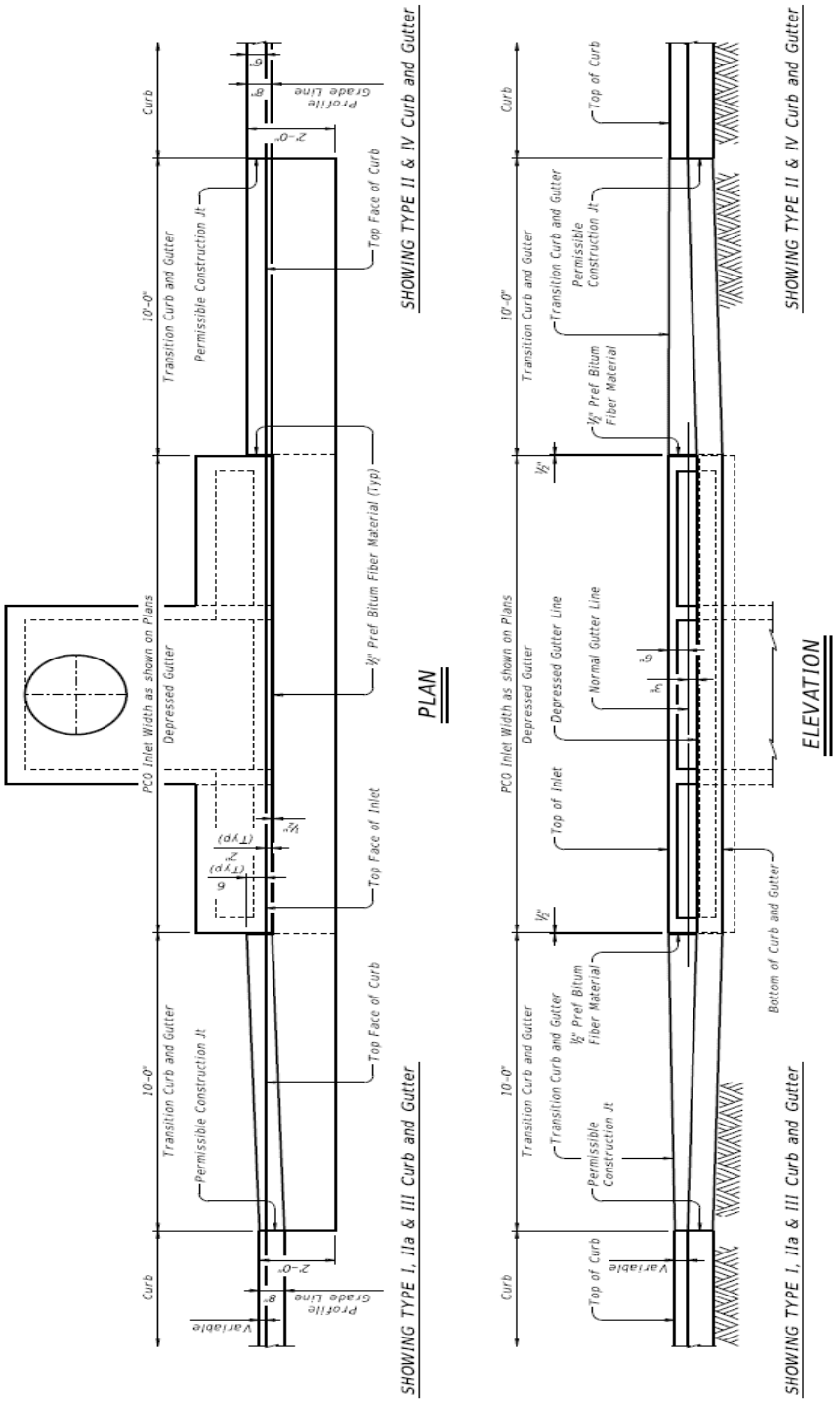


Figure 17. Front and plan view of TxDOT curb and gutter transition sections with TxDOT curb inlet, extracted from TxDOT file prestd13.dgn (January 2015 revisions).

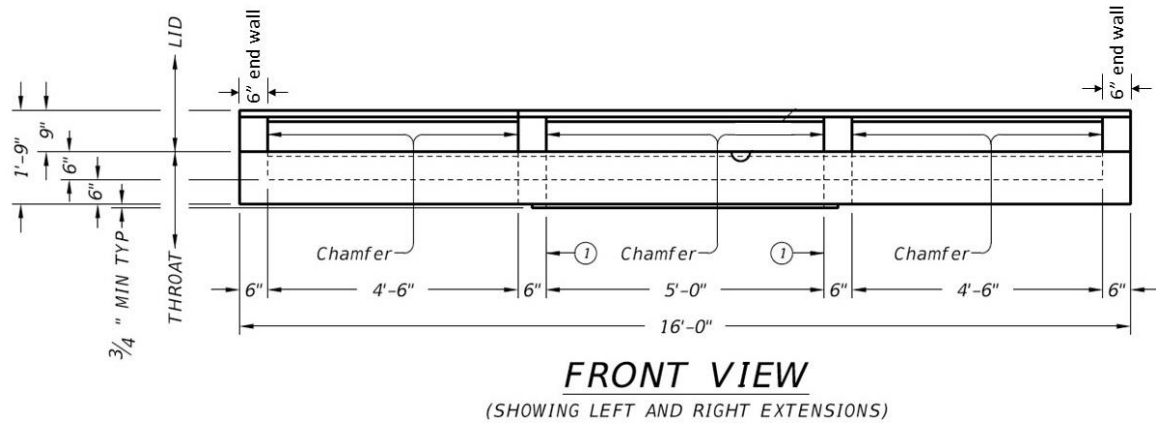


Figure 18. Front view of TxDOT curb inlet, extracted from TxDOT file presd03.dgn (January 2015 revisions), with annotated end walls.

Figure 19. V-notch weirs and approach channels.

Figure 20. Inlet pipe manifold with valves, and headbox.

### 2.3 Flow Measurement Devices and Uncertainty

For the physical model four sharp crested V-notch weir devices were required to measure flow rates. The flow rate from a V-notch weir was calculated with the following equation (Bos, 1989; ASTM Standard D5242)

$$Q = \frac{8}{15} C_e \sqrt{2g} \tan\left(\frac{\theta}{2}\right) H^{5/2} \tag{12}$$

where Q is the discharge (cfs), $C_e$ is the discharge coefficient (a factor of notch angle and contraction type), $\theta$ is the angle of the V-notch weir (degrees), and H is the head on the weir measured from the apex (ft). The three V-notch weir notch angles used were: 60, 90 and 120 degrees. The 60 degree V-notch weir was used to measure flow that bypassed the curb inlet. The 120 degree V-notch weir was used to measure flow rates when calibrating the physical model roughness (see §2.4). Three 90 degree partially-contracted V-notch weirs were used for each of the three curb inlet sections. The term partially-contracted is used when the sidewalls and bottom of the approach channel affect the contraction of the

jet of water flowing over the weir (ASTM Standard D5242). The partially-contracted 90 degree V-notch weirs were not fully contracted due to space constraints in the laboratory. Partial contraction of a 90 degree V-notch weir is an approved method and only increases discharge coefficient uncertainty 1% compared to a fully-contracted weir (ASTM Standard D5242). For a 60 degree V-notch weir $C_e = 0.577$ (Figure 5.9 from Bos, 1989; Figure 6 from ASTM Standard D5242) and eq. (12) becomes

$$Q = 1.426H^{5/2} \tag{13}$$

For a 90 degree partially contracted V-notch weir $C_e = 0.597$ (Figure 5.10 from Bos, 1989; Figure 7 from ASTM Standard D5242) and eq. (12) becomes

$$Q = 2.555H^{5/2} \tag{14}$$

For a 120 degree V-notch weir $C_e = 0.584$ (Grant and Dawson, 2001) and eq. (12) becomes

$$Q = 4.330H^{5/2} \tag{15}$$

Flow rate measurements were made with ISCO 4230 Bubbler Flow Meters. These devices measure head over a weir with two to three decimal places of accuracy for flow rates in cubic feet per second. They use eqs. (13), (14) and (15) and continuously output flow rates.

### 2.3.1 Flow Measurement Uncertainty

Measurement uncertainty is determined by adding the combined standard uncertainty (CSU) with the flow rate variability from the Bubbler Flow Meter. The variability in flow rate from the Bubbler Flow Meter is due to the natural undulation of water levels in the V-notch weir approach channel. The CSU can be expressed as follows:

$$U_{Q,Equation} = \sqrt{\left(\frac{\partial f}{\partial C_e} u_{C_e}\right)^2 + \left(\frac{\partial f}{\partial \theta} u_{\theta}\right)^2 + \left(\frac{\partial f}{\partial H} u_H\right)^2} \tag{16}$$

where $U_{Q,Equation}$ is the CSU of the V-notch weir flow rate in eq. (12). The measured quantities $C_e$, $\theta$, and H, are functions of eq. (12), which have their own respective uncertainty (e.g. $U_H$), which are listed in Table 4. The $U_{Ce}$ value was selected from ASTM Standard D5242. The $U_\theta$ value was estimated based on V-notch weir construction accuracy. The $U_H$ value was estimated from the uncertainty in defining the water level datum compared to the apex of the V-notch. The variability in flow rate outputs due to natural undulation in water levels can be expressed as follows:

$$U_{Q,Measured} = 0.005Q_{Measured} + 0.005 \quad (17)$$

where $U_{Q,Measured}$ is the uncertainty from the flow rate outputs and $Q_{Measured}$ is the flow rate output from the Bubbler Flow Meter.

Table 4. Individual uncertainty quantities in eq. (12).

| Measured Quantities | Unit of Measurement | Uncertainty |
|---|---|---|
| $C_e$ | N/A | ±0.0119 |
| $\theta$ | degree | ±0.01 |
| H | feet | ±0.00984 |

The total measured uncertainty ($U_T$) is the summation of eq. (16) and (17) and is expressed in eq. (18) for a 15-foot curb inlet and eq. (19) for a 5-ft curb inlet. The total uncertainty ranges from ±0.03 cfs at Q=0.5 cfs for a 5-foot curb inlet to ±0.23 cfs at Q=6cfs for a 15-foot curb inlet.

$$U_{T,15ft} = 0.031Q + 0.0397 \quad (18)$$

$$U_{T,5ft} = 0.0256Q + 0.0216 \quad (19)$$

### 2.3.2 Flow Measurement Verification

A sharp crested rectangular weir without end contractions was used to verify V-notch weir flow measurements. By using the rectangular weir, which was downstream of

all V-notch weirs, it is possible to compare the cumulative flow rate of all four V-notch weirs to the rectangular weir.

A sharp crested rectangular weir flow rate is calculated with the following equation (Grant and Dawson, 2001):

$$Q = 3.330LH^{3/2} \tag{20}$$

where Q is the discharge (cfs), L is the length of the weir (ft), and H is the head on the weir measured from the top of the weir (ft). With the weir length of 5 feet eq. (20) becomes

$$Q = 16.65H^{3/2} \tag{21}$$

The flow rate was calculated by measuring and averaging H from both sides of the channel and using eq. (21). A range of flow rates from 1 cfs to 6 cfs were measured for the rectangular weir and all V-notch weirs. Figure 21 provides a comparison of flow rates for the V-notch weirs and rectangular weir. The root mean square difference (RMSD) between the V-notch weirs and rectangular weir was 0.36 cfs. The alignment between the V-notch weirs and rectangular weir shows that the V-notch weir flow measurement devices are reasonable and eqs. (13) - (15) are appropriate.

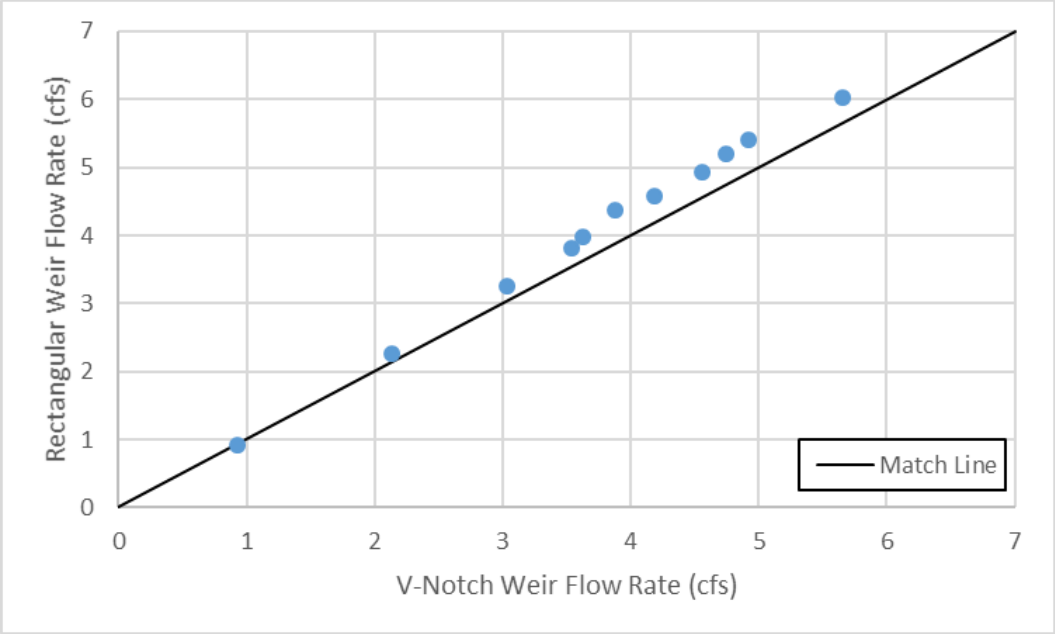


Figure 21. Comparison of flow rates measured by all V-notch weirs and rectangular weir.

## 2.4 Physical Model Roughness Calibration

The physical model's roughness is determined before any experimental data can be collected. Qian et al. (2013) previously calculated a Manning's roughness coefficient (or Manning's n) for the same road surface being used in this study and this study's data are compared to it.

Manning's n is an empirically-derived coefficient to measure surface roughness. HEC-22 uses Manning's n for gutter flow on a road and is commonly expressed as follows (HEC-22; TxDOT, 2014):

$$Q = \frac{K_u}{n} S_x^{5/3} S_L^{1/2} T^{8/3} \quad (22)$$

where:

$K_u$ = 0.56 in English units

n = Manning's roughness coefficient

Q = Flow rate (cfs)

T = Ponded width, (ft)

$S_x$ = Cross slope (ft/ft)

$S_L$ = Longitudinal slope (ft/ft)

To solve for Manning's n, eq. (22) can be rearranged as follows:

$$n = \frac{K_u}{Q} S_x^{5/3} S_L^{1/2} T^{8/3} \quad (23)$$

Equation (23) is used to solve for Manning's n with given road geometries ($S_L$, $S_x$), a measured flow rate (Q), and a measured ponded width (T).

Table 5 shows the values of Manning's n over three longitudinal slopes and an average of all longitudinal slopes. Each longitudinal slope's Manning's n is an average of all three cross slopes (2%, 4%, 6%) for a low and high flow rate condition.

Table 5. Comparison between measured average Manning's n and Qian et al. (2013) average Manning's n.

| **$S_L$ (%)** | **Measured Manning's n** | **Manning's n (Qian et al., 2013)** |
|---|---|---|
| 0.5 | 0.0169 | 0.0166 |
| 1.0 | 0.0152 | 0.0167 |
| 2.0 | 0.0165 | 0.0166 |
| Average | 0.0162 | 0.0166 |

The average Manning's n is 0.0162, a 2.67% difference from the Qian et al. (2013) value of 0.0166. The alignment of data with Qian et al. (2013) is evidence that the road surface roughness has not changed and that using the reported Manning's roughness coefficient of 0.0166 from Qian et al. (2013) for this study is appropriate.

### 2.5 Experimental Procedure for Data Collection

The physical model was tested by varying the following for every possible combination: longitudinal slope, cross slope, inlet configuration, and flow rate conditions. Table 6 provides all the configuration values tested. The inlet configurations included

varying the number of 5-foot curb inlet sections (1 or 3 for a 5 ft or 15 ft curb inlet, respectively) and varying the number of slab supports (0 or 2 for a 5 ft or 15 ft curb inlet, respectively). Two flow rate conditions were measured: 100% gutter flow rate interception by the curb inlet (100% interception), and gutter bypass condition (or bypass) where less than 100% of the gutter flow rate was intercepted by the curb inlet.

Table 6. Physical model test configurations.

| | **Tested** |
|---|---|
| Longitudinal slope (%) | 0.1, 0.5, 1.0, 2.0, 4.0 |
| Cross Slope (%) | 2.0, 4.0, 6.0 |
| Inlet Configuration (# of 5 ft sections / # internal slab supports) | 1/0; 3/2; 3/0 |
| Flow Rate Condition | 100% interception; bypass |

A single flow rate was determined for 100% interception by first slowly increasing the flow rate until bypass flow was noticed. At this point the flow rate was slowly decreased until only a small trickle of bypass flow was occurring. This instance was considered 100% interception.

Multiple bypass flow rates were collected and normally ranged from 0.1 to 0.5 cfs. A bypass flow rate of up to 0.5 cfs is allowed by TxDOT and was selected as the upper limit. Bypass flow was achieved by slowly increasing the flow rate until bypass flow occurs then incrementally increasing the flow rate to obtain the desired bypass flow rate. The range of bypass flow achieved was a function of the pump capacity and physical model limitations (i.e. ponded width limit and water depth at curb limit).

Before data were collected the conditions listed in Table 7 were met. Once conditions in Table 7 were met the following data were collected: flow rate(s), water spread, and water depth. Flow rate measurements were taken from each V-notch weir and repeated after an approximate 5-minute wait. This wait was to confirm the flow rate had

not changed. If the flow rate had changed another 5-minute wait occurred until a steady flow rate had occurred. Water spread measurements were collected every 2 ft along the roadway, starting 18 ft upstream of the beginning of the curb inlet opening and continued until 5 ft downstream of the end of the curb inlet opening. Measurements were taken perpendicular to the curb from the curb edge to the edge of the water surface on the roadway. Water depth was measured at 3 locations upstream of the gutter depression transitions, which corresponded to water spread measurement locations.

Table 7. Conditions before for data collection occurred.

| **Conditions** |
|---|
| Longitudinal and cross slope set |
| Inlet length set |
| Internal slab supports installed/removed |
| Pump(s) turned on |
| Manifold values and headbox opened |
| Selected flow rate condition met (i.e. 100% interception, bypass) by adjusting manifold values and headbox opening |

### 2.6 Experimental Repeatability

Ten tests were performed to study the model's experimental repeatability and to determine if headbox configurations affect physical model data results. Each test was performed for a 15 ft curb inlet at an identical road geometry and flow rate condition (i.e. $S_L$=2%, $S_x$=4%, 100% interception). For each new test the manifold valves were turned fully off and the headbox configuration was changed by adjusting the concrete blocks and the length of the headbox opening.

From the ten tests performed two ponded-width profiles were observed. Figure 22 shows the two profiles, which are each an average of 5 tests. The profile named *Normal Opening* was from a headbox opening that produced the most consistent ponded width upstream of the curb inlet. The profile named *Constricted Opening* was a small headbox opening, which produced a step-like profile upstream of the curb inlet. The *Constricted Opening* was never used in data collection but was a possible configuration. Even with the *Constricted Opening* the ponded width converged with the *Normal Operation* before the end of the curb inlet.

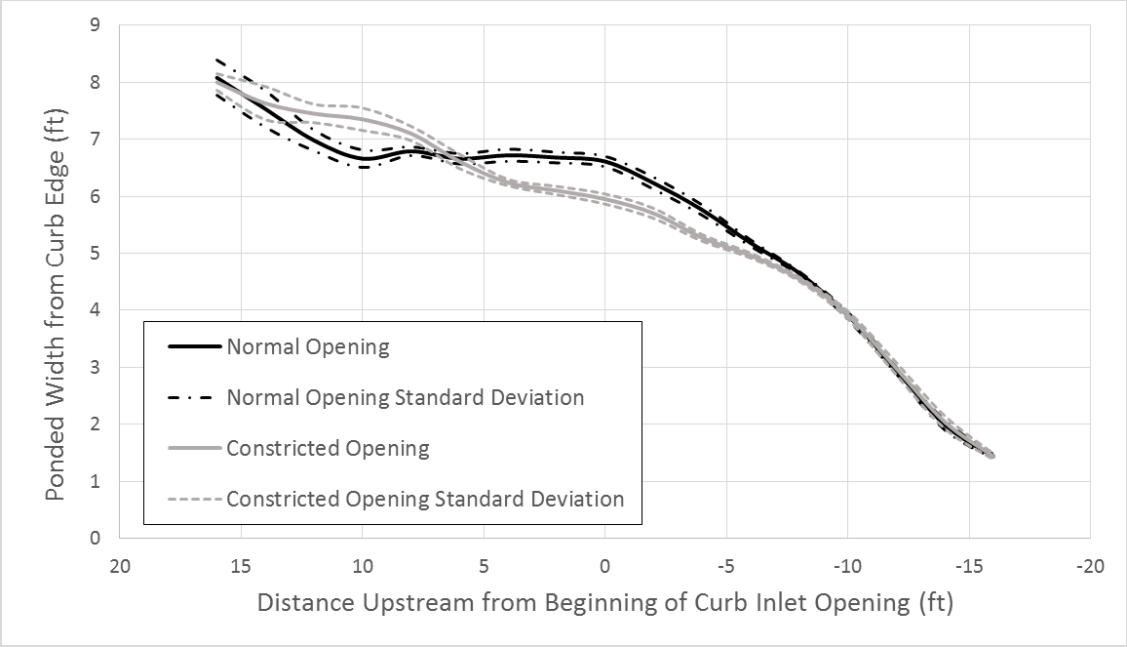


Figure 22. Repeatability test's ponded width profiles at 100% curb inlet interception, 15 ft inlet length and $S_L$=2%, $S_X$=4%.

The ten flow rates measured for each test are listed in Table 8. The flow rates have a standard deviation of 0.07 cfs and are within the measurement uncertainty (see §2.3). From these data it can be concluded that upstream conditions have no measureable effect

on intercepted flow rates. Additionally, if the headbox conditions are reasonably controlled ponded widths can be accurately measured.

Table 8. Repeatability test flow rates, 100% interception condition, 15 ft inlet length and $S_L$=2%, $S_X$=4%.

| Test | Intercepted Flow Rate (cfs) | Condition |
|---|---|---|
| 1 | 2.88 | Normal operation |
| 2 | 2.93 | Constricted opening |
| 3 | 2.93 | Constricted opening |
| 4 | 3.03 | Normal operation |
| 5 | 3.09 | Normal operation |
| 6 | 2.98 | Constricted opening |
| 7 | 2.98 | Constricted opening |
| 8 | 3.03 | Constricted opening |
| 9 | 3.06 | Normal operation |
| 10 | 3.03 | Normal operation |
| Mean | 2.99 | -- |
| Standard Deviation | 0.07 | -- |

# CHAPTER 3: DATA AND ANALYSIS

## 3.1 INTRODUCTION

In this chapter analysis is presented on three topics: the effects (if any) of slab supports on a curb inlet's hydraulic performance, how the physical model data compares to HEC-22 design equations, and how the physical model data compares to other design equations. Data presented in this chapter are provided in Appendix B.

## 3.2 SLAB SUPPORT ANALYSIS

Figure 23 compares flow rates for a 15 ft TxDOT curb inlet with and without slab supports. Each data point represents a slope combination (i.e. longitudinal and cross slope) for both flow rate conditions (i.e. 100% interception, bypass). The root mean square different (RMSD) is 0.08 cfs, which is within the measurement uncertainty (see §2.3). For a 15 ft curb inlet no significant flow interception differences exist between curb inlets with or without slab supports.

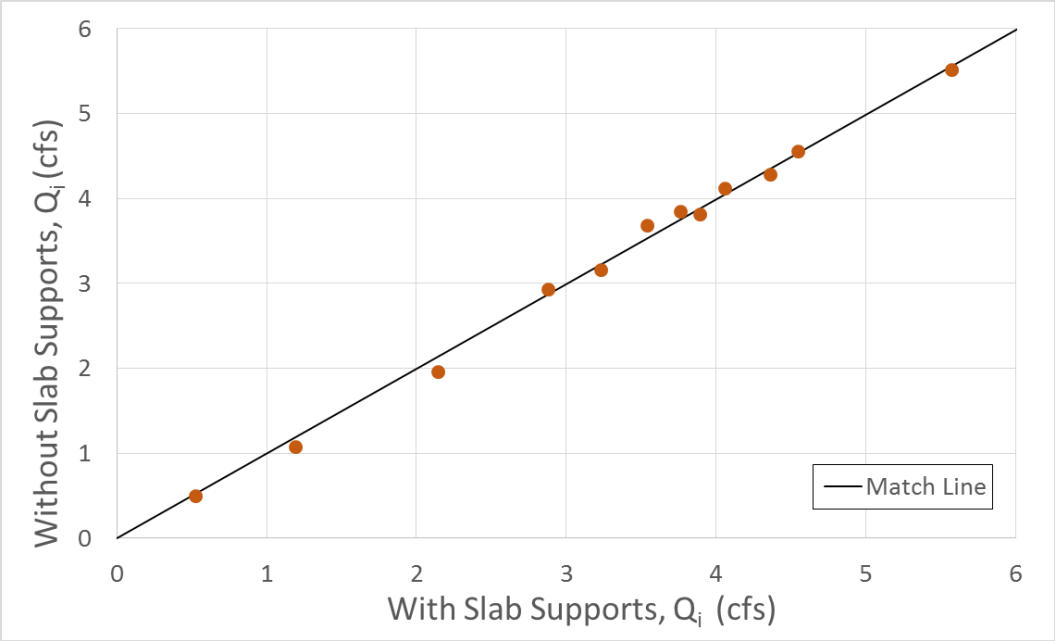


Figure 23. Comparison of intercepted flow rates for the 15 ft TxDOT curb inlet with and without slab supports. Performed at 100% interception and bypass conditions over a variety of $S_L$ and $S_X$.

Figure 24 shows that ponded widths are closely aligned for a 15 ft TxDOT curb inlet with and without slab supports. It shows no evidence that slab supports affect ponded widths.

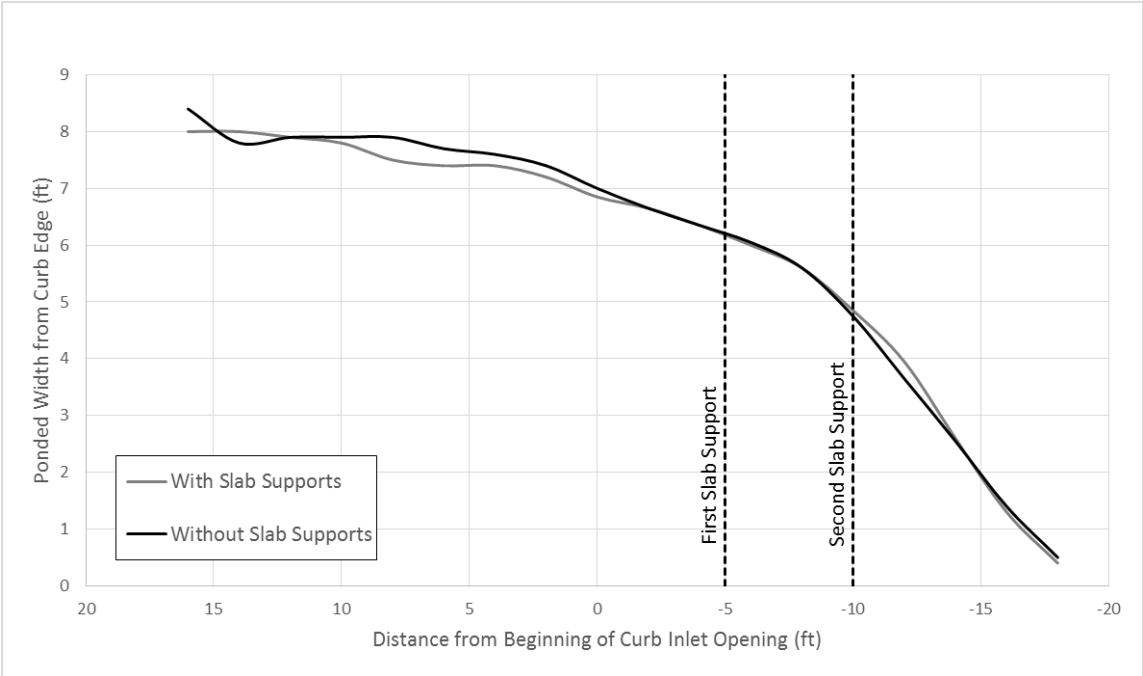


Figure 24. Comparison of ponded widths for a 15 ft TxDOT curb inlet with and without slab supports for $S_L$=1%, $S_X$=6% at 100% interception condition (Test # 24 and 59, Appendix B).

The waves generated at slab supports are shown in Figure 25 and 26. There are waves on both the upstream and downstream side of each internal slab support. These waves extend a maximum of 2 feet on either side of the slab support. Because the intercepted flow rates with and without slab supports are similar (see Figure 23 above), we surmise that the slab supports affect the interception in such a way that their blocking effects are counterbalanced by locally-increased flow into the outlet.

Figure 25. Photo of waves before and after an internal slab support for a 15 ft curb inlet at $S_L$=1%, $S_X$=6%, bypass condition (Test #60, Appendix B).

Figure 26. Photo of waves around both internal slab supports for a 15 ft curb inlet at $S_L$=1%, $S_X$=6%, bypass condition (Test #60, Appendix B).

### 3.3 HEC-22 & PHYSICAL MODEL ANALYSIS

This section provides analyses of the physical model data and HEC-22 design equations. A Matlab script (provided in Appendix B) was written to compute HEC-22 results at similar road geometry configurations as the physical model data. Additionally, Hydraulic Toolbox (Federal Highway Administration, 2015) was used to confirm the accuracy of the Matlab script.

Comparisons of the physical model and HEC-22 are shown in Figure 27 and 28 for a 15 ft TxDOT curb inlet. HEC-22 over-predicts intercepted flow rates by an average factor of 2.3:1 when compared to the physical model. The RMSD between the physical model and HEC-22 is 4.2 cfs. Over-prediction is higher for low cross and longitudinal slopes (e.g. $S_X$=2% and $S_L$=2%), which can be seen in Figure 28.

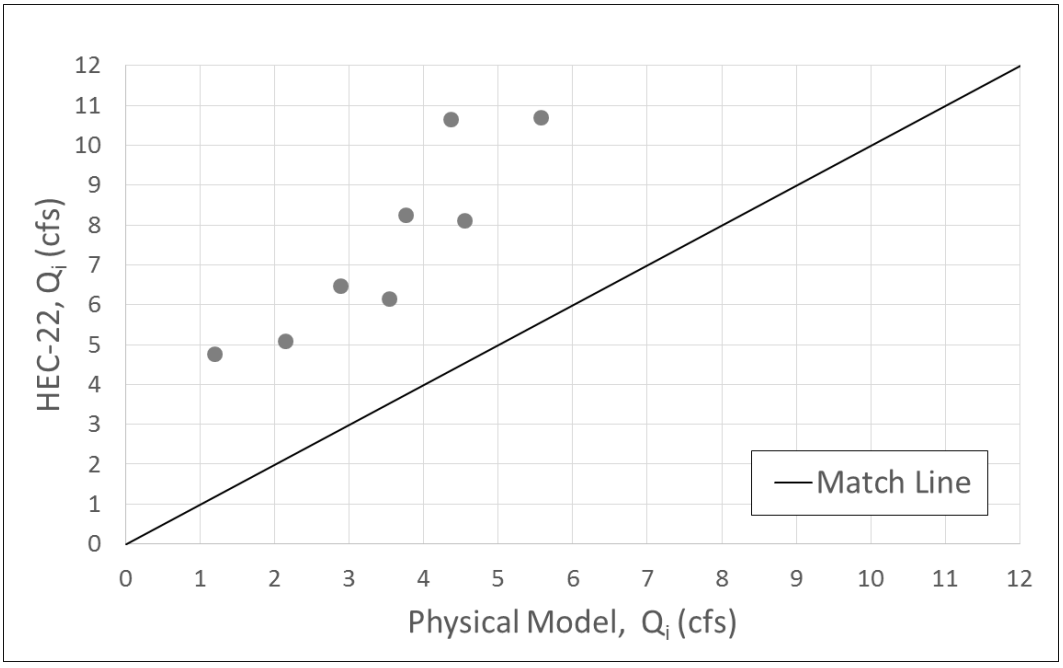


Figure 27. Comparison between physical model and HEC-22 for a 15 ft TxDOT curb inlet at 100% interception condition.

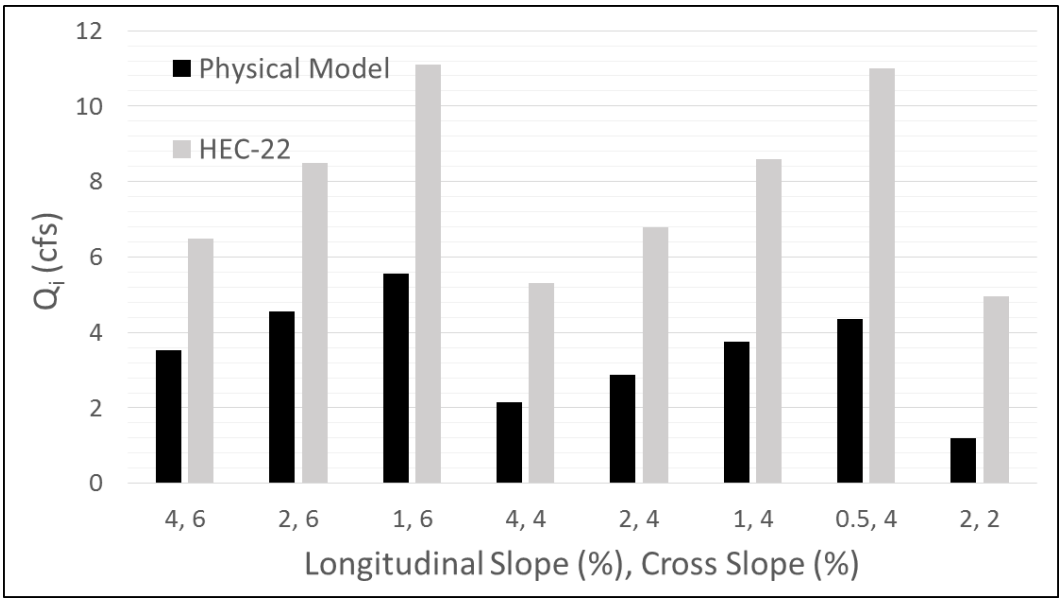


Figure 28. Comparison between physical model and HEC-22 for a 15 ft TxDOT curb inlet at 100% interception condition by individual slope combinations.

Comparisons of the physical model and HEC-22 for a 5 ft TxDOT curb inlet are shown in Figure 29 and 30. In Figure 29 the two HEC-22 points that deviate significantly from the match line are for extremely small longitudinal slopes ($S_L$) of 0.1%. Without considering $S_L$=0.1% data the RMSD is 0.33 cfs; when considering $S_L$=0.1% data the RMSD is 0.73 cfs. Figure 30 shows the comparison of physical model data with HEC-22 according to longitudinal and cross slope and distinguishes the $S_L$=0.1% data differences observed in Figure 29.

With a constant cross slope the intercepted flow rates predicted by HEC-22 increase significantly with decreasing longitudinal slopes, as seen in Figure 30. When comparing that to 4 and 6% cross slopes in the physical model there are no significant differences in intercepted flow rates observed within 2, 1, 0.5 and 0.1% longitudinal slopes.

In general there is alignment of data between HEC-22 and the 5 ft curb inlet physical model except for longitudinal slopes of 0.1%. The significant difference between the physical model and HEC-22 at a longitudinal slope of 0.1% is not yet understood.

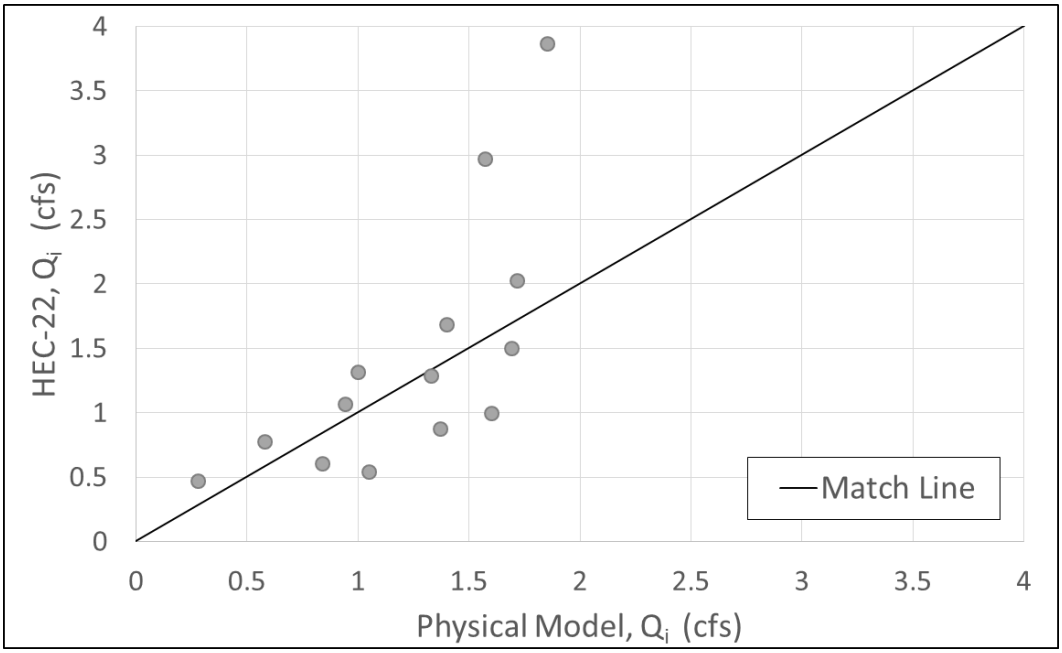


Figure 29. Comparison between the physical model and HEC-22 for a 5 ft TxDOT curb inlet at 100% interception condition.

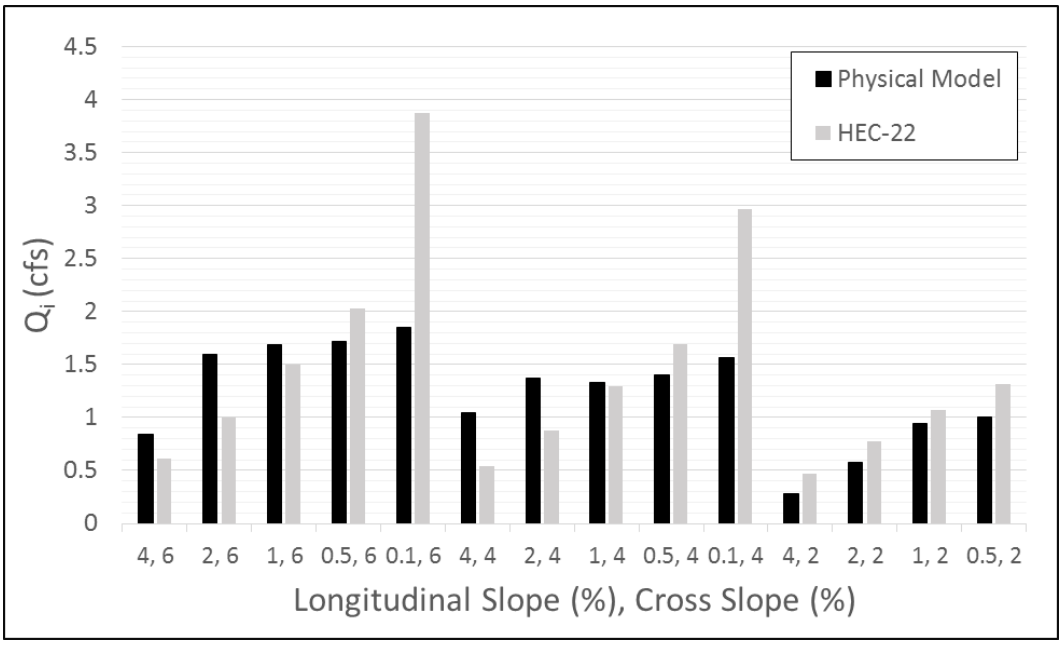


Figure 30. Comparison between physical model and HEC-22 for a 5 ft TxDOT curb inlet at 100% interception condition for individual slope combinations.

### 3.4 Design Equations & Physical Model Analysis

This section provides analysis of the design equations discussed in §1.5 and the physical model data. A Matlab script was written to compute different design equation results at similar road geometry configurations as the physical model data.

Figure 31 and 32 compare the physical model data with the three design equations for a 15 ft TxDOT curb inlet. All three design equations over-predict the physical model data and none reasonably align. In Figure 32, the Comport and Thorton (2012) approach is shown to predict a decrease in intercepted flow rates with decreasing longitudinal slopes. This negative trend is in opposition to other design equations and the physical model data. Table 9 provides RMSD between the physical model and the design equations.

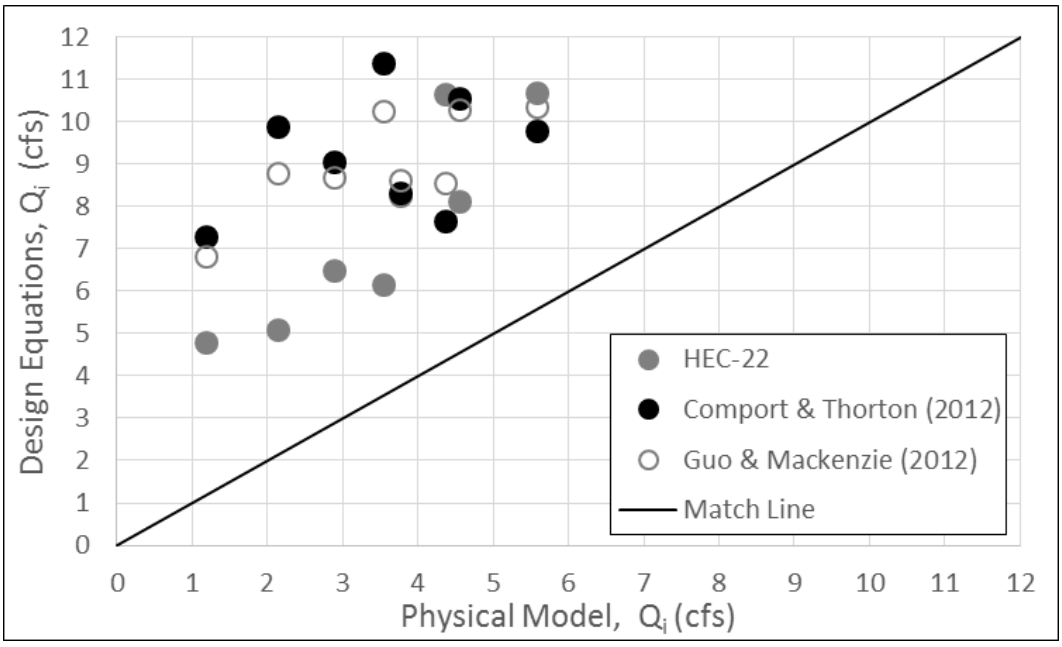


Figure 31. Comparison between the physical model and design equations for a 15 ft TxDOT curb inlet at 100% interception condition.

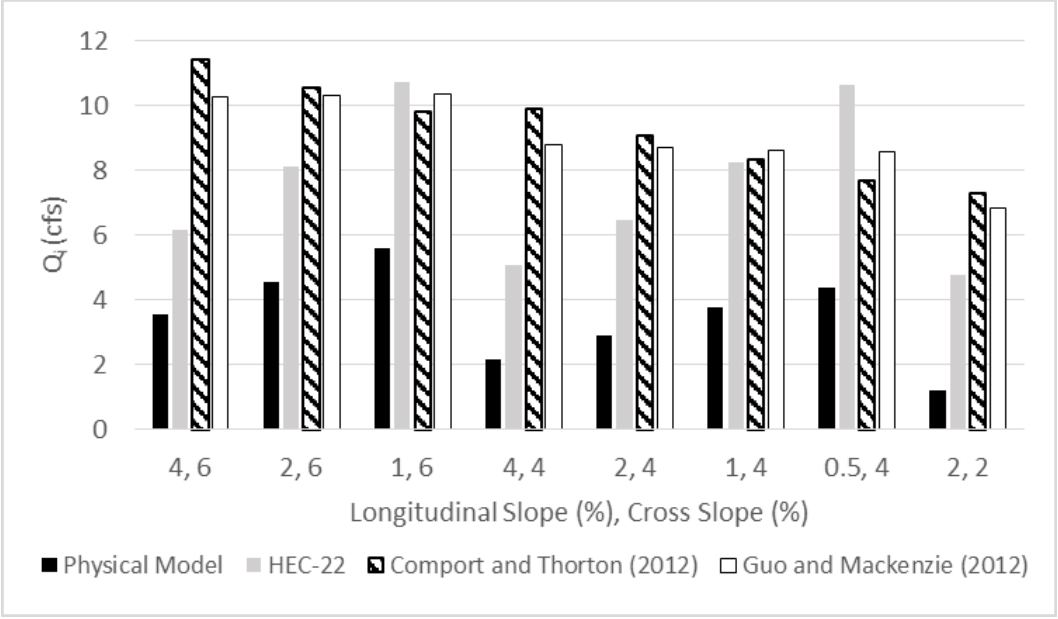


Figure 32. Comparison between physical model and design equations for a 15 ft TxDOT curb inlet at 100% interception condition for individual slope combinations.

Table 9. Root Mean Square Difference between design equations and the physical model for a 15 ft TxDOT curb inlet.

| **Design Equation** | **RMSD (cfs)** |
|---|---|
| HEC-22 | 4.19 |
| Comport and Thorton (2012) | 5.95 |
| Guo and MacKenzie (2012) | 5.62 |

Figure 33 and 34 compare the physical model data with the three design equations for a 5 ft TxDOT curb inlet. The reversed longitudinal slope trend in Comport and Thorton (2012) that was noted for the 15 ft curb inlet occurs here as well. A combination of Guo and MacKenzie (2012) and HEC-22 align best with the physical model, yet neither align with every slope combination that was tested. Table 10 lists RMSD between the physical model and the design equations. Section 3.5 provides design equation recommendations according to longitudinal and cross slope combinations.

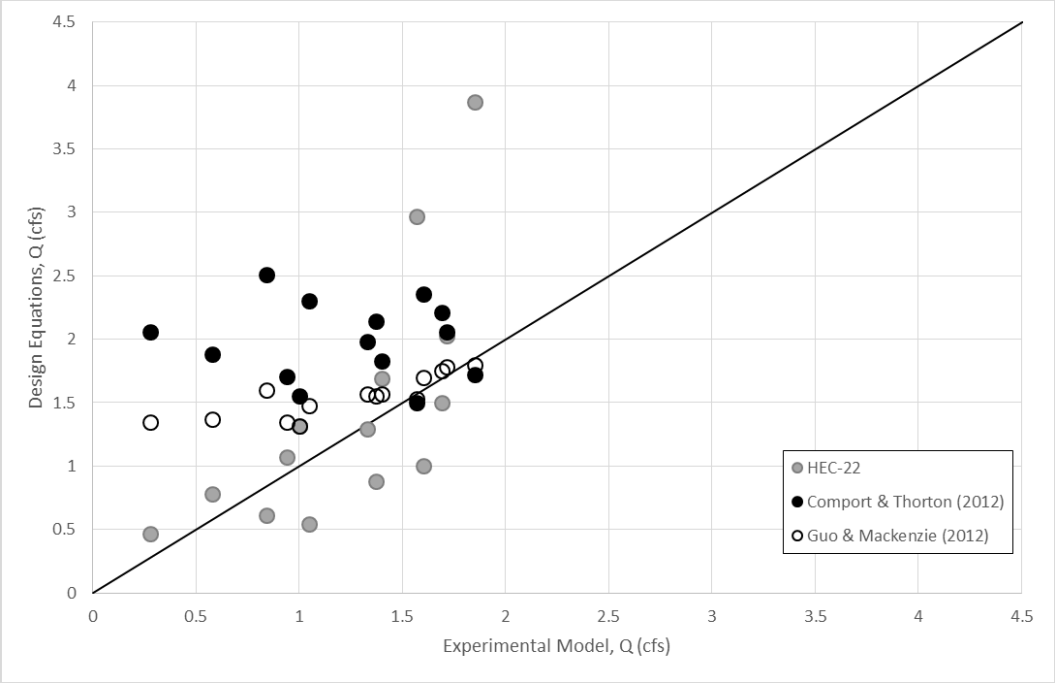


Figure 33. Comparison between physical model and design equations for a 5 ft TxDOT curb inlet at 100% interception condition.

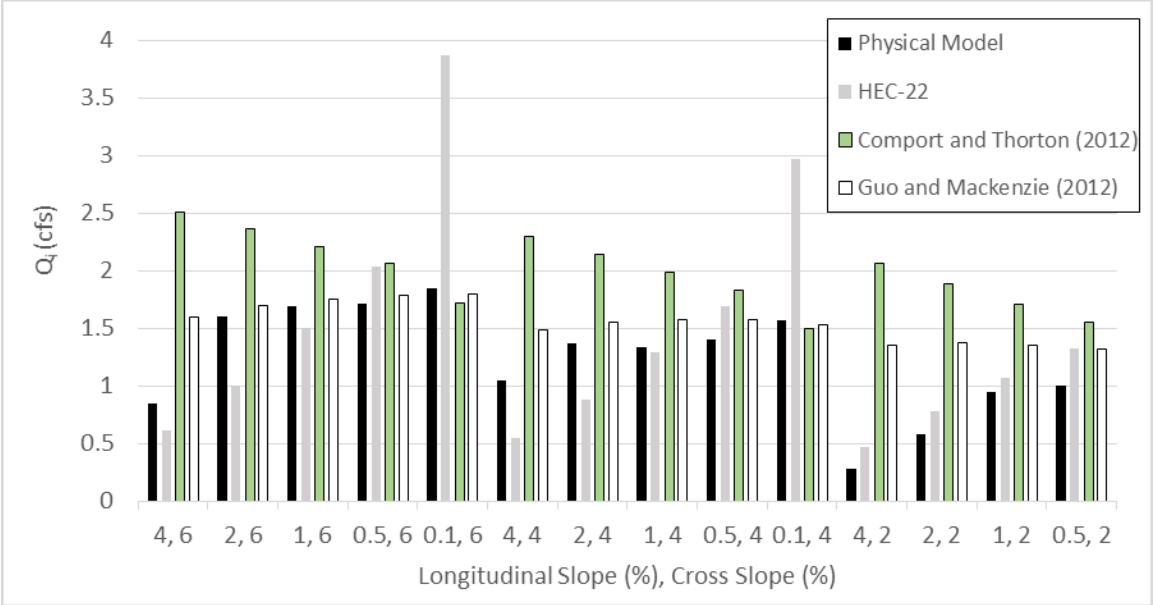


Figure 34. Comparison between physical model and design equations for a 5 ft TxDOT curb inlet at 100% interception condition for individual slope combinations.

Table 10. Root Mean Square Difference between design equations and the physical model for a 5 ft TxDOT curb inlet.

| Design Equation | RMSD (cfs) |
|---|---|
| HEC-22 | 0.73 |
| HEC-22 (without $S_L$=0.1%) | 0.33 |
| Comport and Thorton (2012) | 0.94 |
| Guo and MacKenzie (2012) | 0.46 |

### 3.5 Design Equation Recommendations

For a 5 ft TxDOT curb inlet the recommended design equations that best predict the physical model data under each slope combination are listed in Table 11. The recommended design equations were selected based on minimum RMSD.

Table 11. Recommended design equation according to cross and longitudinal slopes for a 5 ft TxDOT curb inlet.

| Cross Slope (%) | Longitudinal Slope (%) | Recommended Design Equation | RMSD (cfs) |
|---|---|---|---|
| 2 | 4, 2, 1, 0.5 | HEC-22 | 0.22 |
| 4 | 4, 2, 0.5, 0.1 | Guo and MacKenzie (2012) | 0.25 |
| 4 | 1 | HEC-22 | 0.04 |
| 6 | 2, 1, 0.5, 0.1 | Guo and MacKenzie (2012) | 0.07 |
| 6 | 4 | HEC-22 | 0.23 |

None of the present design equations appear to be appropriate for a 15 ft TxDOT curb inlet. A discussion of possible reasons for the divergence between design equations and the physical model from the 5 ft to 15 ft TxDOT curb inlet is presented in the following chapter.

# CHAPTER 4: DISCUSSION AND CONCLUSIONS

## 4.1 DISCUSSION

The design equations for HEC-22 and Guo and MacKenzie (2012) align with physical model data for the 5 ft TxDOT curb inlet but over-predict curb inlet hydraulic performance for the 15 ft TxDOT curb inlet, as shown in Figure 31 and 32. This section discusses possible reasons for this divergence.

One possible explanation is the effect of geometric scaling. Previous studies (Table 2) have been conducted on geometrically-scaled physical models. Geometric scaling of the experiments is accompanied with Froude number scaling of the flow, which requires the assumption that Reynolds number (Re) effects are invariant over a wide range of scales. The Re effects can change significantly at thin water depths, where the boundary layer affects fluid dynamics. Thin water depths have been observed for the 15 ft TxDOT curb inlet model at the curb inlet opening and on the road surface beyond the curb inlet opening (Figure 35). Although thin water depths have been observed for the 5 ft TxDOT curb inlet they only occur at the apex of the cross-section triangle (the edge of the ponded width). This is in contrast to the 15 ft TxDOT curb inlet which in certain conditions, as shown in Figure 35, has thin flow throughout much of the cross-section triangle. To properly account for varying Re effects that could be caused by thin water depths a full-scale model must be used. Both Comport and Thorton (2012) and Guo and MacKenzie (2012) used geometric scaling to develop equation recommendations. It is unknown if geometric scaling was used in the experiments from which HEC-22 equations were derived.

Figure 35. Thin water depth observations on the road surface and gutter section during a 100% interception test for a 15 ft TxDOT curb inlet at $S_L$=2%, $S_X$=2% (Test #57, Appendix B).

Izzard (1950) contributed significantly to the theoretical basis for HEC-22 curb inlet design equations. One assumption made by Izzard (1950) was a linearly decreasing water surface profile along the curb inlet's opening. Figure 36 shows the water surface profile for the 15 ft TxDOT curb inlet compared to a linearly decreasing water surface profile assumed by HEC-22. The TxDOT curb inlet's linearly decreasing water profile ends after only 3 ft of the curb inlet opening. For the remaining length of the curb inlet opening the TxDOT curb inlet has thin water depths. At these thin water depths Re effects can change significantly and may alter the fluid dynamics and assumptions initially made in HEC-22.

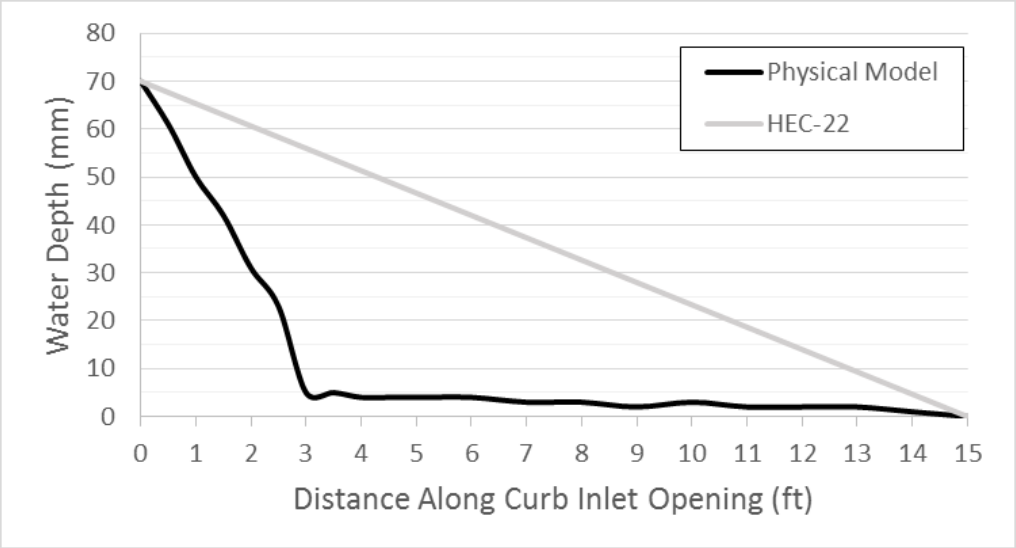


Figure 36. Water surface profile along the length of the curb inlet opening. $S_L$=2%, $S_x$=2%, 100% interception condition.

### 4.2 FINDINGS

The slab support analysis in §3.1 supports the conclusion that no measureable curb inlet interception differences exists between a 15 ft TxDOT curb inlet with or without internal flush slab supports. Slab supports for a 15 ft TxDOT curb inlet have local effects (standing waves) that can reach up to 2 feet both upstream and downstream of the slab supports. These local effects do not influence the ponded width or flow rates at 100% interception. It follows that the correct design approach is Case 2 in §1.6, where slab supports are simply ignored and the inlet length is taken as the distance from the upstream to the downstream ends of the curb opening.

For a 5 ft TxDOT curb inlet a combination of Guo and MacKenzie (2012) and HEC-22 align best with the physical model, yet neither align with every slope combination.

For a 15 ft TxDOT curb inlet none of the present design equations appear to be appropriate as all significantly over-predict the physical model's intercepted flow rates.

## 4.3 FUTURE WORK

There is a need to further investigate the complex fluid dynamics occurring at 15 ft curb inlet lengths as they are not clearly understood. Additionally, an alternative design equation is needed to accurately predict a curb inlet's interception capacities at 15 ft curb inlet lengths.

# Appendix A

## CURB INLET DESIGN EQUATIONS: DERIVATION OF CASE 1, 2 AND 3

For the Case 1 approach, the overall inlet efficiency is evaluated using the sum of the inlet lengths, so that

$$L_c = L_{c1} + L_{c2} + L_{c3} \tag{24}$$

$$E = 1 - \left( 1 - \frac{L_{c1} + L_{c2} + L_{c3}}{K_u \, Q_g^{0.42} \, S_L^{0.3} \left( \frac{1}{n \, S_e} \right)^{0.6}} \right)^{1.8} \tag{25}$$

where the $L_{c1}$, $L_{c2}$ and $L_{c3}$ are the lengths of the three curb inlet openings. This does not include the lengths of any flush slab supports and $L_c$ will be shorter than the total inlet length from beginning to end of inlet.

The Case 2 approach preserves total inlet length, which includes the length of the interior flush slab supports, so that

$$L_c = L_{c1} + L_{s1} + L_{c2} + L_{s2} + L_{c3} \tag{26}$$

$$E = 1 - \left( 1 - \frac{L_{c1} + L_{s1} + L_{c2} + L_{s2} + L_{c3}}{K_u \, Q_g^{0.42} \, S_L^{0.3} \left( \frac{1}{n \, S_e} \right)^{0.6}} \right)^{1.8} \tag{27}$$

where $L_{s1}$ and $L_{s2}$ are the lengths of the two (or one) flush slab supports within the inlet structures.

For the Case 3 approach, each inlet has its own efficiency, $E_1$, $E_2$ and $E_3$, associated with their respective inflows. The total gutter flow ($Q_g$) is the inflow to the first (upstream) inlet and $Q_{g2}$ and $Q_{g3}$ are the gutter inflows to the second and third inlets respectively, which requires

$$Q_{g2} = Q_g \left( 1 - E_1 \right) \tag{28}$$

and

$$Q_{g3} = Q_{g2}\left(1-E_2\right) = Q_g\left(1-E_1\right)\left(1-E_2\right) \tag{29}$$

The total bypass is what remains after the last inlet, which is

$$Q_b = Q_{g3}\left(1-E_3\right) \tag{30}$$

so that substituting eq. (29) provides

$$Q_b = Q_g\left(1-E_1\right)\left(1-E_2\right)\left(1-E_3\right) \tag{31}$$

The overall efficiency of a three-inlet set for Case 3 is then

$$\begin{aligned} E &= \frac{Q_g - Q_b}{Q_g} \\ &= \frac{Q_g - Q_g\left(1-E_1\right)\left(1-E_2\right)\left(1-E_3\right)}{Q_g} \\ &= 1-\left(1-E_1\right)\left(1-E_2\right)\left(1-E_3\right) \end{aligned} \tag{32}$$

If we use the HEC-22 approach for the individual inlets in Case 3, an individual inlet would have an efficiency estimated using the individual inlet length and the individual gutter flow rates $Q_g$, $Q_{g2}$ and $Q_{g3}$, which leads to

$$E_1 = 1-\left(1-\frac{L_{c1}}{K_u Q_g^{0.42} S_L^{0.3}\left(\frac{1}{nS_{e1}}\right)^{0.6}}\right)^{1.8} \tag{33}$$

$$E_2 = 1-\left(1-\frac{L_{c2}}{K_u\left(Q_g\left[1-E_1\right]\right)^{0.42} S_L^{0.3}\left(\frac{1}{nS_{e2}}\right)^{0.6}}\right)^{1.8} \tag{34}$$

$$E_3 = 1-\left(1-\frac{L_{c3}}{K_u\left(Q_g\left[1-E_1\right]\left[1-E_2\right]\right)^{0.42} S_L^{0.3}\left(\frac{1}{nS_{e3}}\right)^{0.6}}\right)^{1.8} \tag{35}$$

where eqs. (28) and (29) are used to provide the flow rate in terms of $Q_g$. Note that eqs. (34) and (35) require recursive substitution of eqs. (33) and (34) to remove $E_1$ and $E_2$ from the denominator. Additionally, the equivalent cross slope $S_e$ is unique for each inlet length

as it depends on $E_o$, the ratio of flow in the depressed section to the total gutter flow. To get an equation for the overall efficiency for Case 3, we substitute eqs. (33) - (35) into (32)

$$E = \left(1 - \frac{L_{c1}}{K_u Q_g^{0.42} S_L^{0.3} \left(\frac{1}{nS_{e1}}\right)^{0.6}}\right)^{1.8} \times \left(1 - \frac{L_{c2}}{K_u \left(Q_g\left[1-E_1\right]\right)^{0.42} S_L^{0.3} \left(\frac{1}{nS_{e2}}\right)^{0.6}}\right)^{1.8} \times \left(1 - \frac{L_{c3}}{K_u \left(Q_g\left[1-E_1\right]\left[1-E_2\right]\right)^{0.42} S_L^{0.3} \left(\frac{1}{nS_{e3}}\right)^{0.6}}\right)^{1.8} \quad (36)$$

where definitions of $E_1$ and $E_2$ must still be recursively applied to obtain efficiency as a function of only the coefficient $K_u$, design parameters of $Q_g$, $L_{c1}$, $L_{c2}$, $L_{c3}$, and road geometry variables $S_L$, $S_e$ and Manning's n, which will be comparable to eqs. (25) and (27).

## EXPERIMENT SCALING: DERIVATION OF DIMENSIONAL ANALYSIS

Geometric scaling of experiments are accompanied with Froude number scaling of the flow. The Froude number (Fr) can be represented as:

$$F_r = \frac{V}{\sqrt{gL}} \quad (37)$$

where V is velocity, g is acceleration due to gravity and L is the geometric length. The Fr number must be equal for the prototype ($F_{r,p}$) and the model ($F_{r,m}$), such that

$$\frac{V_p}{\sqrt{gL_p}} = \frac{V_m}{\sqrt{gL_m}} \quad (38)$$

Rearranging terms in eq. (38) leads to:

$$\frac{V_p}{V_m} = \left[\frac{L_p}{L_m}\right]^{1/2} \tag{39}$$

Finally, to convert velocity to flow rate, both sides are multiplied by cross sectional area ($L^2$) such that:

$$\frac{Q_{prototype}}{Q_{model}} = \left(\frac{L_{prototype}}{L_{model}}\right)^{5/2} \tag{40}$$

which is eq. (11).

## CURB INLET AND CURB AND GUTTER TRANSITION CONSTRUCTION AND DESIGN

The main construction material used for the TxDOT curb inlet was wood due to its ease of adaptation and light-weight. To reduce workload and time to switch curb inlet configurations (between a 5 ft and 15 ft curb inlet) the following were built: three modular curb inlet sections (5 ft lengths), two removable flush slab supports, one modular curb and gutter transition (downstream of the curb inlet), one permanent curb and gutter transition (upstream of the curb inlet), and a modular roadway section (to extend the normal curb and gutter 10 ft when transitioning from a 15 ft to 5 ft curb inlet model). The modular design allowed each section to be easily attached to the existing physical model independent of other sections.

The three modular curb inlet sections (each 5 ft in length) were constructed with 2x6 inch beams which extended beyond their required length. These extensions were secured between the structural steel beam and roadway deck and placed between the existing 2x6 inch roadway beams (Figure 37 and 38). The C-shaped 2x6 inch portion (Figure 38) of the curb inlet section was built to independently support the top of curb inlet with or without flush slab support. The C-shaped portion was built strong enough to support the weight of one person and its respective flume, which would direct the curb inlet's

intercepted flow into an approach channel. On top of the 2x6 inch beams ¾ inch plywood was installed (Figure 39). In addition to the TxDOT curb inlet designs (Figure 4, 5, 16 and 17) detailed construction designs for the curb inlet sections and internal slab supports are shown in Figure 40 - 44.

Curb and gutter transitions were installed upstream and downstream of the curb inlet and depressed the curb and gutter 3 inches over the length of 10 ft. The width of the gutter was 16 inches. The upstream curb and gutter transition section was permanently built into the existing roadway, while the downstream curb and gutter was built as a module section. Three layers of 1/4 inch plywood were installed for the new roadway surface, which provided flexibility but did not jeopardize strength.

Texture was applied on top of the new roadway plywood by layering epoxy sealant and graded sand. The sand particle sizes ranged from 1 to 2 mm in diameter. A variety of graded sands and sand density were tested (Figure 45) to closely match the existing roadway texture.

Figure 37. Photo of the 2x6 inch beams used to construct the TxDOT curb inlet.

Figure 38. Photo of the side of the 2x6 inch beams used to construct the TxDOT curb inlet, with the steel beam visible to the lower right.

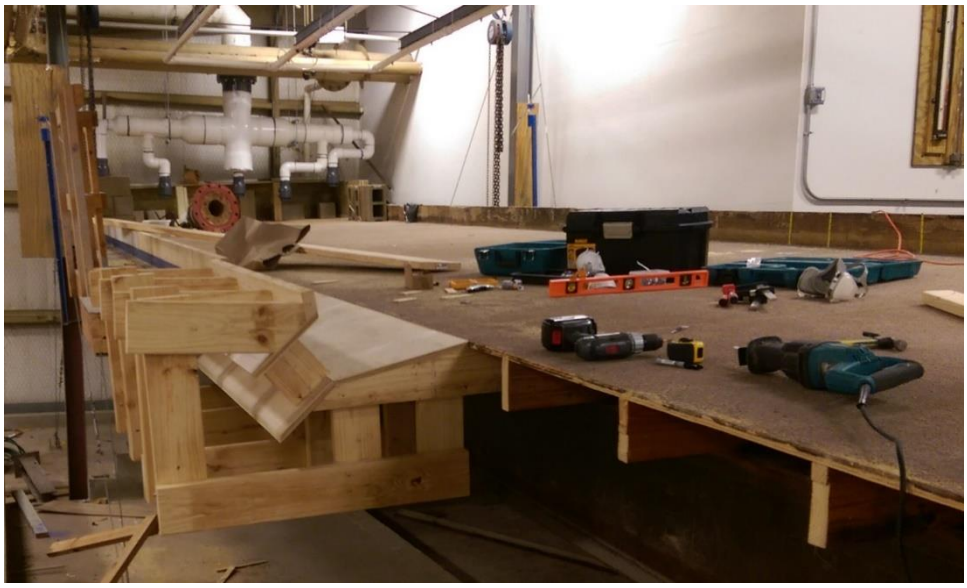

Figure 39. Photo of the side of the 2x6 inch beams and ¾ inch plywood used to construct the TxDOT curb inlet.

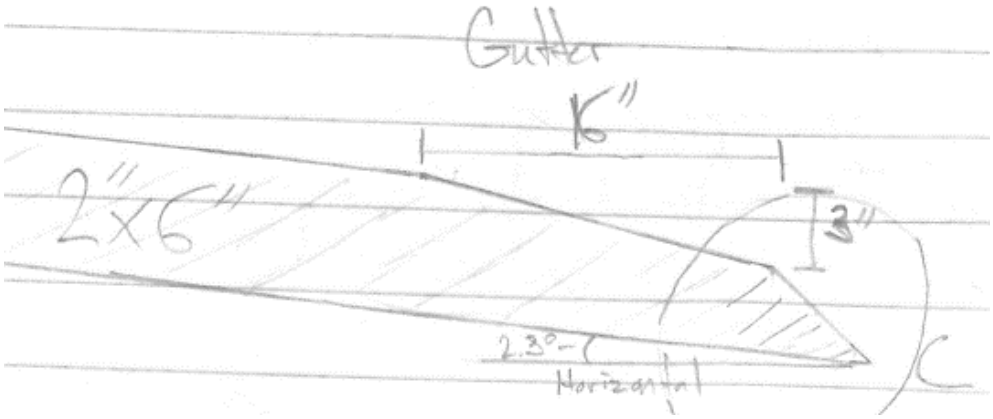


Figure 40. Profile view of 2x6 inch beam construction design.

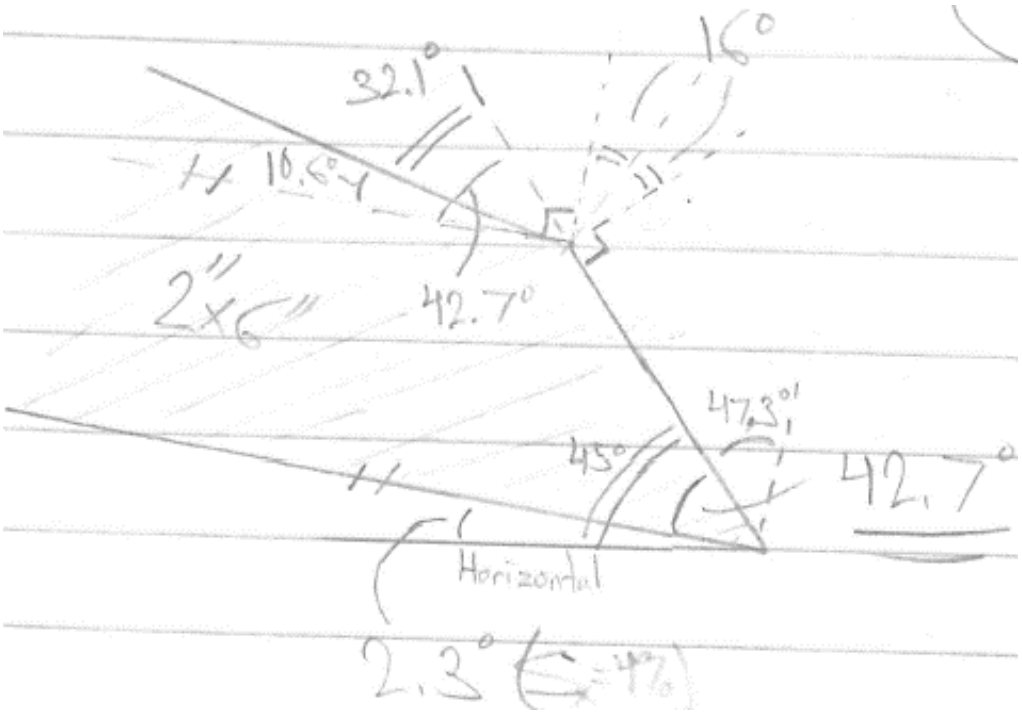


Figure 41. Profile view of Section C from Figure 40[2].

[2] The beam's 45 degree angle from horizontal (the slope of the curb inlet opening; see Figure 4 and 16) was selected based on an assumed 4% cross slope from horizontal. During testing this 45 degree angle will change for 2 and 6% cross slopes. It was assumed that any deviation from 45 degrees would have minimal effect on curb inlet hydraulic performance due to the presumed supercritical nature of the flow at that location.

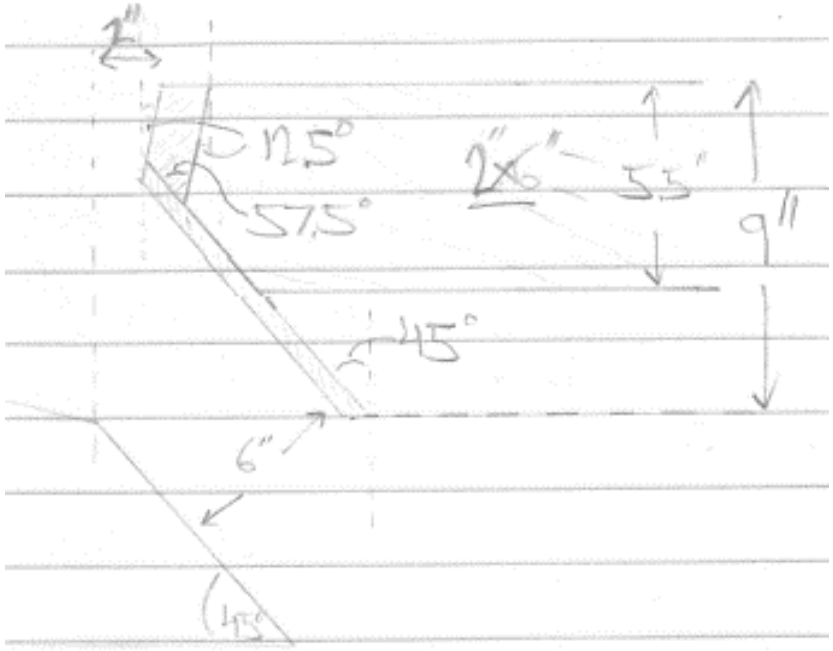


Figure 42. Profile view of construction design for the top of curb inlet opening.

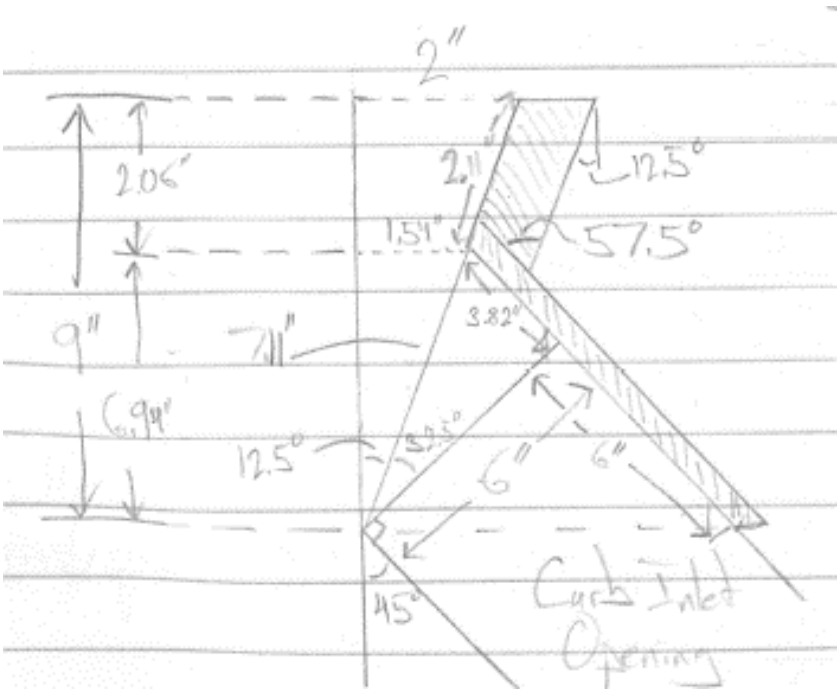


Figure 43. Additional profile view of construction design for the top of curb inlet opening, including ¾" plywood.

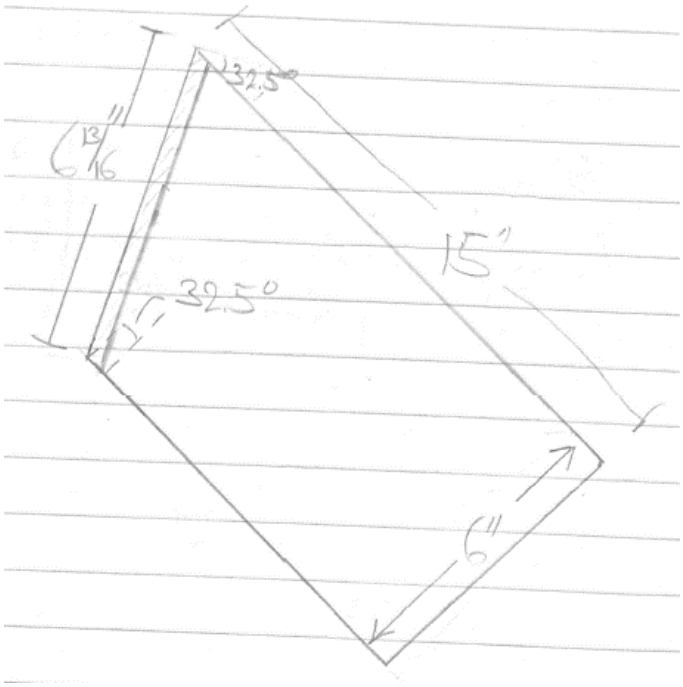


Figure 44. Profile view of a 6 inch wide flush internal slab support construction design.

Figure 45. Graded sand variations for matching existing roadway texture.

### V-NOTCH WEIRS AND APPROACH CHANNELS CONSTRUCTION AND DESIGN

The three 90 degree V-notch weirs for each of the three curb inlet sections (for a 15 ft curb inlet) were identical and fabricated out of steel. Fabrication was performed by The Center for Electromechanics at the J.J. Pickle Research Campus at The University of Texas at Austin. The three V-notch weirs were designed for a maximum head of 1.25 ft above the V-notch apex, which corresponds to an estimated maximum flow rate of 4.5 cfs. Figure 46 shows the construction design of the V-notch weirs.

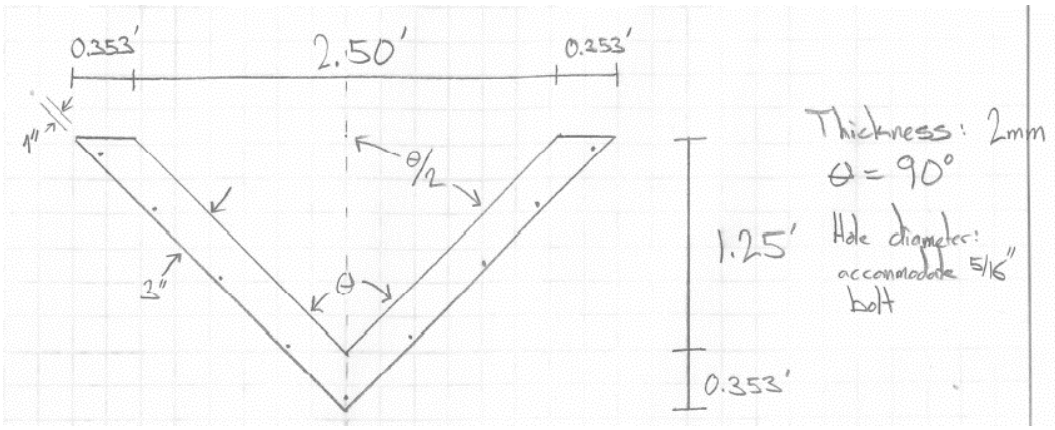


Figure 46. Profile view of the designs for the three V-notch weirs.

The approach channels to each of the 90 degree V-notch weirs were constructed parallel to each other and parallel to the physical model (Figure 47). The approach channels were constructed out of wood, then covered in polyethylene plastic sheeting. These channels were sized for a partially contracted 90 degree V-notch weir, according to the state of the art standards (ASTM Standard D5242; Bos, 1989; Water Measurement Manual). The V-notch weirs were centered on the width of their approach channel. The V-notch apex was installed 1.05 ft above the bottom of the channel. The approach channel dimensions are provided in Table 12.

Figure 47. Photo of three 90 degree v-notch weirs and their approach channels with the physical model on the left side of the photo.

Table 12. Dimensions of the three identical approach channels.

| Approach channel element | Dimension |
|---|---|
| Interior height | 2.3 ft |
| Interior width | 3.125 ft |
| Exterior length | 22 ft |

### INLET PIPE AND HEADBOX CONSTRUCTION AND DESIGN

The water demands for a full scale physical model required modifications to the inlet pipe and headbox. With potential flow rates of 6 cfs, a manifold was designed with five 4 inch pipes, each with a ball value, which increased the distribution and control of flow within the headbox. The manifold and valve design is shown in Figure 48. The valves were positioned to be easily adjusted by an individual standing on a platform at the front of the headbox.

A new headbox was designed with three panels across the exit of the headbox, which could be raised or lowered depending on the experiment's needs. This design provided increased flow control from the headbox onto the roadway. Additionally, a platform was installed in front of the headbox and across the roadway, which provided a walkable surface for an individual to easily adjust the headbox panels. Figure 49 - Figure 51 show the construction plans for the headbox.

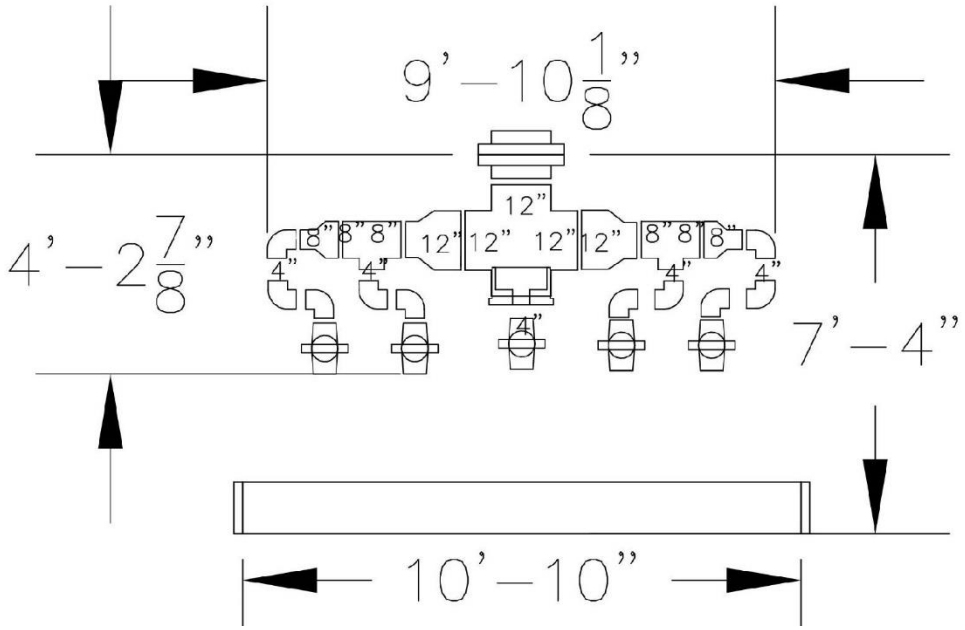


Figure 48. Manifold design.

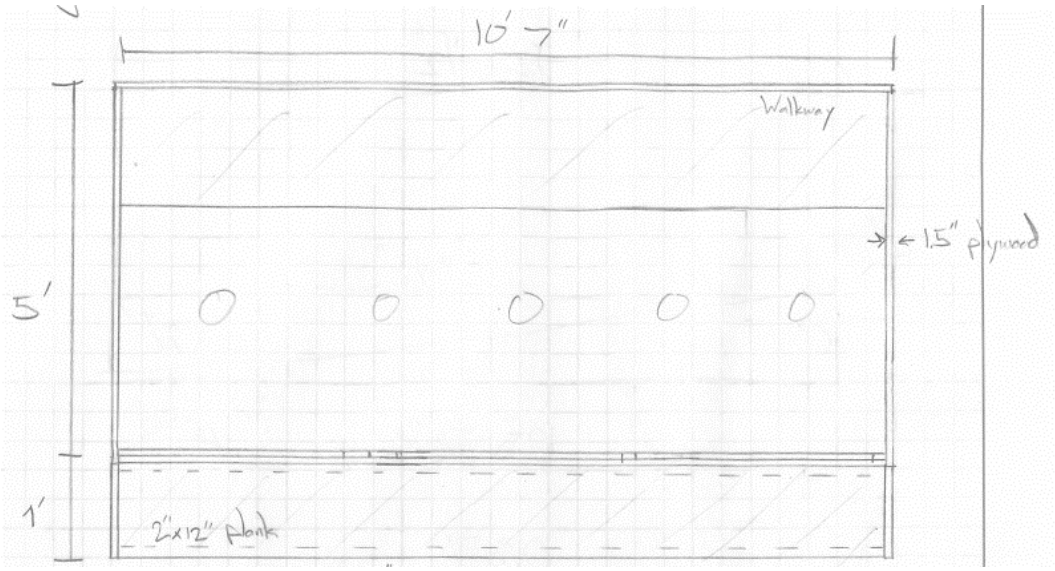


Figure 49. Plan view of headbox construction design.

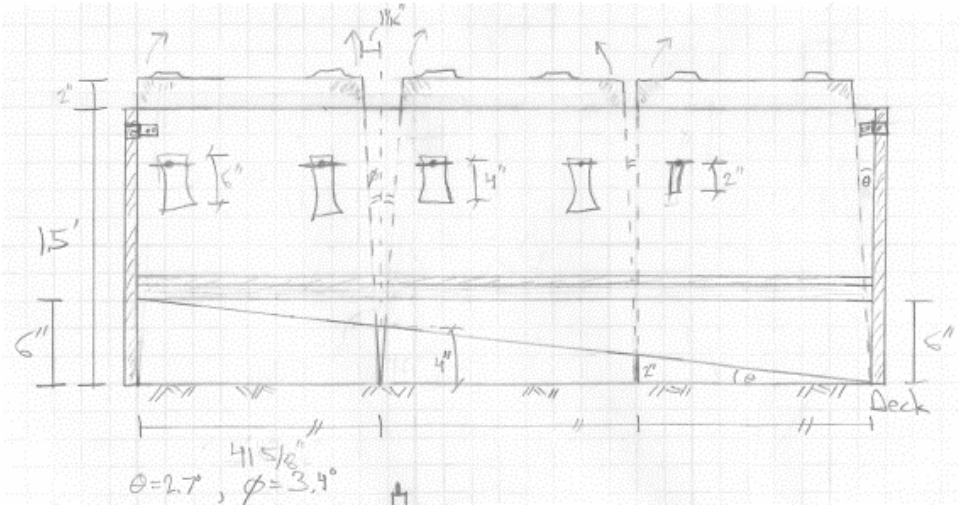


Figure 50. Profile front view of headbox construction design.

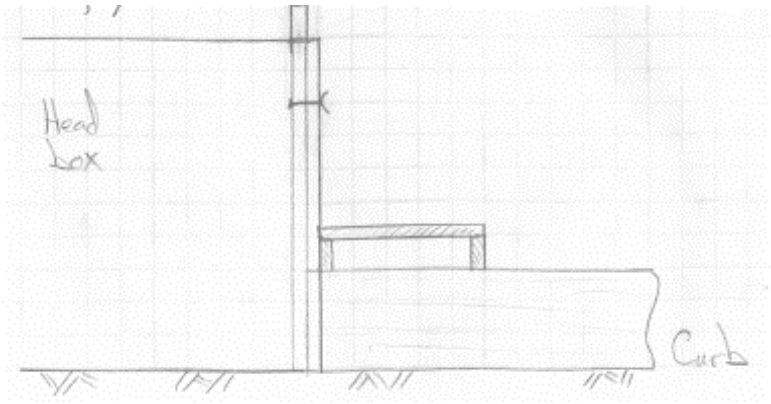


Figure 51. Profile side view of headbox construction design.

## ROUGHNESS COEFFICIENT DATA COLLECTION PROCEDURES

The road geometries and flow rates tested to measure roughness are listed in Table 13. Actual flow rates varied and depended upon road geometries and the physical model's ponded width limitations. All possible combinations of longitudinal slope, cross slope and flow rates listed in Table 13 were used in collecting data.

Table 13. Tested road geometries and flow rates for measuring road roughness.

| | |
|---|---|
| Longitudinal slope (%) | 0.5, 1, 2 |
| Cross slope (%) | 2, 4, 6 |
| Flow Rate (cfs) | ~1cfs (low), ~2cfs (high) |

Road geometries were adjusted based on surveyed longitudinal and cross slope elevations (Holley, 1992). Flow rates were measured with a 120 degree sharp crested V-notch weir and ponded width was measured at five or more evenly spaced locations along the roadway.

Qian et al. (2013) collected extensive data in determining the Manning's roughness coefficient on the same roadway surface used in this study (Figure 52). Since the study, minor road surface alterations in specific locations have been performed to remove previous experimental elements. All alterations were applied a similar texture layered of

epoxy sealant and graded sand. The road roughness is expected to be the same as when analyzed by Qian et al. (2013).

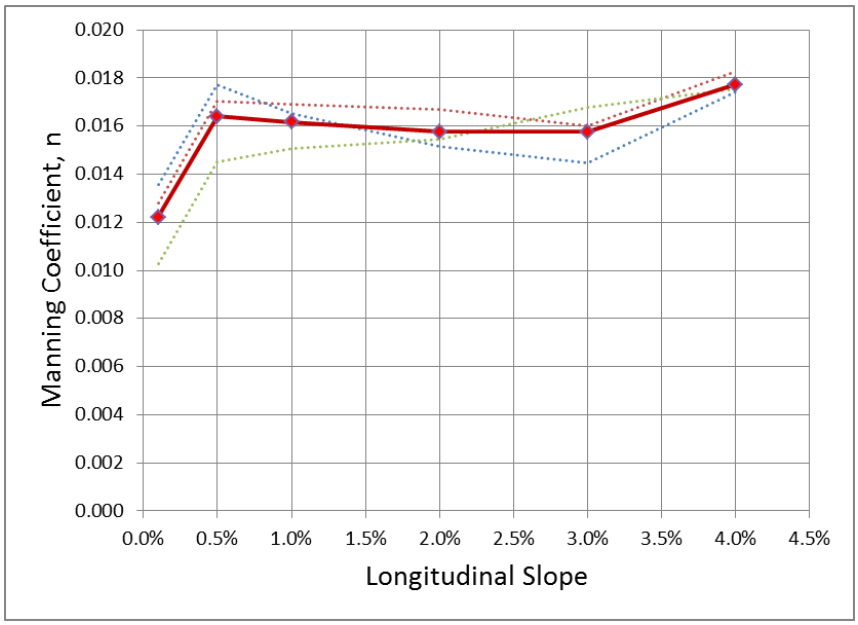


Figure 52. Manning's roughness coefficient as a function of longitudinal slope. 2% cross slope = blue dotted line; 4% cross slope = red dotted line; 6% cross slope = green dotted line; average across cross slopes = heavy red line (Qian et al, 2013)[3].

[3] The low drop in the Manning's roughness coefficient for a longitudinal slope of 0.1% in Figure 52 has since been retracted. It was due to not having sufficient road length to achieve normal flow depth. The Manning's roughness coefficient data for the remaining longitudinal slopes are still valid.

# Appendix B

## PHYSICAL MODEL DATA

In the following tables the columns labeled Flow Rate 1, 2 and 3 correspond to the first, second and third section of the curb inlet while moving downstream, respectively. The spread (or ponded width) and water depth measurements are provided in feet. All spread and water depth measurements locations were in respect to the distance upstream (e.g. +10ft) or downstream (e.g. -6ft) of the beginning of the curb inlet. The beginning of the curb inlet is the furthest upstream point of the curb inlet opening. Tests that do not list a bypass flow rate were performed at 100% interception condition. The variation in water depth at curb measurements was ±0.1 ft.

Table 14: Physical model data recorded during experiments for 15 ft curb inlet without slab supports.

| Test Number | Longit. Slope, % | Cross Slope, % | Flow Rate 1 (CFS) | Flow Rate 2 (CFS) | Flow Rate 3 (CFS) | Flow Rate Bypass (CFS) |
|---|---|---|---|---|---|---|
| 1 | 4 | 6 | 1.43 | 1.88 | 0.38 | 0 |
| 2 | 4 | 6 | 1.66 | 2.26 | 1.11 | 0.21 |
| 3 | 4 | 6 | 1.57 | 2.16 | 0.91 | 0.1 |
| 4 | 4 | 6 | 1.69 | 2.28 | 1.23 | 0.31 |
| 5 | 4 | 4 | 1.129 | 0.814 | 0.015 | 0 |
| 6 | 4 | 4 | 1.436 | 1.85 | 0.688 | 0.3043 |
| 7 | 4 | 4 | 1.42 | 1.72 | 0.55 | 0.19 |
| 8 | 4 | 4 | 1.38 | 1.65 | 0.47 | 0.13 |
| 9 | 4 | 2 | 0.48 | 0.02 | 0.002 | 0 |
| 10 | 4 | 2 | 1.02 | 0.55 | 0.21 | 0.38 |
| 11 | 4 | 2 | 1.01 | 0.38 | 0.14 | 0.2 |
| 12 | 4 | 2 | 0.87 | 0.17 | 0.07 | 0.06 |
| 13 | 2 | 6 | 2.04 | 1.94 | 0.58 | 0 |
| 14 | 2 | 6 | 2.22 | 2.32 | 1.3 | 0.19 |
| 15 | 2 | 6 | 2.17 | 2.21 | 1.17 | 0.099 |
| 16 | 2 | 4 | 1.56 | 1.14 | 0.23 | 0 |
| 17 | 2 | 4 | 1.84 | 1.75 | 0.83 | 0.24 |
| 18 | 2 | 4 | 1.56 | 1.14 | 0.21 | 0 |
| 19 | 2 | 4 | 1.69 | 1.11 | 0.23 | 0 |
| 20 | 2 | 4 | 1.78 | 1.62 | 0.66 | 0.13 |
| 21 | 2 | 4 | 1.85 | 1.82 | 0.89 | 0.36 |
| 22 | 2 | 2 | 0.96 | 0.1 | 0.02 | 0 |
| 23 | 2 | 2 | 1.34 | 0.34 | 0.21 | 0.056 |
| 24 | 1 | 6 | 2.53 | 2.1 | 0.89 | 0 |
| 25 | 1 | 6 | 2.57 | 2.23 | 1.13 | 0.03 |
| 26 | 1 | 4 | 1.96 | 1.26 | 0.56 | 0 |
| 27 | 1 | 4 | 2.02 | 1.31 | 0.59 | 0 |
| 28 | 1 | 4 | 2.07 | 1.48 | 0.77 | 0.07 |
| 29 | 1 | 4 | 2.13 | 1.55 | 0.85 | 0.07 |
| 30 | 1 | 2 | | | | |
| 31 | 0.5 | 6 | | | | |
| 32 | 0.5 | 4 | 2.2 | 1.37 | 0.72 | 0 |
| 33 | 0.5 | 2 | | | | |
| 34 | 0.1 | 6 | | | | |
| 35 | 0.1 | 4 | | | | |
| 36 | 0.1 | 2 | | | | |

Table 14: Continued.

| Test Number | Spread (ft) at +18ft | Depth (ft) at +18ft | Spread (ft) at +16ft | Spread (ft) at +14ft | Depth (ft) at +14ft | Spread (ft) at +12ft | Spread (ft) at +10ft | Depth (ft) at +10ft |
|---|---|---|---|---|---|---|---|---|
| 1 | 6.9 | 0.28 | 6.5 | 6 | 0.3 | 5.25 | 5.1 | 0.29 |
| 2 | 8 | 0.32 | 7.6 | 7.4 | 0.33 | 6.9 | 6.3 | 0.32 |
| 3 | 7.8 | 0.31 | 7.4 | 7 | 0.31 | 6.25 | 5.7 | 0.31 |
| 4 | 8.3 | | 8.1 | 7.65 | | 7 | 6.45 | |
| 5 | 6.65 | 0.2 | 6.25 | 5.9 | 0.23 | 5.3 | 5.1 | 0.18 |
| 6 | 8.7 | 0.28 | 8.5 | 8.6 | 0.26 | 8.35 | 8.05 | 0.23 |
| 7 | 8.9 | 0.24 | 8.9 | 8.9 | 0.24 | 8.7 | 8.2 | 0.22 |
| 8 | 8.8 | 0.23 | 8.8 | 8.7 | 0.23 | 8.3 | 8 | 0.21 |
| 9 | 5.8 | 0.08 | 5.7 | 5.35 | 0.1 | 5.2 | 5.1 | 0.06 |
| 10 | 9.4 | 0.13 | 9.9 | 9.9 | 0.14 | 10 | 10 | 0.12 |
| 11 | 8.8 | 0.13 | 9 | 9.2 | 0.14 | 9.2 | 9.1 | 0.12 |
| 12 | 8.1 | 0.1 | 8.1 | 8.1 | 0.11 | 8.1 | 7.95 | 0.1 |
| 13 | 7.4 | 0.35 | 6.9 | 6.65 | 0.36 | 6.6 | 6.55 | 0.34 |
| 14 | 8.2 | 0.4 | 7.9 | 7.2 | 0.39 | 6.95 | 7 | 0.4 |
| 15 | 8 | 0.36 | 7.7 | 7.4 | 0.38 | 7.3 | 7.1 | 0.37 |
| 16 | 8.1 | 0.24 | 7.95 | 7.4 | 0.275 | 7.25 | 7.1 | 0.25 |
| 17 | 9.3 | 0.3 | 9.4 | 9.3 | 0.28 | 9 | 8.95 | 0.28 |
| 18 | 8 | 0.25 | 7.6 | 7.2 | 0.26 | 7 | 6.9 | 0.24 |
| 19 | | | | | | | | |
| 20 | 9 | 0.27 | 9 | 8.85 | 0.26 | 8.6 | 8.6 | 0.26 |
| 21 | 9.7 | | 9.8 | 9.6 | | 9.3 | 8.95 | |
| 22 | 8.2 | 0.11 | 8.2 | 8.3 | 0.13 | 8.1 | 8 | 0.11 |
| 23 | 10 | 0.15 | 10.4 | 10.2 | 0.16 | 10.2 | 10 | 0.14 |
| 24 | 8.9 | | 8.4 | 7.8 | | 7.9 | 7.9 | |
| 25 | 8.7 | 0.39 | 5.8 | 8.3 | 0.42 | 8.4 | 8.2 | 0.41 |
| 26 | 9.7 | 0.3 | 9.5 | 9.4 | 0.31 | 9.4 | 9.4 | 0.3 |
| 27 | 8.9 | 0.35 | 8.8 | 8.7 | 0.36 | 8.9 | 8.9 | 0.32 |
| 28 | 10.1 | 0.28 | 9.9 | 9.7 | 0.3 | 9.7 | 9.6 | 0.31 |
| 29 | 9.6 | | 9.5 | 9.3 | 0.35 | 9.4 | 9.5 | 0.36 |
| 30 | | | | | | | | |
| 31 | | | | | | | | |
| 32 | 10.4 | 0.29 | 10.3 | 10.4 | 0.33 | 10.4 | 10.3 | 0.33 |
| 33 | | | | | | | | |
| 34 | | | | | | | | |
| 35 | | | | | | | | |
| 36 | | | | | | | | |

Table 14: Continued.

| Test Number | Spread (ft) at +8ft | Spread (ft) at +6ft | Spread (ft) at +4ft | Spread (ft) at +2ft | Spread (ft) at 0ft | Spread (ft) at -2ft | Spread (ft) at -4ft | Spread (ft) at -6ft |
|---|---|---|---|---|---|---|---|---|
| 1 | 5.05 | 5.1 | 5.1 | 5.1 | 5 | 4.85 | 4.5 | 4.05 |
| 2 | 5.8 | 5.8 | 5.7 | 5.65 | 5.5 | 5.35 | 5.15 | 4.95 |
| 3 | 5.6 | 5.6 | 5.5 | 5.5 | 5.4 | 5.25 | 5 | 4.85 |
| 4 | 6.1 | 6 | 5.8 | 5.8 | 5.7 | 5.55 | 5.3 | 5 |
| 5 | 5.05 | 5.05 | 5.1 | 5.15 | 4.95 | 4.85 | 4.3 | 3.8 |
| 6 | 7.65 | 7.45 | 7.3 | 7.15 | 6.95 | 6.75 | 6.55 | 6.25 |
| 7 | 7.8 | 7.3 | 7 | 6.6 | 6.6 | 6.4 | 6.3 | 6.05 |
| 8 | 7.6 | 7.1 | 6.7 | 6.4 | 6.4 | 6.25 | 6.15 | 5.8 |
| 9 | 4.9 | 4.9 | 4.9 | 4.95 | 4.9 | 4.65 | 4.3 | 3.65 |
| 10 | 9.9 | 9.8 | 9.8 | 9.7 | 9.6 | 9.35 | 9.15 | 9 |
| 11 | 9 | 8.9 | 8.7 | 8.5 | 8.2 | 8.15 | 8.05 | 8.15 |
| 12 | 7.7 | 7.4 | 7.3 | 7.1 | 6.9 | 6.75 | 6.75 | 6.6 |
| 13 | 6.4 | 6.3 | 6.3 | 6.2 | 5.95 | 5.65 | 5.15 | 4.85 |
| 14 | 7 | 6.7 | 6.7 | 6.7 | 6.7 | 6.4 | 6.1 | 5.7 |
| 15 | 7.1 | 6.8 | 6.7 | 6.7 | 6.55 | 6.25 | 5.95 | 5.55 |
| 16 | 7.2 | 6.85 | 6.7 | 6.6 | 6.4 | 6.15 | 5.65 | 5.15 |
| 17 | 8.8 | 8.75 | 8.4 | 7.95 | 7.7 | 7.45 | 7.3 | 6.75 |
| 18 | 7.1 | 6.95 | 6.95 | 6.8 | 6.6 | 6.25 | 5.75 | 5.2 |
| 19 | | | | | | | | |
| 20 | 8.5 | 8.3 | 8.05 | 7.5 | 7.4 | 7.2 | 6.9 | 6.3 |
| 21 | 8.9 | 8.9 | 8.6 | 8.3 | 8.1 | 8 | 7.75 | 7.35 |
| 22 | 7.8 | 7.7 | 7.3 | 7.2 | 7.1 | 6.75 | 6.3 | 5.55 |
| 23 | 9.9 | 9.7 | 9.7 | 9.4 | 9 | 8.85 | 8.65 | 8.35 |
| 24 | 7.9 | 7.7 | 7.6 | 7.4 | 7 | 6.65 | 6.35 | 6.05 |
| 25 | 8.1 | 7.8 | 7.75 | 7.45 | 7.25 | 6.9 | 6.65 | 6.35 |
| 26 | 9.3 | 9 | 8.7 | 8.2 | 7.9 | 7.45 | 7.15 | 6.75 |
| 27 | 8.9 | 8.6 | 8.4 | 8 | 7.7 | 7.4 | 7.25 | 6.75 |
| 28 | 9.2 | 9.2 | 8.8 | 8.6 | 8.3 | 7.85 | 7.65 | 7.25 |
| 29 | 9.4 | 9.1 | 8.9 | 8.6 | 8.3 | 8 | 7.95 | 7.65 |
| 30 | | | | | | | | |
| 31 | | | | | | | | |
| 32 | 9.9 | 9.8 | 9.5 | 9 | 8.8 | 8.6 | 8.3 | 7.85 |
| 33 | | | | | | | | |
| 34 | | | | | | | | |
| 35 | | | | | | | | |
| 36 | | | | | | | | |

Table 14: Continued.

| Test Number | Spread (ft) at -8ft | Spread (ft) at -10ft | Spread (ft) at -12ft | Spread (ft) at -14ft | Spread (ft) at -16ft | Spread (ft) at -18ft | Spread (ft) at -20ft |
|---|---|---|---|---|---|---|---|
| 1 | 3.5 | 2.95 | 2.35 | 1.7 | 0.1 | 0.1 | 0.1 |
| 2 | 4.65 | 4.35 | 3.95 | 3.35 | 2.6 | 2 | 1 |
| 3 | 4.45 | 4.05 | 3.65 | 2.9 | 2.3 | 1.6 | 0.7 |
| 4 | 4.8 | 4.6 | 4.15 | 3.8 | 3 | 2.3 | 1.7 |
| 5 | 3.15 | 2.2 | 1.6 | 1.45 | 0.15 | 0.1 | 0.05 |
| 6 | 5.95 | 5.65 | 5.2 | 4.8 | 4.25 | 3.2 | 2.65 |
| 7 | 5.75 | 5.3 | 4.9 | 4.4 | 3.8 | 2.85 | 2.4 |
| 8 | 5.6 | 5.05 | 4.55 | 4 | 3.2 | 2.5 | 2.1 |
| 9 | 2.8 | 2.2 | 1.7 | 1.5 | 0.2 | 0.1 | 0.1 |
| 10 | 9.05 | 8.85 | 8.7 | 8.3 | 8 | 8.1 | 7.7 |
| 11 | 8.05 | 7.95 | 7.35 | 7.2 | 7 | 6.55 | 6 |
| 12 | 6.45 | 6.15 | 6.2 | 5.8 | 5.3 | 5 | 4.7 |
| 13 | 4.45 | 3.85 | 2.95 | 2 | 0.2 | 0.15 | 0.3 |
| 14 | 5.4 | 5 | 4.45 | 3.4 | 2.6 | 1.7 | 1.2 |
| 15 | 5.3 | 4.75 | 4.15 | 3.35 | 2.35 | 1 | 1 |
| 16 | 4.6 | 3.9 | 3.05 | 2.15 | 1.3 | 0.2 | 0.4 |
| 17 | 6.3 | 6.05 | 5.95 | 5.4 | 4.6 | 3.35 | 2.1 |
| 18 | 4.6 | 3.85 | 2.9 | 2 | 1.5 | 0.2 | 0.3 |
| 19 | | | | | | | |
| 20 | 6 | 5.55 | 5.25 | 4.7 | 3.8 | 2.4 | 1.6 |
| 21 | 6.7 | 6.25 | 6 | 5.6 | 4.9 | 4.15 | 2.8 |
| 22 | 4.95 | 4.3 | 2.55 | 1.95 | 1.6 | 1.6 | 0.4 |
| 23 | 8.05 | 7.25 | 6.45 | 6 | 5.5 | 4.8 | 4 |
| 24 | 5.6 | 4.75 | 3.65 | 2.55 | 1.4 | 0.5 | 0.6 |
| 25 | 5.95 | 5.2 | 4.55 | 3 | 1.9 | 0.9 | 1 |
| 26 | 6.25 | 5.55 | 4.65 | 3.3 | 2 | 0.6 | 0.7 |
| 27 | 6.3 | 5.6 | 4.75 | 3.5 | 2 | 0.6 | 0.7 |
| 28 | 6.85 | 6.15 | 5.45 | 4.6 | 3.2 | 1.8 | 1.3 |
| 29 | 7 | 6.35 | 5.75 | 4.9 | 3.3 | 1.7 | 1.6 |
| 30 | | | | | | | |
| 31 | | | | | | | |
| 32 | 6.9 | 6 | 5.3 | 4 | 2.2 | 0.8 | 0.9 |
| 33 | | | | | | | |
| 34 | | | | | | | |
| 35 | | | | | | | |
| 36 | | | | | | | |

Table 14: Continued.

| Test Number | NOTES |
|---|---|
| 1 | |
| 2 | |
| 3 | |
| 4 | |
| 5 | |
| 6 | |
| 7 | |
| 8 | |
| 9 | |
| 10 | |
| 11 | |
| 12 | |
| 13 | |
| 14 | |
| 15 | |
| 16 | |
| 17 | |
| 18 | |
| 19 | |
| 20 | |
| 21 | |
| 22 | |
| 23 | Maximum ponded width |
| 24 | |
| 25 | Maximum flow obtained |
| 26 | |
| 27 | |
| 28 | Ponded width at maximum |
| 29 | Could only get 0.07 cfs of bypass with both pumps and all valves open |
| 30 | Ponding width exceeded, could not achieve 100% |
| 31 | Maximum flow, not at 100% |
| 32 | Ponded width at maximum, bypass conditions not possible |
| 33 | Ponding width exceeded, could not achieve 100% |
| 34 | Depth exceeded, could not achieve 100% |
| 35 | Ponding width exceeded, could not achieve 100% |
| 36 | Ponding width exceeded, could not achieve 100% |

Table 15: Physical model data recorded during experiments for 15 ft curb inlet with slab supports.

| Test Number | Longit. Slope, % | Cross Slope, % | Flow Rate 1 (CFS) | Flow Rate 2 (CFS) | Flow Rate 3 (CFS) | Flow Rate Bypass (CFS) | Spread (ft) at +18ft |
|---|---|---|---|---|---|---|---|
| 37 | 4 | 6 | 2.05 | 1.35 | 0.14 | 0 | 6.7 |
| 38 | 4 | 6 | 2.61 | 2.18 | 0.7 | 0.29 | 8.2 |
| 39 | 4 | 6 | 2.54 | 2.06 | 0.64 | 0.22 | 8 |
| 40 | 4 | 6 | 2.3 | 1.75 | 0.48 | 0.05 | 7.75 |
| 41 | 4 | 4 | 1.54 | 0.56 | 0.04 | 0 | 8 |
| 42 | 4 | 4 | 2.1 | 1.49 | 0.56 | 0.41 | 10 |
| 43 | 4 | 4 | 1.95 | 1.26 | 0.42 | 0.18 | 9.55 |
| 44 | 4 | 4 | 1.89 | 1.14 | 0.34 | 0.09 | 9.3 |
| 45 | 4 | 2 | 0.5 | 0.02 | 0.003 | 0 | 5.5 |
| 46 | 4 | 2 | 1.26 | 0.42 | 0.22 | 0.46 | 10.2 |
| 47 | 4 | 2 | 1.14 | 0.29 | 0.15 | 0.24 | 9.4 |
| 48 | 4 | 2 | 0.93 | 0.14 | 0.08 | 0.08 | 8.3 |
| 49 | 2 | 6 | 2.584 | 1.586 | 0.375 | 0 | 7.25 |
| 50 | 2 | 6 | 2.748 | 1.977 | 0.815 | 0.069 | 7.4 |
| 51 | 2 | 6 | 2.752 | 1.959 | 0.826 | 0.071 | 7.7 |
| 52 | 2 | 6 | 2.73 | 2.03 | 0.92 | 0.15 | 8.8 |
| 53 | 2 | 4 | 1.85 | 0.85 | 0.18 | 0 | 8.7 |
| 54 | 2 | 4 | 2.25 | 1.39 | 0.68 | 0.27 | 10.3 |
| 55 | 2 | 4 | 2.15 | 1.27 | 0.59 | 0.16 | 10.1 |
| 56 | 2 | 4 | 2.07 | 1.16 | 0.51 | 0.08 | 9.7 |
| 57 | 2 | 2 | 1.03 | 0.13 | 0.03 | 0 | 8.3 |
| 58 | 2 | 2 | 1.25 | 0.28 | 0.16 | 0.04 | 10.3 |
| 59 | 1 | 6 | 2.97 | 1.85 | 0.75 | 0 | 8.2 |
| 60 | 1 | 6 | 3.03 | 1.96 | 0.89 | 0.02 | 8.2 |
| 61 | 1 | 4 | 2.21 | 1.08 | 0.47 | 0 | 9.5 |
| 62 | 1 | 4 | 2.42 | 1.33 | 0.74 | 0.1 | 10.2 |
| 63 | 1 | 2 | | | | | |
| 64 | 0.5 | 6 | | | | | |
| 65 | 0.5 | 4 | 2.45 | 1.26 | 0.65 | 0 | 10 |
| 66 | 0.5 | 2 | | | | | |
| 67 | 0.1 | 6 | | | | | |
| 68 | 0.1 | 4 | | | | | |
| 69 | 0.1 | 2 | | | | | |

Table 15: Continued.

| Test Number | Depth (ft) at +18ft | Spread (ft) at +16ft | Spread (ft) at +14ft | Depth (ft) at +14ft | Spread (ft) at +12ft | Spread (ft) at +10ft | Depth (ft) at +10ft | Spread (ft) at +8ft | Spread (ft) at +6ft | Spread (ft) at +4ft |
|---|---|---|---|---|---|---|---|---|---|---|
| 37 | 0.23 | 6.5 | 6.2 | 0.25 | 5.8 | 5.6 | 0.28 | 5.3 | 5 | 4.8 |
| 38 | | 8.2 | 8.1 | | 7.6 | 7 | | 6.7 | 6.35 | 6.2 |
| 39 | 0.29 | 8.1 | 7.9 | 0.29 | 7.3 | 6.8 | 0.29 | 6.45 | 6.2 | 6 |
| 40 | | 7.5 | 7.1 | | 6.6 | 6.1 | | 5.75 | 5.6 | 5.4 |
| 41 | 0.19 | 7.6 | 7.3 | 0.2 | 7 | 6.3 | 0.19 | 5.7 | 5.3 | 5.3 |
| 42 | 0.24 | 10 | 9.75 | 0.25 | 9.6 | 9.4 | 0.22 | 9 | 8.7 | 8.2 |
| 43 | | 9.6 | 9.5 | | 9.3 | 8.95 | | 8.4 | 8 | 7.3 |
| 44 | 0.23 | 9.3 | 9.2 | 0.23 | 9 | 8.6 | 0.21 | 8.1 | 7.5 | 7 |
| 45 | 0.08 | 5.5 | 5.25 | 0.1 | 5.2 | 5.1 | 0.08 | 4.95 | 4.9 | 4.9 |
| 46 | 0.16 | 10.3 | 10.3 | 0.16 | 10.3 | 10.3 | 0.13 | 10.3 | 10.1 | 10.05 |
| 47 | 0.13 | 9.6 | 9.6 | 0.14 | 9.6 | 9.6 | 0.12 | 9.4 | 9.3 | 9.1 |
| 48 | 0.11 | 8.5 | 8.5 | 0.13 | 8.2 | 8.1 | 0.1 | 7.9 | 7.7 | 7.3 |
| 49 | 0.46 | 6.3 | 6.05 | 0.42 | 6.2 | 6.35 | 0.35 | 6.5 | 6.35 | 6.2 |
| 50 | 0.47 | 6.9 | 6.9 | 0.49 | 7 | 6.95 | 0.43 | 7.1 | 6.9 | 6.95 |
| 51 | 0.46 | 7.2 | 6.05 | 0.46 | 7.05 | 6.95 | 0.44 | 7.05 | 6.95 | 7 |
| 52 | 0.38 | 8.5 | 7.7 | 0.39 | 7.15 | 7.15 | 0.4 | 7.1 | 6.9 | 6.8 |
| 53 | | 8.6 | 8.05 | | 7.2 | 6.8 | | 6.9 | 6.6 | 6.6 |
| 54 | 0.27 | 10.2 | 9.9 | 0.28 | 9.5 | 9 | 0.28 | 8.6 | 8.6 | 8.1 |
| 55 | | 9.9 | 9.5 | | 9.1 | 8.6 | | 8.15 | 8 | 7.6 |
| 56 | 0.25 | 9.6 | 9.3 | 0.26 | 8.7 | 8.1 | 0.26 | 7.8 | 7.65 | 7.25 |
| 57 | 0.11 | 8.6 | 8.4 | 0.14 | 8 | 7.9 | 0.11 | 7.7 | 7.3 | 7.1 |
| 58 | 0.15 | 10.4 | 10.3 | 0.15 | 10.2 | 10 | 0.13 | 9.8 | 9.6 | 9.5 |
| 59 | | 8 | 8 | | 7.9 | 7.8 | | 7.5 | 7.4 | 7.4 |
| 60 | 0.36 | 8.1 | 8 | 0.41 | 8 | 7.8 | 0.41 | 7.6 | 7.35 | 7.3 |
| 61 | | 9.4 | 9.3 | | 9.1 | 9 | | 8.65 | 8.4 | 8 |
| 62 | 0.25 | 10.1 | 10.1 | 0.28 | 10 | 10 | 0.3 | 9.7 | 9.4 | 8.7 |
| 63 | | | | | | | | | | |
| 64 | | | | | | | | | | |
| 65 | 0.26 | 9.8 | 10 | 0.31 | 10.1 | 10 | 0.3 | 9.7 | 9.5 | 9.2 |
| 66 | | | | | | | | | | |
| 67 | | | | | | | | | | |
| 68 | | | | | | | | | | |
| 69 | | | | | | | | | | |

Table 15: Continued.

| Test Number | Spread (ft) at +2ft | Spread (ft) at 0ft | Spread (ft) at -2ft | Spread (ft) at -4ft | Spread (ft) at -6ft | Spread (ft) at -8ft | Spread (ft) at -10ft | Spread (ft) at -12ft | Spread (ft) at -14ft | Spread (ft) at -16ft |
|---|---|---|---|---|---|---|---|---|---|---|
| 37 | 4.65 | 4.65 | 4.45 | 4.05 | 3.65 | 3.35 | 2.85 | 2.05 | 1.5 | 0.05 |
| 38 | 6 | 5.7 | 5.65 | 5.3 | 4.95 | 4.7 | 4.4 | 4.1 | 3.8 | 3 |
| 39 | 5.75 | 5.5 | 5.35 | 5.1 | 4.85 | 4.6 | 4.4 | 3.95 | 3.5 | 2.75 |
| 40 | 5.25 | 5.1 | 4.95 | 4.75 | 4.5 | 4.3 | 3.8 | 3.3 | 2.45 | 2 |
| 41 | 5.4 | 5.3 | 5.1 | 4.75 | 4.3 | 3.65 | 2.85 | 2.05 | 1.6 | 1.3 |
| 42 | 7.85 | 7.5 | 7.25 | 7.1 | 6.85 | 6.5 | 6.15 | 5.8 | 5.4 | 4.9 |
| 43 | 7 | 6.7 | 6.6 | 6.45 | 6.15 | 5.8 | 5.35 | 5 | 4.4 | 3.9 |
| 44 | 6.4 | 6.35 | 6.2 | 6.15 | 5.7 | 5.35 | 4.9 | 4.4 | 4 | 3 |
| 45 | 4.95 | 4.9 | 4.7 | 4.3 | 3.6 | 2.85 | 2.25 | 1.75 | 1.45 | 0 |
| 46 | 9.95 | 9.7 | 9.55 | 9.4 | 9.3 | 9.2 | 9.05 | 8.9 | 8.6 | 8.2 |
| 47 | 8.7 | 8.5 | 8.45 | 8.25 | 8.25 | 8.25 | 8 | 7.7 | 7.5 | 7.3 |
| 48 | 7.15 | 7.05 | 6.9 | 7 | 6.8 | 6.55 | 6.35 | 6.15 | 5.9 | 5.6 |
| 49 | 3.15 | 6.05 | 5.7 | 5.25 | 4.85 | 4.35 | 3.7 | 3 | 2.05 | 0.3 |
| 50 | 6.7 | 6.7 | 6.65 | 6.25 | 5.75 | 5.4 | 4.95 | 4.3 | 3.4 | 2.15 |
| 51 | 6.95 | 6.65 | 6.5 | 6.05 | 5.85 | 5.45 | 4.95 | 4.3 | 3.35 | 2.2 |
| 52 | 6.85 | 6.8 | 6.45 | 6.2 | 5.8 | 5.4 | 4.95 | 4.3 | 3.8 | 2.5 |
| 53 | 6.6 | 6.5 | 6.15 | 5.65 | 5.2 | 4.65 | 3.85 | 2.95 | 2 | 1.45 |
| 54 | 7.75 | 7.6 | 7.25 | 7.1 | 6.75 | 6.45 | 6.15 | 5.65 | 5.3 | 4.55 |
| 55 | 7.4 | 7.3 | 7.05 | 6.85 | 6.3 | 6.15 | 5.75 | 5.35 | 4.8 | 4.1 |
| 56 | 7.1 | 7.1 | 6.75 | 6.6 | 6.05 | 5.85 | 5.4 | 4.8 | 4.1 | 3.1 |
| 57 | 7.1 | 7 | 6.5 | 6.15 | 5.5 | 4.75 | 3.85 | 2.25 | 1.9 | 1.45 |
| 58 | 8.9 | 8.6 | 8.65 | 8.35 | 8.1 | 7.9 | 6.85 | 6.35 | 5.9 | 5.3 |
| 59 | 7.2 | 6.85 | 6.65 | 6.35 | 6 | 5.6 | 4.85 | 3.95 | 2.6 | 1.3 |
| 60 | 7.2 | 7.1 | 6.8 | 6.45 | 6.2 | 5.85 | 4.95 | 4 | 2.85 | 1.6 |
| 61 | 7.8 | 7.6 | 7.3 | 6.95 | 6.4 | 6.05 | 5.4 | 4.5 | 3.45 | 1.9 |
| 62 | 8.25 | 8.1 | 7.9 | 7.7 | 7.35 | 6.85 | 6.35 | 5.55 | 5.1 | 3.7 |
| 63 | | | | | | | | | | |
| 64 | | | | | | | | | | |
| 65 | 8.8 | 8.6 | 8.35 | 8.15 | 7.75 | 6.85 | 6.05 | 5.15 | 4.1 | 2.1 |
| 66 | | | | | | | | | | |
| 67 | | | | | | | | | | |
| 68 | | | | | | | | | | |
| 69 | | | | | | | | | | |

Table 15: Continued.

| Test Number | Spread (ft) at -18ft | Spread (ft) at -20ft | Notes |
|---|---|---|---|
| 37 | 0.05 | 0.05 | |
| 38 | 2.3 | 1.7 | |
| 39 | 2 | 1.5 | |
| 40 | 1.45 | 0.6 | |
| 41 | 0.1 | 0.1 | |
| 42 | 4.4 | 3.4 | |
| 43 | 2.8 | 2.2 | |
| 44 | 2.4 | 1.8 | |
| 45 | 0 | 0 | |
| 46 | 8.1 | 7.9 | |
| 47 | 6.7 | 6.3 | |
| 48 | 5.2 | 4.9 | |
| 49 | 0.25 | 0.1 | |
| 50 | 0.85 | 1 | |
| 51 | 0.95 | 1 | |
| 52 | 1.5 | 1.1 | |
| 53 | 0.2 | 0.35 | |
| 54 | 3.25 | 2.2 | |
| 55 | 2.5 | 1.8 | |
| 56 | 2 | 1 | |
| 57 | 0.2 | 0.35 | |
| 58 | 4.6 | 3.95 | Maximum bypass due to nearly being at maximum ponded width |
| 59 | 0.4 | 0.5 | |
| 60 | 0.75 | 0.9 | Maximum flow rate |
| 61 | 0.5 | 0.7 | |
| 62 | 2 | 1.4 | Maximum ponded width |
| 63 | | | Maximum ponded width, could not reach 100% capture |
| 64 | | | Maximum flow, could not reach 100% capture |
| 65 | 0.8 | 0.85 | Nearly maximum ponded width, bypass flow not possible |
| 66 | | | Ponded width exceeded, 100% capture not possible |
| 67 | | | Depth exceeded, 100% not possible |
| 68 | | | Ponded width exceeded, 100% capture not possible |
| 69 | | | Ponded width exceeded, 100% capture not possible |

Table 16: Physical model data recorded during experiments for 5 ft curb inlet without slab supports.

| Test Number | Longit. Slope, % | Cross Slope, % | Flow Rate 1 (CFS) | Flow Rate 2 (CFS) | Flow Rate 3 (CFS) | Flow Rate Bypass (CFS) | Spread (ft) at +18ft | Depth (ft) at +18ft |
|---|---|---|---|---|---|---|---|---|
| 70 | 4 | 6 | 0.84 | 0 | 2.9 | 0.17 | 2.9 | 3 |
| 71 | 4 | 6 | 1.98 | 0.54 | 5.6 | 0.2 | 5.2 | 5 |
| 72 | 4 | 6 | 1.89 | 0.29 | 5.15 | 0.2 | 4.9 | 4.7 |
| 73 | 4 | 6 | 1.75 | 0.09 | 4.85 | 0.2 | 4.5 | 4.2 |
| 74 | 4 | 4 | 1.05 | 0 | 4.6 | | 4.4 | 4.2 |
| 75 | 4 | 4 | 1.02 | 0 | 4.6 | 0.16 | 4.1 | 4 |
| 76 | 4 | 4 | 1.79 | 0.52 | 6.7 | 0.17 | 6.7 | 6.6 |
| 77 | 4 | 4 | 1.7 | 0.34 | 6.4 | 0.17 | 6.3 | 6.15 |
| 78 | 4 | 4 | 1.52 | 0.12 | 5.7 | 0.16 | 5.7 | 5.4 |
| 79 | 4 | 2 | 0.28 | 0 | 4 | | 3.8 | 3.8 |
| 80 | 4 | 2 | 1.11 | 0.52 | 7.7 | 0.11 | 8 | 8.2 |
| 81 | 4 | 2 | 0.96 | 0.29 | 7.1 | 0.1 | 7.2 | 7.3 |
| 82 | 4 | 2 | 0.76 | 0.12 | 6.3 | 0.09 | 6.4 | 6.3 |
| 83 | 2 | 6 | 1.6 | 0 | 4.2 | | 4.2 | 4.3 |
| 84 | 2 | 6 | 2.31 | 0.45 | 5.9 | 0.24 | 5.5 | 5.25 |
| 85 | 2 | 6 | 2.24 | 0.32 | 5.7 | 0.24 | 5.3 | 5 |
| 86 | 2 | 6 | 2.05 | 0.11 | 5 | 0.25 | 4.8 | 4.65 |
| 87 | 2 | 4 | 1.37 | 0 | 5.8 | 0.19 | 5.5 | 5.3 |
| 88 | 2 | 4 | 1.97 | 0.47 | 7.6 | 0.2 | 7.4 | 7.1 |
| 89 | 2 | 4 | 1.88 | 0.33 | 7.3 | 0.21 | 7.15 | 6.75 |
| 90 | 2 | 4 | 1.79 | 0.12 | 7 | 0.19 | 6.6 | 6.2 |
| 91 | 2 | 2 | 0.58 | 0 | 6.2 | 0.09 | 6 | 5.75 |
| 92 | 2 | 2 | 1.36 | 0.33 | 9.4 | 0.14 | 10 | 9.65 |
| 93 | 2 | 2 | 1.2 | 0.17 | 8.9 | 0.11 | 9.15 | 9.25 |
| 94 | 2 | 2 | 1.01 | 0.08 | 8.25 | 0.1 | 8.4 | 8.2 |
| 95 | 1 | 6 | 1.69 | 0 | 5.05 | 0.26 | 5.15 | 5.05 |
| 96 | 1 | 6 | 2.54 | 0.49 | 6.1 | 0.33 | 6.05 | 6.1 |
| 97 | 1 | 6 | 2.34 | 0.28 | 5.7 | 0.32 | 5.7 | 6 |
| 98 | 1 | 6 | 2.1 | 0.1 | 5.4 | 0.3 | 5.6 | 5.7 |
| 99 | 1 | 4 | 1.33 | 0 | 5.9 | 0.2 | 6.05 | 6.2 |
| 100 | 1 | 4 | 2.23 | 0.51 | 8.1 | 0.25 | 7.95 | 7.55 |
| 101 | 1 | 4 | 2.01 | 0.29 | 7.4 | 0.24 | 7.25 | 7.15 |
| 102 | 1 | 4 | 1.7 | 0.09 | 6.7 | 0.22 | 6.4 | 6.5 |
| 103 | 1 | 2 | 0.94 | 0 | 8.1 | 0.12 | 8.1 | 8.1 |
| 104 | 1 | 2 | 1.39 | 0.25 | 10.3 | 0.14 | 10.25 | 10.15 |
| 105 | 1 | 2 | 1.3 | 0.16 | 10.1 | 0.14 | 9.7 | 9.6 |
| 106 | 1 | 2 | 1.17 | 0.07 | 9.3 | 0.13 | 9.3 | 9.1 |
| 107 | 0.5 | 6 | 1.717 | 0 | 5.9 | 0.32 | 5.9 | 5.85 |
| 108 | 0.5 | 6 | 2.7 | 0.51 | 7 | 0.39 | 6.95 | 7.2 |
| 109 | 0.5 | 6 | 2.51 | 0.3 | 6.7 | 0.37 | 6.7 | 6.75 |
| 110 | 0.5 | 6 | 2.24 | 0.11 | 6.35 | 0.34 | 6.35 | 6.35 |
| 111 | 0.5 | 4 | 1.4 | 0 | 7.1 | 0.25 | 6.9 | 7 |
| 112 | 0.5 | 4 | 2.23 | 0.51 | 8.35 | 0.27 | 8.4 | 8.65 |

Table 16: Continued.

| Test Number | Spread (ft) at +16ft | Spread (ft) at +14ft | Depth (ft) at +14ft | Spread (ft) at +12ft | Spread (ft) at +10ft | Depth (ft) at +10ft | Spread (ft) at +8ft | Spread (ft) at +6ft | Spread (ft) at +4ft |
|---|---|---|---|---|---|---|---|---|---|
| 70 | 0.17 | 3.1 | 3 | 0.14 | 2.9 | 2.8 | 2.4 | 1.7 | 1.2 |
| 71 | 0.25 | 4.9 | 4.7 | 0.24 | 4.4 | 4.1 | 4.3 | 4.25 | 4 |
| 72 | 0.26 | 4.55 | 4.35 | 0.23 | 4.05 | 4.05 | 4.2 | 4.05 | 3.75 |
| 73 | 0.23 | 4.1 | 3.9 | 0.21 | 3.85 | 4 | 4 | 3.85 | 3.4 |
| 74 | | 4.1 | 4 | | 4.05 | 4.1 | 4.1 | 4 | 3.6 |
| 75 | 0.16 | 4 | 4.1 | 0.13 | 4.1 | 4.15 | 4.15 | 4.05 | 3.8 |
| 76 | 0.17 | 6.5 | 6.25 | 0.18 | 6.2 | 6 | 5.7 | 5.4 | 5.1 |
| 77 | 0.18 | 6 | 5.9 | 0.17 | 5.8 | 5.5 | 5.3 | 5 | 4.9 |
| 78 | 0.18 | 5.4 | 5.3 | 0.16 | 5 | 4.9 | 4.8 | 4.7 | 4.6 |
| 79 | | 3.6 | 3.7 | | 3.8 | 3.7 | 3.7 | 3.3 | 2.95 |
| 80 | 0.11 | 8.2 | 8.3 | 0.1 | 8.5 | 8.6 | 8.5 | 8.4 | 8.2 |
| 81 | 0.11 | 7.3 | 7.6 | 0.1 | 7.6 | 7.6 | 7.3 | 7.3 | 7.3 |
| 82 | 0.1 | 6.4 | 6.4 | 0.09 | 6.4 | 6.25 | 6.25 | 6.15 | 6.15 |
| 83 | | 4.4 | 4.4 | | 4.3 | 4.1 | 3.9 | 3.3 | 2.8 |
| 84 | 0.31 | 5.05 | 4.95 | 0.28 | 5.1 | 5.2 | 5.2 | 4.9 | 4.5 |
| 85 | 0.3 | 4.9 | 4.9 | 0.27 | 5 | 5 | 5 | 4.7 | 4.3 |
| 86 | 0.29 | 4.7 | 4.7 | 0.25 | 4.8 | 4.7 | 4.6 | 4.2 | 3.65 |
| 87 | 0.2 | 5.3 | 5.2 | 0.16 | 5.1 | 5.1 | 5.1 | 4.8 | 4.35 |
| 88 | 0.25 | 6.85 | 6.5 | 0.23 | 6.35 | 6.2 | 6.25 | 6.15 | 5.85 |
| 89 | 0.24 | 6.5 | 6.25 | 0.22 | 6.15 | 6.05 | 6.05 | 6.05 | 5.75 |
| 90 | 0.22 | 5.95 | 5.95 | 0.2 | 5.9 | 5.8 | 5.75 | 5.6 | 5.2 |
| 91 | 1.1 | 5.9 | 6 | 0.08 | 5.85 | 5.65 | 5.55 | 5.5 | 5 |
| 92 | 0.16 | 9.7 | 9.5 | 0.13 | 9.45 | 9.35 | 9.1 | 8.65 | 8.5 |
| 93 | 0.14 | 8.9 | 8.7 | 0.12 | 8.55 | 8.65 | 8.25 | 7.8 | 7.7 |
| 94 | 0.13 | 7.9 | 7.85 | 0.11 | 7.9 | 7.65 | 7.4 | 7.3 | 7.15 |
| 95 | 0.28 | 5 | 4.9 | 0.25 | 4.85 | 4.5 | 4.1 | 3.75 | 3.5 |
| 96 | 0.34 | 6.25 | 6.15 | 0.31 | 5.95 | 5.85 | 5.5 | 5.15 | 4.85 |
| 97 | 0.33 | 5.95 | 5.9 | 0.3 | 5.55 | 5.5 | 5.25 | 4.7 | 4.5 |
| 98 | 0.31 | 5.55 | 5.4 | 0.29 | 5.25 | 5.05 | 4.75 | 4.4 | 4.1 |
| 99 | 0.21 | 6.15 | 6.05 | 0.19 | 5.7 | 5.55 | 5.25 | 4.7 | 4.1 |
| 100 | 0.27 | 7.7 | 7.8 | 0.26 | 7.85 | 7.45 | 7.3 | 7 | 6.5 |
| 101 | 0.26 | 7.25 | 7.25 | 0.23 | 7.3 | 6.9 | 6.75 | 6.35 | 5.58 |
| 102 | 0.24 | 6.8 | 6.7 | 0.24 | 6.45 | 6.25 | 6 | 5.6 | 5 |
| 103 | 0.15 | 8.15 | 8.1 | 0.12 | 8.1 | 7.7 | 7.3 | 7.05 | 6.4 |
| 104 | 0.16 | 10.2 | 10.15 | 0.15 | 9.9 | 9.75 | 9.4 | 9.05 | 8.65 |
| 105 | 0.16 | 9.85 | 9.8 | 0.15 | 9.6 | 9.5 | 8.9 | 8.55 | 8.3 |
| 106 | 0.15 | 9.15 | 9.4 | 0.14 | 9.2 | 9.1 | 8.5 | 7.95 | 7.75 |
| 107 | 0.31 | 5.8 | 5.6 | 0.26 | 5.3 | 4.9 | 4.65 | 4.4 | 4 |
| 108 | 0.36 | 7.15 | 7.05 | 0.32 | 6.95 | 6.5 | 6.15 | 6 | 5.8 |
| 109 | 0.35 | 6.8 | 6.6 | 0.31 | 6.35 | 6.05 | 5.8 | 5.5 | 5.3 |
| 110 | 0.33 | 6.4 | 6.25 | 0.29 | 5.9 | 5.55 | 5.35 | 5 | 4.8 |
| 111 | 0.24 | 7.05 | 6.75 | 0.2 | 6.45 | 6 | 5.55 | 5.1 | 4.8 |
| 112 | 0.29 | 8.8 | 8.7 | 0.25 | 8.6 | 8.1 | 7.65 | 7.4 | 7.15 |

Table 16: Continued.

| Test Number | Spread (ft) at +2ft | Spread (ft) at 0ft | Spread (ft) at -2ft | Spread (ft) at -4ft | Spread (ft) at -6ft | Spread (ft) at -8ft | Spread (ft) at -10ft | Spread (ft) at -12ft |
|---|---|---|---|---|---|---|---|---|
| 70 | 1 | 0.5 | 0.05 | 0.05 | 0.05 | 0.05 | 0.05 | 0.05 |
| 71 | 3.5 | 3.1 | 2.4 | 1.7 | 1.6 | 1.9 | 1.6 | 1.9 |
| 72 | 3.3 | 2.65 | 1.9 | 1.15 | 1.1 | 1.1 | 1.1 | 1.1 |
| 73 | 2.9 | 2 | 0.6 | 0.6 | 0.7 | 0.8 | 0.7 | 0.8 |
| 74 | 2.95 | 2 | 0.1 | 0.1 | 0.1 | 0.1 | 0.1 | 0.1 |
| 75 | 3.05 | 2.1 | 0.1 | 0.1 | 0.1 | 0.1 | 0.1 | 0.1 |
| 76 | 4.9 | 4.55 | 4.1 | 3.4 | 2.75 | 2.1 | 2.75 | 2.1 |
| 77 | 4.65 | 4.3 | 3.7 | 3 | 2.15 | 1.7 | 2.15 | 1.7 |
| 78 | 4.3 | 3.6 | 2.8 | 2 | 0.8 | 1 | 0.8 | 1 |
| 79 | 2.2 | 1.6 | 0.1 | 0.1 | 0.1 | 0.1 | 0.1 | 0.1 |
| 80 | 8.15 | 8.2 | 8.1 | 8.1 | 7.9 | 7.1 | 7.9 | 7.1 |
| 81 | 7.1 | 7.1 | 6.9 | 6.7 | 6.4 | 6 | 6.4 | 6 |
| 82 | 6.15 | 6 | 5.7 | 5.4 | 5 | 4.7 | 5 | 4.7 |
| 83 | 2.5 | 2 | 0.25 | 0.2 | | | | |
| 84 | 3.8 | 3.4 | 2.9 | 2.05 | 1.8 | 2.3 | 1.8 | 2.3 |
| 85 | 3.5 | 3.15 | 2.6 | 1.7 | 1.3 | 1.9 | 1.3 | 1.9 |
| 86 | 3.1 | 2.8 | 2 | 0.95 | 1.1 | 1.2 | 1.1 | 1.2 |
| 87 | 3.25 | 2.3 | 0.3 | 0.3 | | | | |
| 88 | 5.45 | 4.9 | 4.45 | 3.65 | 2.9 | 2.85 | 2.9 | 2.85 |
| 89 | 5.35 | 4.7 | 4 | 3.5 | 2.45 | 2.4 | 2.45 | 2.4 |
| 90 | 4.7 | 4.05 | 3.15 | 2.2 | 1.2 | 1.5 | 1.2 | 1.5 |
| 91 | 4.65 | 3.65 | 2 | 1.6 | 0.35 | 0.35 | 0.35 | 0.35 |
| 92 | 8.45 | 8.2 | 8 | 7.15 | 6.15 | 5.5 | 6.15 | 5.5 |
| 93 | 7.65 | 7.25 | 6.8 | 6.1 | 5.4 | 4.3 | 5.4 | 4.3 |
| 94 | 6.65 | 6.25 | 5.55 | 5.05 | 4.2 | 2.7 | 4.2 | 2.7 |
| 95 | 3.25 | 2.55 | 1.2 | 0.7 | 0.65 | 0.55 | 0.65 | 0.55 |
| 96 | 4.7 | 4.35 | 3.8 | 2.9 | 2.55 | 2.85 | 2.55 | 2.85 |
| 97 | 4.3 | 4 | 3.15 | 2.2 | 2.1 | 2.4 | 2.1 | 2.4 |
| 98 | 3.8 | 3.4 | 2.7 | 1.3 | 1.5 | 1.7 | 1.5 | 1.7 |
| 99 | 3.75 | 3.2 | 1.9 | 0.7 | 0.6 | 0.55 | 0.6 | 0.55 |
| 100 | 6.1 | 5.7 | 5.3 | 4.65 | 3.35 | 3.45 | 3.35 | 3.45 |
| 101 | 5.35 | 5.1 | 4.5 | 3.65 | 2.5 | 2.95 | 2.5 | 2.95 |
| 102 | 4.7 | 4.1 | 3.35 | 2.5 | 1.65 | 1.9 | 1.65 | 1.9 |
| 103 | 5.75 | 4.8 | 3.9 | 2.2 | 0.8 | 0.8 | 0.8 | 0.8 |
| 104 | 8.45 | 8.05 | 7 | 6.25 | 5.35 | 4.5 | 5.35 | 4.5 |
| 105 | 7.9 | 7.3 | 6.2 | 5.5 | 4.7 | 3.2 | 4.7 | 3.2 |
| 106 | 6.95 | 6.4 | 5.5 | 4.6 | 3.4 | 2.3 | 3.4 | 2.3 |
| 107 | 3.55 | 3 | 1.7 | 0.8 | 0.75 | 0.6 | 0.75 | 0.6 |
| 108 | 5.45 | 5 | 4.2 | 3.25 | 3.1 | 3.2 | 3.1 | 3.2 |
| 109 | 4.95 | 4.45 | 3.65 | 2.35 | 2.55 | 2.7 | 2.55 | 2.7 |
| 110 | 4.45 | 0.39 | 2.9 | 1.65 | 1.8 | 1.9 | 1.8 | 1.9 |
| 111 | 4.45 | 3.5 | 2.2 | 0.9 | 0.8 | 0.75 | 0.8 | 0.75 |
| 112 | 6.75 | 6.3 | 5.6 | 4.6 | 3.65 | 3.85 | 3.65 | 3.85 |

Table 16: Continued.

| Test Number | Notes |
|---|---|
| 70 | |
| 71 | |
| 72 | |
| 73 | |
| 74 | |
| 75 | |
| 76 | |
| 77 | |
| 78 | |
| 79 | |
| 80 | |
| 81 | |
| 82 | |
| 83 | |
| 84 | |
| 85 | |
| 86 | |
| 87 | |
| 88 | |
| 89 | |
| 90 | |
| 91 | |
| 92 | Maximum bounded width |
| 93 | |
| 94 | |
| 95 | |
| 96 | |
| 97 | |
| 98 | |
| 99 | |
| 100 | |
| 101 | |
| 102 | |
| 103 | |
| 104 | Maximum bounded width that we can model |
| 105 | |
| 106 | |
| 107 | |
| 108 | |
| 109 | |
| 110 | |
| 111 | |
| 112 | |

Table 16: Continued.

| Test Number | 113 | 114 | 115 | 116 | 117 | 118 | 119 | 120 | 121 | 122 | 123 | 124 |
|---|---|---|---|---|---|---|---|---|---|---|---|---|
| Longit. Slope, % | 0.5 | 0.5 | 0.5 | 0.5 | 0.1 | 0.1 | 0.1 | 0.1 | 0.1 | 0.1 | 0.1 | 0.1 |
| Cross Slope, % | 4 | 4 | 2 | 2 | 6 | 6 | 6 | 6 | 4 | 4 | 4 | 2 |
| Flow Rate 1 (CFS) | 2 | 1.7 | 1 | 1.15 | 1.9 | 3 | 2.7 | 2.2 | 1.6 | 2.16 | 1.9 | |
| Flow Rate 2 (CFS) | 0.3 | 0.1 | 0 | 0.02 | 0 | 0.5 | 0.3 | 0.1 | 0 | 0.27 | 0.1 | |
| Flow Rate 3 (CFS) | 7.9 | 7.4 | 10 | 10.4 | 7 | 8.9 | 8.7 | 7.8 | 8.9 | 10.2 | 9.8 | |
| Flow Rate Bypass (CFS) | 0.3 | 0.3 | 0.2 | 0.15 | 0.4 | 0.5 | 0.4 | 0.4 | 0.3 | 0.32 | 0.3 | |
| Spread +18' | 8 | 7.5 | 9.6 | 10 | 6.9 | 8.9 | 8.5 | 7.6 | 8.5 | 9.9 | 9.5 | |
| Depth +18' | 8.2 | 7.7 | 10 | 10.3 | 6.8 | 8.8 | 8.3 | 7.6 | 8.5 | 9.9 | 9.5 | |
| Spread +16' | 0.3 | 0.3 | 0.2 | 0.16 | 0.4 | 0.5 | 0.4 | 0.4 | 0.3 | 0.34 | 0.3 | |
| Spread +14' | 8.3 | 7.8 | 10 | 10.3 | 6.6 | 8.6 | 8.2 | 7.4 | 8.3 | 9.8 | 9.3 | |
| Depth +14' | 8.1 | 7.6 | 10 | 10.4 | 6.2 | 8.2 | 7.7 | 7 | 7.9 | 9.5 | 8.8 | |
| Spread +12' | 0.2 | 0.2 | 0.1 | 0.13 | 0.3 | 0.4 | 0.4 | 0.4 | 0.3 | 0.31 | 0.3 | |
| Spread +10' | 8 | 7.5 | 9.4 | 9.9 | 5.9 | 8 | 7.4 | 6.6 | 7.4 | 9.05 | 8.5 | |
| Depth +10' | 7.3 | 6.8 | 9.2 | 9.7 | 5.6 | 7.4 | 6.9 | 6.2 | 6.8 | 8.5 | 7.7 | |
| Spread +8' | 7.1 | 6.3 | 8.2 | 9 | 5.4 | 7.1 | 6.6 | 6 | 6.4 | 8.15 | 7.4 | |
| Spread +6' | 6.7 | 6.1 | 7.5 | 8.2 | 5 | 6.8 | 6.3 | 5.7 | 6.1 | 7.7 | 7.1 | |
| Spread +4' | 6.4 | 5.7 | 7.3 | 7.8 | 4.7 | 6.5 | 6 | 5.4 | 5.7 | 7.45 | 6.7 | |
| Spread +2' | 6.2 | 5.3 | 6.4 | 7.1 | 4 | 6.1 | 5.6 | 4.9 | 5 | 6.85 | 6.2 | |
| Spread 0' | 5.6 | 4.7 | 5.7 | 6.25 | 3.2 | 5.4 | 4.9 | 4.1 | 4.1 | 6.1 | 5.3 | |
| Spread -2' | 4.8 | 3.8 | 4.7 | 5.3 | 1.8 | 4.6 | 4 | 2.8 | 2.6 | 5.1 | 4.2 | |
| Spread -4' | 3.7 | 2.5 | 3.2 | 4.6 | 0.9 | 3.6 | 3 | 1.9 | 1.1 | 3.9 | 2.7 | |
| Spread -6' | 3.1 | 2.1 | 1.6 | 2.8 | 0.9 | 3.6 | 3.1 | 2 | 1 | 3.8 | 2.9 | |
| Spread -8' | 325 | 2.3 | 0.7 | 2 | 0.8 | 3.6 | 3.1 | 2 | 0.9 | 3.8 | 2.9 | |
| Spread -10' | 3.1 | 2.1 | 1.6 | 2.8 | 0.9 | 3.6 | 3.1 | 2 | 1 | 3.8 | 2.9 | |
| Spread -12' | 325 | 2.3 | 0.7 | 2 | 0.8 | 3.6 | 3.1 | 2 | 0.9 | 3.8 | 2.9 | |
| Notes | | | | Max ponded width | | | | | | Max ponded width | | Max T, 100% not possible |

## MATLAB SCRIPT

Three potential design equations could be used in both scripts, which correspond to eq. (10) and Table 3.

The first Matlab script was used for calculating the intercepted and bypass flow rates of a curb inlet by inputting the following: upstream gutter flow rate, curb inlet length, road geometry (i.e. $S_L$, $S_X$, depression) and road roughness.

The second Matlab script was used for calculating the upstream gutter flow rate for 100% interception of flow based on the following: curb inlet length, road geometry (i.e. $S_L$, $S_X$, depression) and road roughness.

### First Matlab Script

```
%Cal_Eff version 2.2 2/19/2016

disp('Enter the total flow and geometry of the gutter')
qt=input('Total flow, qt (cfs): ');
w=input('Depressed width, w (ft): ');
a=input('Gutter depression, a (inch): ');
sl=input('Longitudinal slope, sl (%): ');
sx=input('Crossectional slope, sx (%): ');
n=input('Manning coefficient, n: ');

sl=sl/100;
sx=sx/100;
i=0;
err=100;
sw=sx+a/12/w;
qs=0;
s=sw/sx;
qwmax=0.56/n*sw^1.67*sl^0.5*w^2.67;
if (qt<=1.02*qwmax)
    qw=qt;
    qs=0;
    t=(qw*n/0.56/sw^(5/3)/sl^0.5)^(1/(8/3));
    se=sw;
    e=1;
    x=[0 w 1.25*w];
y=[0 a/12+w*sx a/12+1.25*w*sx];
w1=[t 0];
```

```
w2=[t*sw t*sw];
k=1;
elseif (qt<=1.25*qwmax)
while(err>0.1 && i<1000000)
    qs=qs+0.000001*qt;
    qw=qt-qs;
    e=qw/qt;
    t=w*(s/((s*e/(1-e)+1)^(1/2.67)-1)+1);
    ts=t-w;
    qscal=0.56/n*sx^1.67*sl^0.5*ts^2.67;
    err=abs(qscal-qs)/((qscal+qs)/2)*100;
    i=i+1;
end
k=100;
sw1=a/12/w;
se=sx+sw1*e;
x=[0 w 1.25*t];
y=[0 a/12+w*sx a/12+1.25*t*sx];
w1=[t 0];
w2=[a/12+t*sx a/12+t*sx];
else
    while(err>0.1 && i<10000)
    qs=qs+0.0001*qt;
    qw=qt-qs;
    e=qw/qt;
    t=w*(s/((s*e/(1-e)+1)^(1/2.67)-1)+1);
    ts=t-w;
    qscal=0.56/n*sx^1.67*sl^0.5*ts^2.67;
    err=abs(qscal-qs)/((qscal+qs)/2)*100;
    i=i+1;
    end
 k=1;
sw1=a/12/w;
se=sx+sw1*e;
x=[0 w 1.25*t];
y=[0 a/12+w*sx a/12+1.25*t*sx];
w1=[t 0];
w2=[a/12+t*sx a/12+t*sx];
end
if i>=k*10000
    disp('Error in spread, try increaseing accuracy of calculation')
end
disp('  ')
disp(['Spread, t= ', num2str(roundn(t,-2)), ' ft '])
disp(['Flow in depressed section, qw= ', num2str(roundn(qw,-2)), ' cfs '])
disp(['Ratio of gutter flow to total flow, e= ', num2str(roundn(e,-2))])
plot(x,y,'k',w1,w2,'b')
title('Road cross-section at gutter')

disp(' ')
```

```
disp('enter 1,2,or 3 to choose the equation of the 100% capture Length (Lt), where:')
disp('Lt= N Qt^a Sl^b (1 / nSe)^c')
disp('(1) HEC-22/TxDOT (2014):         N=0.6    a=0.42   b=0.3     c=0.6')
disp('(2) Comport and Thornton (2012): N=0.176  a= 0.62  b=-0.021  c=0.49')
disp('(3) Guo and Mackenzie (2012):    N=0.38   a=0.51   b=0.06    c=0.46')
disp(' ')
eqno=input('Use equation no.:');
if (eqno~=1) && (eqno~=2) && (eqno~=3)
    disp('wrong choice of equation, code will exit')
    return
end

Lt=0.6*qt^0.42*sl^0.3*(1/(n*se))^0.6*(2-eqno)*((3-eqno)/2)+...
   0.176*qt^0.62*sl^-0.021*(1/(n*se))^0.49*(eqno-1)*(3-eqno)+...
   0.38*qt^0.51*sl^0.06*(1/(n*se))^0.46*((eqno-1)/2)*(eqno-2);
disp(' ')
disp(['Lenth of 100% capture: ', num2str(roundn(Lt,-2)),' ft'])
disp('Enter curb length to calculate effeciency or Enter 0 to exit')
Lc=input('Curb Length, ft: ');
if (Lc==0)
    return
elseif (Lc>Lt)
Eff=1;
Qby=0;
else
Eff=1-(1-Lc/Lt)^1.8;
Qby=qt*(1-Lc/Lt)^1.8;
end

disp(' ')
disp(['Effeciency: ', num2str(roundn(Eff*100,-2)), '%'])
disp(['Bypass flow, Qby: ', num2str(roundn(Qby,-2)), ' cfs'])

clear variables
```

## Second Matlab Script

```
%Cal_Q version 2.2 2/19/2016

disp(' ')
disp('Enter the total flow and geometry of the gutter')
Lc=input('Curb Length, ft: ');
w=input('Depressed width, w (ft): ');
a=input('Gutter depression, a (inch): ');
n=input('Manning coefficient, n: ');
sl=input('Longitudinal slope, sl (%): ');
sx=input('Crossectional slope, sx (%): ');


disp('enter 1,2,or 3 to choose the equation of the 100% capture Length (Lt), where:')
disp('Lt= N Qt^a Sl^b (1 / nSe)^c')
disp('(1) HEC-22/TxDOT (2014):         N=0.6    a=0.42   b=0.3     c=0.6')
disp('(2) Comport and Thornton (2012): N=0.176  a= 0.62  b=-0.021  c=0.49')
disp('(3) Guo and Mackenzie (2012):    N=0.38   a=0.51   b=0.06    c=0.46')
disp('')
eqno=input('Use equation no.:');
if (eqno~=1) && (eqno~=2) && (eqno~=3)
    disp('wrong choice of equation, code will exit')
    return
end

sl=sl/100;
sx=sx/100;
i=0;
j=0;
err1=100;
err=100;
sw=sx+a/12/w;
qt=0;
qs=0;
s=sw/sx;
qwmax=0.56/n*sw^1.67*sl^0.5*w^2.67;

while(err1>0.2 && j<20000)
    qt=0.005+qt;
    qs=0;
    i=0;
    err=100;
if (qt<=1.02*qwmax)
    qw=qt;
    qs=0;
    t=(qw*n/0.56/sw^(5/3)/sl^0.5)^(1/(8/3));
    se=sw;
    e=1;
```

```
    x=[0 w 1.25*w];
y=[0 a/12+w*sx a/12+1.25*w*sx];
w1=[t 0];
w2=[t*sw t*sw];
k=1;
elseif (qt<=1.25*qwmax)
while(err>1 && i<1000000)
    qs=qs+0.000001*qt;
    qw=qt-qs;
    e=qw/qt;
    t=w*(s/((s*e/(1-e)+1)^(1/2.67)-1)+1);
    ts=t-w;
    qscal=0.56/n*sx^1.67*sl^0.5*ts^2.67;
    err=abs(qscal-qs)/((qscal+qs)/2)*100;
    i=i+1;
end
k=100;
sw1=a/12/w;
se=sx+sw1*e;
x=[0 w 1.25*t];
y=[0 a/12+w*sx a/12+1.25*t*sx];
w1=[t 0];
w2=[a/12+t*sx a/12+t*sx];
else
    while(err>1 && i<10000)
    qs=qs+0.0001*qt;
    qw=qt-qs;
    e=qw/qt;
    t=w*(s/((s*e/(1-e)+1)^(1/2.67)-1)+1);
    ts=t-w;
    qscal=0.56/n*sx^1.67*sl^0.5*ts^2.67;
    err=abs(qscal-qs)/((qscal+qs)/2)*100;
    i=i+1;
    end
k=1;
sw1=a/12/w;
se=sx+sw1*e;
x=[0 w 1.25*t];
y=[0 a/12+w*sx a/12+1.25*t*sx];
w1=[t 0];
w2=[a/12+t*sx a/12+t*sx];
end

Lt=0.6*qt^0.42*sl^0.3*(1/(n*se))^0.6*(2-eqno)*((3-eqno)/2)+...
   0.176*qt^0.62*sl^-0.021*(1/(n*se))^0.49*(eqno-1)*(3-eqno)+...
   0.38*qt^0.51*sl^0.06*(1/(n*se))^0.46*((eqno-1)/2)*(eqno-2);

err1=abs(Lc-Lt)/Lc*100;
j=j+1;
end
```

```
if i>=k*10000
    disp(' ')
    disp('**Error in spread, try increaseing accuracy of calculation')
    return
end

if j>=20000
  disp(' ')
  disp('**Error in Q (or Qt >= 100 cfs), try increasing acceptable error')
  return
end

disp(' ')
disp(['Q of 100% capture: ', num2str(roundn(qt,-2)),' cfs'])
disp(['Spread, t= ', num2str(roundn(t,-2)), ' ft '])
disp(['error in Lt (%) = ', num2str(roundn(err1,-2))])
disp(['Flow in depressed section, qw= ', num2str(qw), ' cfs '])
disp(['Ratio of gutter flow to total flow, e= ', num2str(e)])
plot(x,y,'k',w1,w2,'b')
title('Road cross-section at gutter')

clearvars
```

# Appendix C: Photos

Figure 53. Physical model flumes, directing curb inlet intercepted flow into V-notch weir approach channels (when slab supports are installed, a division of flow between sections is achieved through vertical flow dividers).

Figure 54. Photo of upstream curb and gutter transition under construction and before texture is applied.

Figure 55. Photo of approach channels under construction.

Figure 56. Physical model before modifications.

Figure 57. Physical model looking downstream before modifications.

Figure 58. Photo of roadway model before modifications and location of approach channels before construction.

Figure 59. Headbox and inlet pipe before modifications.

Figure 60. Photo of bypass V-notch weir and existing approach channel.

Figure 61. Photo of physical model pumps and exterior reservoir.

# Bibliography


Argue, J.R. and D. Pezzaniti (1996). “How reliable are inlet (hydraulic) models at representing stormwater flow?” The Science of the Total Environment, 189/190:355-359.

ASTM Standard D5242, 2013, "Standard test method for open-channel flow measurement of water with thin-plate weirs," ASTM International, West Conshohocken, PA, 2013, DOI: 10.1520/D5242-92R13, www.astm.org.

Bos, M. G. Discharge Measurement Structures. 3rd ed. Wageningen, Netherlands: International Institute for Land Reclamation and Improvement, 1989. Print.

Bowman, N. K. (1988). “Hydraulic analysis of alternative South Carolina curb inlet structures” Thesis. Clemson University. Print.

Comport, B.C. and C.I. Thornton (2012). “Hydraulic efficiency of grate and curb inlets for urban storm drainage.” ASCE Journal of Hydraulic Engineering, 138:10:878:884.

Drainage Criteria Manual (2002). Urban Drainage and Flood Control District, Denver, Colorado, Streets / Inlets / Storm Sewers Chapter, V. 1, pg. ST-20.

Fang, X., S. Jiang, and S. R. Alam (2010). “Numerical simulations of efficiency of curb-opening inlets.” ASCE Journal of Hydraulic Engineering, 136:1:62-66.

Fiuzat, A. A., C. E. Soares, and B. L. Sill (2000). "Design of Curb Opening Inlet Structure." Iranian Journal of Science & Technology, 24:11-21.

Guo, J.C.Y. (2006). “Design of street curb opening inlets using a decay-based clogging factor.” ASCE Journal of Hydraulic Engineering, 132:11:1237:1241.

Guo, J.C.Y., K.A. MacKenzie, and A. Mommandi (2009). “Design of street sump inlet.” ASCE Journal of Hydraulic Engineering, 135:11:1000-1004.

Guo, J.C.Y. and K. MacKenzie (2012). Hydraulic Efficiency of Grate and Curb-Opening Inlets Under Clogging Effect. Report No. CDOT-2012-3. Colorado Department of Transportation, DTD Applied Research and Innovation Branch, April 2012, 92 pgs.

Gomez, M. and B. Russo (2005). “Comparative study among different methodologies to determine storm sewer inlet efficiency from test data.” Proceedings of the 10th International Conference on Urban Drainage, Copenhagen (Denmark), 21-26 August 2005, 8 pgs.

Gomez, M. and B. Russo (2011). “Methodology to estimate hydraulic efficiency of drain inlets.” Water Management, Proceedings of the Institution of Civil Engineers, 164:WM2:81-90.

Grant, Douglas M., and Brian D. Dawson. ISCO Open Channel Flow Measurement Handbook. 5th ed. Lincoln, Neb.: ISCO, 2001. Print.

Hammonds, M.A. and E. Holley (1995). Hydraulic Characteristics of Flush Depressed Curb Inlets and Bridge Deck Drains. Research Report 0-1409-01, Center for Transportation Research, University of Texas at Austin. December 1995. 171 pgs.

HEC-22: Brown, S.A., J.D. Schall, J.L. Morris, C.L. Doherty, S.M. Stein, and J.C. Warner (2009). Urban Drainage Design Manual, Hydraulic Engineering Circular 22, Third Edition. U.S. Department of Transportation, Federal Highway Administration Publication No. FHWA-NHI-10-009, September 2009, Revised August 2013, 478 pgs.

Holley, E.R., C. Woodward, A. Brigneti, and C. Ott (1992). "Hydraulic Characteristics of Recessed Curb Inlets and Bridge Drains." Research Report FHWA/TX-03+1267-1F, Center for Transportation Research, University of Texas at Austin. December 1992, 89 pgs.

Hotchkiss, R. H, D. E. Bohac (1991). Efficiency of highway storm water inlets. Final Report RES (0099) P440 Nebraska Department of Roads, Department of Civil Engineering, University of Nebraska-Lincoln. October 1991. 53 pgs.

Hotchkiss, R. H. (1994). "Improvements in curb opening and grate inlet efficiency." Recent research on hydraulics and hydrology, 1471:24-30.

Hydraulic Toolbox. Computer software. Vers. 4.2. Federal Highway Administration, Web. Nov. 2015. <https://www.fhwa.dot.gov/engineering/hydraulics/software/toolbox404.cfm>.

Izzard, C. F. (1950). Tentative results on capacity of curb opening inlets, with discussion. Highway Research Board, Research Report No. 11-B, December 1950, p.36-54.

Izzard, C. F. (1977). "Simplified method for design of curb opening inlets." Transportation Research Record, 631:39-46.

Jiang, S. (2007). Numerical Simulations of Shallow Flow Through Curb-Opening Inlets at Various Longitudinal and Cross Slopes. Ph.D. Dissertation, Lamar University, Texas. 176 pgs.

Kranc, S.C., C.J. Cromwell, C.J. Rabens, and J.D. Killian (2001). Hydraulic Performance of Several Curb and Gutter Inlets. Research Report FL/DOT/RMC/0895-BB895, Department of Civil and Environmental Engineering, University of South Florida, May 2001, 37 pgs.

Kranc, S.C., F. Romano, S. Ethier, J. Wilmot, R. Deavers, J. Kromolicki, G. Rabens, and C. Cowell (1998). Hydraulic Performance of Drainage Structures Phase I and II. Research Report FL/DOT/RMC/0790-BA515, Department of Civil and Environmental Engineering, University of South Florida, November 1998, 48 pgs.

MacCallan, R.M. and R.H. Hotchkiss (1996). Hydraulic Efficiency of Highway Stormwater Inlets-Final Report. Research Report NE-DOT-R-96-1, Department of Civil Engineering, University of Nebraska-Lincoln, May 1996, 140 pgs.

McEnroe, B.M., R.P. Wade and A.K. Smith (1999). Hydraulic Performance of Curb and Gutter Inlets. Report No. K-TRANL KU-99-1, Department of Transportation, Kansas, September 1999, 61 pgs.

McEnroe, B.M. and R.P. Wade (1998). Hydraulic Performance of Set-Back Curb Inlets. Final Report K-TRAN Research Project KU-98-3, Department of Civil and Environmental Engineering, University of Kansas, June 1998, 112 pgs.

Pisano, P., Goodwin, L., and Rossetti, M. (2008). U.S. Highway Crashes in Adverse Road Weather Conditions, Advances and Applications in Surface Transportation Weather, 24th Conference on Institutional Information Processing Systems.

Qian, Q., X. Liu, R. Charbeneau, and M. Barrett (2013). Hydraulic Performance of Small Scale Bridge Deck Drains, Report FHWA/TX-12/0-6653-1. Center for Transportation Research, University of Texas at Austin. 112 pgs.

Russo, B. and M. Gomez (2012). 'Discussion of "Hydraulic efficiency of grate and curb inlets for urban storm drainage." by Brendan C. Comport and Christopher I. Thornton.' ASCE Journal of Hydraulic Engineering, 140:1:121-122.

Soares, C. E. (1991). "Analysis of the efficiency of an alternative South Carolina storm water drainage structure" Thesis. Clemson University. Print.

Spaliviero, F., R.W.P. May, and M. Escarameia (2000). Spacing of Road Gullies: Hydraulic performance of BS EN 124 gully gratings and kerb inlets. Report SR 533 HR Wallingford, September 2000, 25 pgs.

Subramanya, K., and S. C. Awasthy (1972). "Spatially varied flow over side weirs." Journal of Hydraulics Division, 98:1:1-10.

Thompson, D., X. Fang, and G.-C. Om Bahadur (2003). Synthesis of TxDOT Storm Drain Design. Report 4553-1, Center for Multidisciplinary Research in Transportation, Department of Civil Engineering, Texas Tech University, 157 pgs.

TxDOT (2014). Hydraulic Design Manual. Effective date May 01, 2014. Chapter 10, Section 6, Sub-heading Curb Inlets On-Grade. Online resource. Accessed August 11, 2014. http://onlinemanuals.txdot.gov/txdotmanuals/hyd/gutter_and_inlet_equations.htm #i1017364.

Uyumaz, A. (1992). "Discharge Capacity for Curb-Opening Inlets." ASCE Journal of Hydraulic Engineering, 118:7:1048-1051.

Uyumaz, A. (1994). "Highway storm drainage with kerb-opening inlets." The Science of the Total Environment, 146/147:471-478.

Uyumaz, A. (2002). "Urban Drainage with Curb Opening Inlets." Global Solutions for Urban Drainage, Proceedings of the Ninth International Conference on Urban Drainage, Portland, Oregon (USA), September 8-13, 2002, 9 pgs.

Water Measurement Manual. U.S. Department of the Interior. Bureau of Reclamation. Washington, DC: Government Printing Office, 2001.